5-2009

Functional Interaction of RacF2 and the WASp Family Protein, SCAR, in the Rab8 Signaling Pathway of the Social Amoeba, *Dictyostelium discoideum*

Terri Bruce
Clemson University, terrib@clemson.edu

FUNCTIONAL INTERACTION OF RACF2 AND THE WASP FAMILY PROTEIN, SCAR, IN THE RAB8 SIGNALING PATHWAY OF THE SOCIAL AMOEBA, *DICTYOSTELIUM DISCOIDEUM*

A Dissertation
Presented to
the Graduate School of
Clemson University

In Partial Fulfillment
of the Requirements for the Degree
Doctor of Philosophy
Biological Sciences

---

by
Terri Lane Foster Bruce
May 2009

Accepted by:
Lesly A. Temesvari, Committee Chair
Kenneth A. Christensen
James C. Morris
Alfred P. Wheeler

ABSTRACT

The small GTPase, Rab8, has been shown to play a role in cell-cell adhesion and restructuring of the actin cytoskeleton in both mammalian cells and the lower eukaryote, *Dictyostelium discoideum*. In *D. discoideum*, cells expressing constitutively activated Rab8 (Rab8CA) display reduced cell-cell adhesion and increased actin-rich protrusions as well as delayed aggregation. Rab8 has been implicated in the restructuring of the actin cytoskeleton, but no specific pathway for this action has been identified. In other systems, actin-rich membrane extension formation is regulated by WASp family proteins, including SCAR. Here we provide evidence of a functional relationship between the WASp family protein, SCAR, and Rab8. This provides the first genetic evidence in any cell system of a functional interaction between Rab8 and a WASp family protein.

SCAR is known to be directly activated by Rac. Our results indicate that Rab8 interacts directly with RacF2 to rescue aggregation in cells expressing Rab8CA. While we were unable to demonstrate that RacF2 interacts directly with SCAR, we have demonstrated that RacF2 likely interacts directly with Rab8 to control cell-cell adhesion.

Additionally, we have begun to conduct similar experiments in mammalian cells. To this end, we have developed and expressed EGFP (enhanced green fluorescent protein) chimeras of wildtype as well as constitutively active and dominant negative mutant forms of Rab8 in mammalian cells. In addition, we have designed a Rab8 activation assay based on its interaction with GCK, a germinal center kinase, which interacts directly with the active, GTP-bound form of Rab8. We have also investigated the effect of expression of mutant versions of Rab8 on GCK intracellular levels.

DEDICATION

To my wonderful husband, Dr. David Bruce, and my two beautiful children, Samuel Namon and Madelyn Patricia, who have supported me through my journey. Sam and Maddie, you are the best part of my life. Your sweet smiles, hugs and kisses have helped keep Mama going. Mama loves you both very much.

David, I quite simply could not have done this without you. You are a wonderful father and husband, and you are truly my best friend. Thank you for all of your support and love, not just through this crazy scheme, but through all of the ones I have come up (or will come up with) over our years together. I thank God that I get to grow old with you. I love you.

ACKNOWLEDGMENTS

Words seem inadequate when the time comes to acknowledge and express appreciation to all of those who help us through the greatest journeys of our lives. I feel this failing especially acutely here at the end of this part of my academic journey.

First, to my advisor, Dr. Lesly Temesvari, I would like to express my appreciation for being allowed to join your research team. You have been supportive and accommodating throughout my tenure in your lab. Thank you for giving me such an immensely interesting problem and the freedom to work on it in my own unique way. Thank you for your patience, advice and friendship along the way.

Second, to my committee members, Dr. Hap Wheeler, Dr. Ken Christensen, and Dr. Jim Morris, thank you all for your insight and guidance over the last few years. You have all helped to make my time at Clemson very productive and pleasant. I appreciate all of you for taking the time out of your extremely busy schedules to attend committee meetings, read my manuscripts and scrutinize my work. You have all been fair and fun, and I count you among my most esteemed colleagues.

Next, to my lab "family" members both past and present, I would like to thank all of you for making my time in the Temesvari lab so much fun. Thanks to Dr. Glen McGugan for encouraging me to pursue my doctorate, and being so kind and helpful through my first year back to school. Thanks to Dr. Rick Laughlin for rooster glove, secret projects and midnight movies with Glenny, even if you were wearing one of your creepy guy shirts. I enjoyed goofing around with you! Thanks to Kriti Mittal and Gina

Byekova for being so sweet and fun. Kriti, you always had a smile, and Gina, you always filled a room with your bubbly personality. Thanks to the little army of undergraduates over the years, notably Dr. Carreen Attaway, Ms. Colleen Fenn, and Mr. Chris Attaway, aka Mr. Hannah Montana. You guys always made me laugh. To Ms. Brennan Palazola, thank you so much. I could not have finished this without you. I can't tell you how much I admire your dedication through all of the late nights and long hours in the microscopy dungeon! You are a wonderful, bright, intelligent young woman. I wish you all the best. I know you will succeed in whatever you choose to do. Thanks to Ms. Amanda Goldston for rotating through the Temesvari at the best time for me to put her to work! You have helped me immensely, and I appreciate all of the late nights! A very special thanks to Ms. Brenda Welter and Ms. Rhonda Powell for your friendship and technical advice. I often drove you both crazy, and I appreciate the leeway you have always given me. Here's to all of the lab lunches we have shared. You two are more than friends, you are family.

Finally, to my family, I love you all. To my parents, Pat and Jack Foster, your support for me has never wavered. You instilled in me a love of learning that I can only hope to pass to my own children. I owe too much to you to speak of here. To my brother, Greg Foster, aka "Dookie Feet," I love you for driving me crazy while we were growing up! To my husband, David Bruce, and my beautiful children, Sam and Maddie, thank you for letting Mama do this.

Financial assistance for this project was provided by a grant to Dr. Temesvari by the National Science Foundation (MCB-0621552) and by the Clemson Research Initiative Fund.

TABLE OF CONTENTS

Page

Table of Contents (Continued)

Page

LIST OF FIGURES

List of Figures (Continued)

CHAPTER ONE

LITERATURE REVIEW

Dictyostelium discoideum

Background

Dictyostelium discoideum is a non-pathogenic, eukaryotic amoeba that is normally found in the soil or leaf litter of deciduous forest environments. The first person to describe the organism was the mycologist, Oskar Brefeld, in 1869 (Eichinger and Rivero, 2006). Today, *D. discoideum* is one of the most well studied model systems in biology. The organism is often referred to as a "social" amoeba due to its remarkable life cycle, which involves both a single cell, vegetative stage and a multi-cellular stage. Under favorable environmental conditions, including adequate sources of food, moisture, and light, *D. discoideum* cells exist as free living, single cell amoebae. However, when resources become scarce, the amoebae have the ability to trigger a developmental program which initiates chemotaxis towards other amoebae, aggregation into a multi-cellular structure, and differentiation that results in the production of spores for long term survival (Loomis, 1975).

D. discoideum is a model system that can be used to study a variety of cellular processes including chemotaxis, cell motility, cell differentiation, pinocytosis and phagocytosis, and cell sorting and patterning. *D. discoideum* is inexpensive to maintain, simple to subculture, and grows at room temperature. It has a haploid genome, making genetic knockout straightforward, and the genome of the organism has been sequenced (Eichinger and Noegel, 2003). Having been a subject of study by biologists for nearly

140 years, a wealth of information regarding manipulation of the organism exists. These advantages put *Dictyostelium* on par with such powerful model systems as *Drosophila melanogaster*, *Sacchoromyces cerevisiae* and *Caenorhabditis elegans* (Eichinger and Rivero, 2006).

Life Cycle

The life cycle of *Dictyostelium* is one of its most characteristic and intriguing features (Figure 1.1). Under favorable environmental conditions, the amoebae exist as free-living, single cells. They subsist primarily on bacteria. The bacteria secrete folic acid, which acts as a chemoattractant to the *Dictyostelium*. When food resources become scarce, the ensuing starvation induces changes in gene expression in the amoebae. As a result, a number of adhesion molecules, cAMP generating protein machinery and cAMP receptor molecules are produced. After approximately 5 hours of starvation, founder cells begin to secrete cAMP, which induces cAMP secretion and chemotaxis towards the cAMP source in surrounding cells. As cells chemotax, they move collectively, as streams of cells, towards the central founder cell and begin to adhere to one another. Cell-cell adhesion is mediated by a 24-kilodalton glycoprotein adhesion molecule, gp24. This process culminates in the formation of aggregates of approximately 100,000 cells (Gilbert, 2003).

Once the initial aggregation has occurred, the resulting group of cells, or aggregate, is further stabilized by the 80-kilodalton adhesion glycoprotein, gp80. During late aggregation, gp80 is replaced by the 150-kilodalton adhesion glycoprotein, gp150. At

this stage, known as the tight aggregate stage, cells are piled on top of one another. Eventually, a tip forms in the center of the aggregate, and the tight aggregate rises up and bends over to form the slug, or pseudoplasmodium stage. The slug is composed of cells that have already begun to differentiate. The anterior portion of the slug is composed of prestalk cells that will eventually become support cells for the culminating fruiting body, while the posterior portion is composed of prespore cells, which will eventually become spore cells within the fruiting body (Gilbert, 2003).

D. discoideum slugs have the ability to chemotax, thermotax, and phototax. The anterior portion of the 2-4 mm slug secretes a slimy, cellulose sheath, which the slug can then move through, leaving behind a slime trail. The slug migrates to an illuminated area, settles, forming the “Mexican hat” stage, and begins culmination. At this point, the prestalk cells secrete an extracellular cellulose coat and form a tube that pushes up, moving the anterior prestalk cells to the bottom and the posterior prespore cells to the top. This cell rearrangement forms the fruiting body, which is approximately 1-2 mm tall. The prestalk cells die and become the support structure of the mature fruiting body, while the prespore cells are encased and become mature spore cells. The spores are then dispersed into the environment where they will germinate when conditions become favorable (Gilbert, 2003).

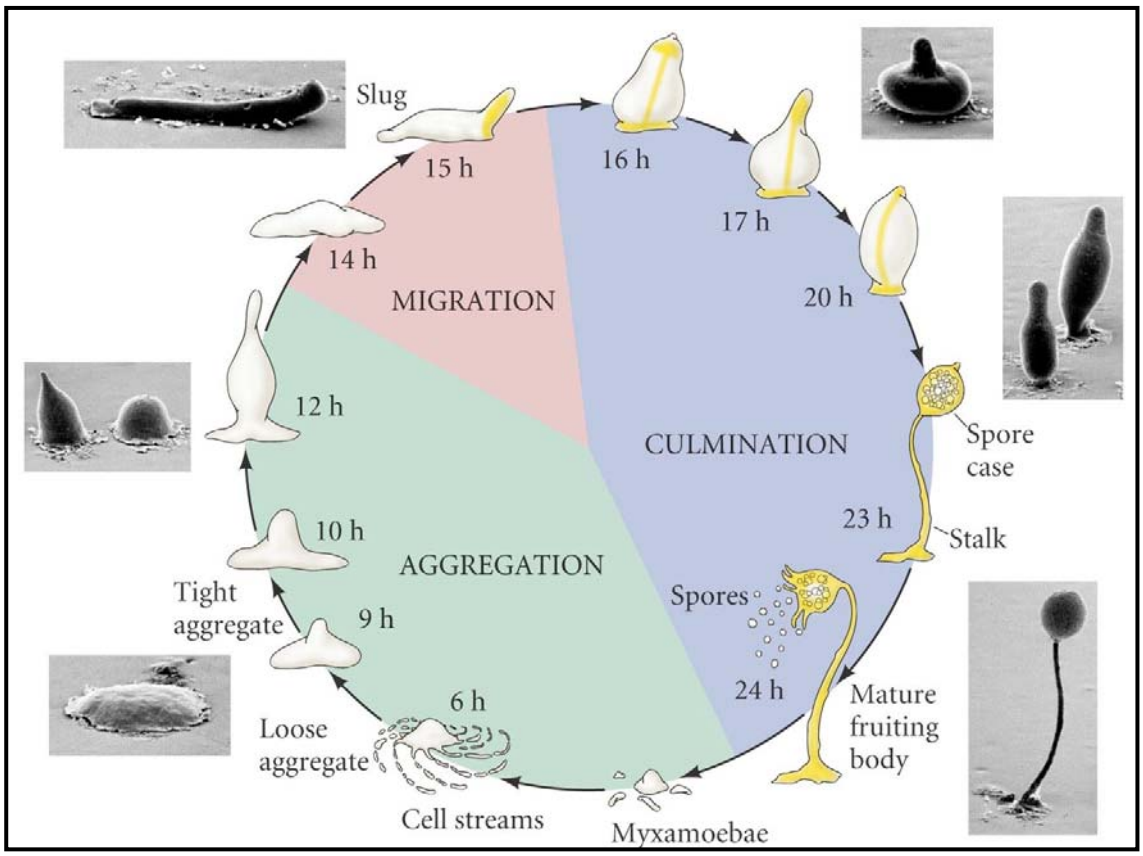

Figure 1.1. ***Dictyostelium discoideum Life Cycle***. When resources become limiting, amoebae form groups of cells called aggregates. Aggregated amoebae form a slug, which has the ability to migrate. Amoebae within the slug undergo cellular differentiation to become specialized cells, including stalk cells and spores. A fruiting body is formed from the stalk cells, which encases the spores. The spores are distributed and germinate to become single amoebae. Taken from *Developmental Biology*, p. 39 (Gilbert, 2003).

cAMP and Chemotaxis

The ability to sense and move directionally along a chemical gradient is a process known as chemotaxis. It is a process utilized by a wide variety of cells to signal directional movement. During chemotaxis, cells are able to detect a chemical gradient and respond to it by polarizing and orienting themselves in the direction of the gradient. Cell polarization is accomplished by the formation of actin-rich pseudopods at the

leading edge and the trafficking of myosin II to the lagging edge, where it is instrumental in retraction (Kriebel, Barr, *et al.*, 2008). The process of chemotaxis is important during a variety of cellular and tissue processes including nutrient acquisition, angiogenesis, wound-healing and embryological development. It is also associated with disease pathologies including inflammation associated with conditions such as asthma and arthritis, as well as cancer metastasis (Ridley, Schwartz, *et al.*, 2003).

D. discoideum utilizes the process of chemotaxis during nutrient acquisition and during development. During nutrient acquisition, the organism is able to sense a gradient of folic acid. Bacteria, which serves as the main source of nutrition for *Dictyostelium*, secrete folic acid, towards which the amoeba chemotax. When nutrients become limiting, *Dictyostelium* begin the process of development. Founder cells begin secretion of cAMP, which acts as a chemoattractant by binding to cell surface receptors on neighboring cells (Kriebel, Barr, *et al.*, 2008; Postma, Roelofs, *et al.*, 2004).

The *Dictyostelium* cAMP cell surface receptors are serpentine, seven transmembrane, G-protein coupled receptors. Upon binding to extracellular cAMP, these heterotrimeric G-proteins disassociate into a Gα subunit and a Gβγ subunit (Postma, Roelofs, *et al.*, 2004; Postma, Roelofs, *et al.*, 2004). This triggers the activation of adenylyl cyclase, phospholipase C, Ca^{++} transporters, and guanylyl cyclase, which, in turn, respectively activate the production and accumulation of the intracellular secondary messengers, cAMP, Ca++, IP3 and cGMP (Saxe, Ginsburg, *et al.*, 1993).

D. discoideum has four different cAMP receptor (cAR) proteins, cAR1, cAR2, cAR3, and cAR4. cAR1 and cAR3 are expressed during early development and are high

affinity cAMP receptors, while cAR2 and cAR4 are expressed during later development and are lower affinity receptors (Ginsburg and Kimmel, 1997). Each cAR is expressed at a different time and is targeted to a unique location on the plasma membrane. As a result of this differential expression, each cAR plays a specific role in the process of development (Ginsburg and Kimmel, 1997).

The first cAMP receptor that is expressed during development is cAR1. It is required for the proper streaming and aggregation of individual cells during the initiation of development (Ginsburg and Kimmel, 1997). When cAMP is released from founder cells, it binds to cAR1 on neighboring cells. This results in the production of intracellular cAMP and secretion of cAMP. This relay action leads to an overabundance of extracellular cAMP, which results in the desensitization of the cAR1 receptors due to hyperphosphorylation. *D. discoideum* concomitantly secretes phosphodiesterases, which break down extracellular cAMP. This attenuates the cAR1 binding and returns the receptor to a sensitive state. The result is an oscillatory pattern of cAMP release. These cAMP "waves" occur regularly every six minutes during the onset of streaming and aggregation (Saxe, Ginsburg, *et al.*, 1993). *D. discoideum* cAR1 null mutants fail to aggregate and demonstrate changes from the gene expression normally seen in early development (Klein, Sun, *et al.*, 1988; Sun and Devreotes, 1991).

cAR3 is the second cAMP receptor expressed during *D. discoideum* development. The highest level of cAR3 occurs at approximately 10 hours of development (Johnson, Van Haastert, *et al.*, 1992). It has the ability to substitute for cAR1 in cAR1 null cells when they are pulsed with cAMP in suspension (Ginsburg and Kimmel, 1997).

cAR2 and cAR4 are expressed during later developmental stages. cAR2 is a prestalk marker and is necessary for proper tip formation following the tight mound stage of development. In cAR2 null cells, development is arrested prior to tip formation (Bear, Rawls, and Saxe, 1998). It is believed that it may play a role in the sorting of prestalk and prespore cells within the slug (Saxe, Ginsburg, *et al.*, 1993). cAR4 expression begins during the tight aggregate stage of development and continues through to the fruiting body stage (Ginsburg and Kimmel, 1997; Louis, Ginsburg, and Kimmel, 1994). Although it is expressed most in prestalk cells, it is also expressed at low levels in prespore cells. It is responsible for initiating prestalk intracellular differentiation and inhibiting prespore intracellular differentiation (Ginsburg and Kimmel, 1997).

During chemotaxis, cAMP binds to cAR1, and adenylyl cyclase A is activated. In addition, a gradient of cAMP is created within the cell through the activities of phosphoinositide-3-kinase (PI3K), PI(3,4,5)P_3-phosphatase (PTEN) and phospholipase A2 (PLA2) (Vicker and Grutsch, 2008; Chen, Iijima, *et al.*, 2007; Keizer-Gunnink, Kortholt, and Van Haastert, 2007). Following cAMP stimulation, PIP_3 accumulates exclusively at the leading edge of the cell (Loovers, Postma, *et al.*, 2006), while PTEN, which degrades PIP_3, is accumulated at the lagging edge. CRAC (cytosolic regulator of adenylyl cyclase), which is a pleckstrin homology (PH) domain-containing protein, binds to PIP_3 at the leading edge membrane. It is hypothesized that this binding event stimulates the induction of signaling pathways, which lead to cell polarization, intracellular cAMP synthesis, and the assembly of actin filaments necessary for chemotaxis (Condeelis, 1993; Dormann, Weijer, *et al.*, 2004; Dormann and Weijer, 2006;

Parent, Blacklock, *et al.*, 1998; Ridley, Schwartz, *et al.*, 2003; Vicker and Grutsch, 2008; Westphal, Jungbluth, *et al.*, 1997; Xu, Meier-Schellersheim, *et al.*, 2005; Xu, Meier-Schellersheim, *et al.*, 2005).

The Cytoskeleton

Cells contain a three dimensional scaffolding system referred to as the cytoskeleton. The cytoskeletal system is composed of three types of protein filaments; intermediate filaments, microtubules and actin filaments, or microfilaments. These filaments provide structural stability to the cell and form protein "highways" for the vesicle transport of proteins within the cell. The cell cytoskeleton is a vital component of cell locomotion, cell division, cell polarity and tissue morphogenesis (Fuchs and Yang, 1999).

Intermediate Filaments

Intermediate filaments are a group of cytoskeletal fibers found primarily in eukaryotic cells within multicellular organizations. A primary role for intermediate filaments is to provide mechanical stability by distributing tensile forces across cells within a tissue. They are primarily found in muscle tissue and sheets of epithelial skin cells, which must withstand substantial mechanical forces, as well as in long, fragile nerve processes. Intermediate filaments also form the nuclear lamina, which provides support for the nuclear envelope in eukaryotic cells (Lodish, Berk, *et al.*, 2000).

The subunits of intermediate filaments are alpha-helical protein monomers. Individual subunits are paired to form coiled-coil dimers. These dimers are paired in a

staggered configuration to form a tetramer. Eight tetramers are then twisted into a ropelike filament (Alberts, Johnson, *et al.*, 2008). There are a number of different intermediate fiber proteins, which are divided into six groups based on their sequence homology; Type I(acid keratins), Type II(basic keratins), Type III (desmin, glial fibrillary acid protein, peripherin, vimentin), Type IV (NF-L, NF-M, NF-H, internexin), Nonstandard Type IV (filensin, phakinin) and Type V (laminA, B, and C) (Hattula, 2007). The type of intermediate filament protein is cell type specific. For example, keratin is primarily found in epithelial cells. As a result, the type of intermediate filament protein in tumor cells can be used to help identify their cellular origin (Lodish, Berk, *et al.*, 2000).

Microtubules

Microtubules are cytoskeletal structures which are involved in determining the position of cellular organelles and in directed transport within a cell. They are hollow tubes composed of thirteen protofilaments, which are polymers composed of α– and β–tubulin heterodimers. The heterodimer subunit has an integral GTP nucleotide binding site. This GTP is subsequently hydrolyzed when the subunit is incorporated into the protofilament. Microtubules are organized by the centrosome, which is often referred to as the microtubule organizing center (MTOC). This structure is the primary organizing center of the cell and is also responsible for the organization of the mitochondria, Golgi complex and endoplasmic reticulum (Lodish, Berk, *et al.*, 2000). The MTOC is a complex that contains a host of proteins that are instrumental in the assembly of

microtubules. One of these MTOC latticework proteins is γ-tubulin, which forms a ring-like structure. β-tubulin binds to the γ-tubulin ring, which guides the protofilaments to form a hollow tube.

Microtubules are dynamic structures. They are continuously assembled and disassembled in a process called dynamic instability (Alberts, Johnson, *et al.*, 2008). The dynamic microtubule is a polar structure with plus and minus ends. The plus end is the end that has the higher rate of assembly, while the minus end is the end with the slower rate of assembly. In most microtubules, the minus end is associated with the MTOC, while the more dynamic plus end is extended into the cytoplasm (Lodish, Berk, *et al.*, 2000).

An important process within cells is the directed delivery of proteins and vesicles. Microtubules act as tracks within the cell and help direct the timely and spatially precise delivery of proteins and vesicles to specific sites within the cytoplasm or to the plasma membrane. Cargo is carried along microtubule tracks by the interaction with the motor molecules, kinesin and dynein. Kinesins are dimers composed of two heavy and two light chains. The heavy end has globular heads with ATP hydrolysis activity that bind to the microtubule, and the light end binds to the cargo vesicle to be transported. There are several different kinesins, which are specific for different cargo vesicles. Nearly all of the kinesin molecules are responsible for the movement of cargo towards the plus end of the microtubule away from the MTOC, and are often involved in the transport of secretory vesicles to the plasma membrane (Lodish, Berk, *et al.*, 2000).

Dyneins are composed of two or three heavy chains, and a number of intermediate and light chains. They must be associated with a group of microtubule-binding proteins in order to facilitate transport. Nearly all dyneins are responsible for minus end directed movement of cargo vesicles. Both kinesins and dyneins utilize energy from ATP hydrolysis to facilitate vesicle transport. While diffusion may be sufficient for short range transport of vesicles, microtubules are required to move vesicles over long distances like those of nerve axons. Microtubule disruption has been linked to neurodegenerative diseases including Parkinson's (Ren, Jiang, *et al.*, 2009) and Alzheimer disease (Iqbal, Liu, *et al.*, 2009).

Actin

The actin cytoskeleton of a cell is composed of actin filaments and associated proteins. It is involved in cellular processes including motility, chemotaxis, endocytosis, and changes in cell shape (Noegel and Schleicher, 2000). Actin is one of the most abundant and highly evolutionarily conserved proteins found in eukaryotic cells (Nefsky and Bretscher, 1992). Actin filaments, called F-actin, are assembled from globular actin monomers, called G-actin. The G-actin monomers polymerize into polar filaments with a fast growing plus end and a slower growing minus end. The plus end and minus end are often referred to respectively as the barbed end and the pointed end. These terms arise from the appearance of pointed actin filaments as seen in electron micrographs (Millard, Sharp, and Machesky, 2004). G-actin binds to ATP, making it available to bind to the fast growing plus end of an actin filament. This ATP is hydrolyzed within the filament

conformation, and G-actin, bound to ADP, is released from the minus end of the actin filament (Carlier, 1998). This dynamic process of assembly and disassembly of actin filaments is referred to as treadmilling (Lodish, Berk, *et al.*, 2000).

Actin dimers and trimers are inherently unstable complexes, and the assembly of actin monomers is energetically unfavorable. Therefore, in order for actin filaments to form, the process must be regulated by accessory proteins. Cells have mechanisms by which the generation of barbed, or plus, ends is regulated. Proteins that play a role in the regulation of filament growth at the barbed end include gelsolin and capping proteins, ADF (actin-depolymerizing factor)/ cofilin, and the Arp2/3 (actin-related proteins 2 and 3) complex (Chan, Bailly, *et al.*, 2000; Ichetovkin, Grant, and Condeelis, 2002; Millard, Sharp, and Machesky, 2004).

Gelsolin and capping proteins bind to the barbed end, preventing further elongation. These caps may be removed when cellular events trigger the elongation of actin filaments (Silacci, Mazzolai, *et al.*, 2004). Membrane phosphoinosotides may play a role in signaling the release of capping proteins, so that actin filaments may elongate during cell migration (Millard, Sharp, and Machesky, 2004; Ridley, Schwartz, *et al.*, 2003; Rozelle, Machesky, *et al.*, 2000).

ADF/cofilin are severing proteins that can break actin filaments and create new barbed ends, which may be utilized for elongation. The action of these severing proteins has been shown to play a role in the formation of new actin filaments during cell spreading and epidermal growth factor induced lamellipodia generation (Chan, Bailly, *et al.*, 2000; Ichetovkin, Grant, and Condeelis, 2002; Millard, Sharp, and Machesky, 2004).

The formation of new actin filaments is accomplished through the process of nucleation. As actin dimers and trimers are unstable, it was hypothesized that accessory proteins must be acting as nucleating agents for the beginning of new filament formation. It has been demonstrated that the Arp2/3 protein complex acts as such a nucleator. The complex works in conjunction with other actin associated proteins, including capping and severing proteins, to stabilize actin dimers and trimers at the beginning of new filament formation. Arp2/3 was isolated from human platelets and shown to be sufficient to drive actin polymerization in tail formation and motility in *Listeria monocytogenes* (Welch, Iwamatsu, and Mitchison, 1997). The evolutionarily conserved and diverse role of this protein complex has been demonstrated in human cell lines and such organisms as *Dictyostelium discoideum*, and *Caenorhabditis elegans*, in such processes as motility, phagocytosis, and development (Insall, Muller-Taubenberger, *et al.*, 2001; May, Caron, *et al.*, 2000; Sawa, Suetsugu, *et al.*, 2003).

WASp Family Proteins

The assembly of actin filaments is essential for many cellular functions including chemotactic movement, endocytosis and cell morphological changes (Blagg and Insall, 2004; Pinyol, Haeckel, *et al.*, 2007). The Arp 2/3 complex plays a crucial role in the process of actin polymerization in these diverse cellular functions. Therefore, specificity is modulated through Arp 2/3 activator proteins. One group of Arp 2/3 activators is the WASp (Wiskott-Aldrich Syndrome protein) family proteins. There have been five WASp family proteins identified: WASp, N-WASp, SCAR/WAVE1, SCAR/WAVE2, and

SCAR/WAVE3 (Millard, Sharp, and Machesky, 2004; Suetsugu, Miki, and Takenawa, 1999). These Arp2/3 activators have been implicated in actin-based processes such as the generation of lamellipodia, filipodia, and membrane ruffling (Legg, Bompard, *et al.*, 2007), as well as cell migration, extension of neurites, and vesicle trafficking (Suetsugu, Miki, and Takenawa, 1999; Ward, Wu, and Rao, 2004). WASp family proteins are believed to link Rho-GTPases to actin cytoskeletal dynamics (Blagg, Stewart, *et al.*, 2003; Blagg and Insall, 2004; Oikawa, Yamaguchi, *et al.*, 2004).

WASp and N-WASp

Wiskott-Aldrich Syndrome (WAS) is an X-chromosome linked immunodeficiency disorder characterized by pathologies caused by the failure of T and B cell functions and defects in monocyte chemotaxis. WAS patients suffer from recurrent infections, eczema, and thrombocytopenia, and experience a higher rate of lymphomas and leukemias (Millard, Sharp, and Machesky, 2004; Myers, Han, *et al.*, 2005; Seastone, Harris, *et al.*, 2001). In 1994, the cause of Wiskott-Aldrich Syndrome was identified as being the result of a mutation in the gene encoding a 501-amino-acid proline-rich protein expressed only in hematopoietic cells. This protein was subsequently named WASp (Wiskott-Aldrich protein) (Derry, Ochs, and Francke, 1994; Millard, Sharp, and Machesky, 2004).

An isoform of WASp was found in brain tissue in 1996. This WASp isoform became known as N-WASP (neural-WASp), and was shown to be widely expressed (Miki, Miura, and Takenawa, 1996). WASp homologues have subsequently been

identified in several organisms including *D. discoideum* (WASp), *C. elegans* (WSP-1), *Drosophila* (WASp) and *Saccharomyces cerevisiae* (Las17p) (Bear, Rawls, and Saxe, 1998; Ben-Yaacov, Le Borgne, *et al.*, 2001; Millard, Sharp, and Machesky, 2004; Sawa, Suetsugu, *et al.*, 2003; Zallen, Cohen, *et al.*, 2002).

WASp family proteins are characterized by a conserved arrangement of domains. The C-terminus contains a module of three domains including the verprolin-homology domain (V), also referred to as the WH2 (WASP-homology-2) domain, the cofilin-homology domain, also referred to as the central-domain (C), and the acidic domain (A). Collectively, this C-terminal module is known as the VCA or WCA region. This region binds to a monomer of actin and to the Arp2/3 complex. This activates the Arp2/3 complex and actin nucleation and filament formation is initiated (Millard, Sharp, and Machesky, 2004; Takenawa and Suetsugu, 2007).

The N-termini of WASp and N-WASp differ from SCAR/WAVE proteins. WASp and N-WASp contain a WH1 (WASP-homology-1) domain, which is also known as the Ena-VASP-homology-1 (EVH1) domain. This domain binds to a proline-rich area of WIP (WASP-interacting protein) protein family members as well as corticosteroids. The EVH1 domain is followed by a basic region that binds to the phospholipid, PIP_2 (phosphatidylinositol 4, 5-bisphosphate). In WASp and N-WASp, the basic region lies adjacent to a GBD (GTPase binding domain) domain, or CRIB (Cdc42 and Rac interactive binding) binding site for the GTP-bound forms of Cdc42 and Rac, which are key actin cytoskeleton regulators (Millard, Sharp, and Machesky, 2004; Myers, Han, *et al.*, 2005; Takenawa and Suetsugu, 2007). Studies of dominant- negative Cdc42 showed

reduced WASp and N-WASp induction of actin filaments (Miki, Sasaki, *et al.*, 1998; Symons, Derry, *et al.*, 1996). Therefore, it is believed that Cdc42 acts upstream of WASp and N-WASp. GTP-bound Cdc42 binds to the CRIB region and leads to the activation of WASp or N-WASp, which, in turn, activate the Arp2/3 complex and induce actin filament formation (Figure 1.2 A) (Aspenstrom, Lindberg, and Hall, 1996).

SCAR/WAVE

In 1998, Bear *et al.* identified a WASp- related protein during a genetic screen in *D. discoideum*. The identified protein, named SCAR (suppressor of cAMP receptor), acts as a suppressor of the defect caused by the loss of the *D. discoideum* cAMP receptor, cAR2. The absence of cAR2 causes disruption of tip formation during development. By disrupting SCAR in cAR2 null cells, normal tip formation was restored (Bear, Rawls, and Saxe, 1998). During the same year, two independent labs isolated a mammalian SCAR homologue. One group named the homologue SCAR, while the other dubbed it WAVE (WASp family verprolin homologous protein) (Machesky and Insall, 1998; Miki, Suetsugu, and Takenawa, 1998). The two names are both used in the literature. Two further isoforms, SCAR2/WAVE2 and SCAR3/WAVE3, were subsequently identified in mammals. In mammals, SCAR1/WAVE1 and SCAR3/WAVE3 are primarily expressed in the brain, while SCAR2/WAVE2 is expressed in a variety of tissues (Oikawa, Yamaguchi, *et al.*, 2004). SCAR homologues have also been identified in several organisms including *C. elegans* (WVE-1) (Sawa, Suetsugu, *et al.*, 2003), and *Drosophila*

(SCAR) (Bear, Rawls, and Saxe, 1998; Ben-Yaacov, Le Borgne, *et al.*, 2001; Millard, Sharp, and Machesky, 2004; Zallen, Cohen, *et al.*, 2002).

SCAR/WAVE proteins share the same C-terminal triple domain module and phospholipid binding basic region seen in WASp and N-WASp. However, SCAR/WAVE proteins differ from WASp and N-WASp in their N-termini configuration. In WASp and N-WASp, the N-termini include a WH1 domain, which is absent in SCAR/WAVE proteins. Instead, SCAR/WAVE proteins contain a SCAR homology domain (SHD) at their N-termini. In addition, unlike WASp and N-WASp, SCAR/WAVE proteins do not contain a CRIB domain for binding Cdc42 and Rac. It is the CRIB domain in WASp and N-WASp proteins that leads to their activation and regulation of Arp2/3. The binding of Cdc42 to the CRIB regions of WASp and N-WASp releases them from their autoinhibition. SCAR/WAVE proteins were originally thought to exist only in the constitutively active state (Machesky and Insall, 1998; Millard, Sharp, and Machesky, 2004; Seastone, Harris, *et al.*, 2001). More recent studies suggest that these proteins may actually exist in an inhibited state. However, instead of being autoinhibitors like WASp and N-WASp, their activation appears to be regulated by existing within a complex of proteins (Blagg, Stewart, *et al.*, 2003; Blagg and Insall, 2004; Caracino, Jones, *et al.*, 2007; Eden, Rohatgi, *et al.*, 2002; Ho, Rohatgi, *et al.*, 2004).

Eden *et al*. showed that SCAR/WAVE exists in a heteropentameric complex along with PIR121 (p53-inducible mRNA 121), Nap125 (Nck-associated protein 1), Abi2 (Abl-interactor 2) and HSPC300 (Blagg, Stewart, *et al.*, 2003; Eden, Rohatgi, *et al.*, 2002). Each of the complex proteins has been linked to cytoskeletal dynamics. When

associated with the complex, SCAR/WAVE is inactive. However, it has been shown that activated Rac or Nck leads to disassociation of SCAR/WAVE and HSPC300 from the complex and the subsequent activation of SCAR/WAVE. This demonstrates indirect regulation of SCAR/WAVE activation by Rac (Figure 1.2 B) (Caracino, Jones, *et al.*, 2007; Eden, Rohatgi, *et al.*, 2002). PIR121 has been shown to bind to Rac, which suggests that it may provide a link between SCAR/WAVE and the GTPase. SCAR2/WAVE2 has also been shown to bind to insulin receptor substrate (IRS) p53, which in turn binds to active Rac1, providing another indirect link between SCAR/WAVE and Rac (Miki, Yamaguchi, *et al.*, 2000; Miki and Takenawa, 2002; Roy, Kakinuma, and Kiyama, 2009). Many additional studies support a functional link between SCAR/WAVE and Rac, but no direct interaction has ever been demonstrated (Millard, Sharp, and Machesky, 2004).

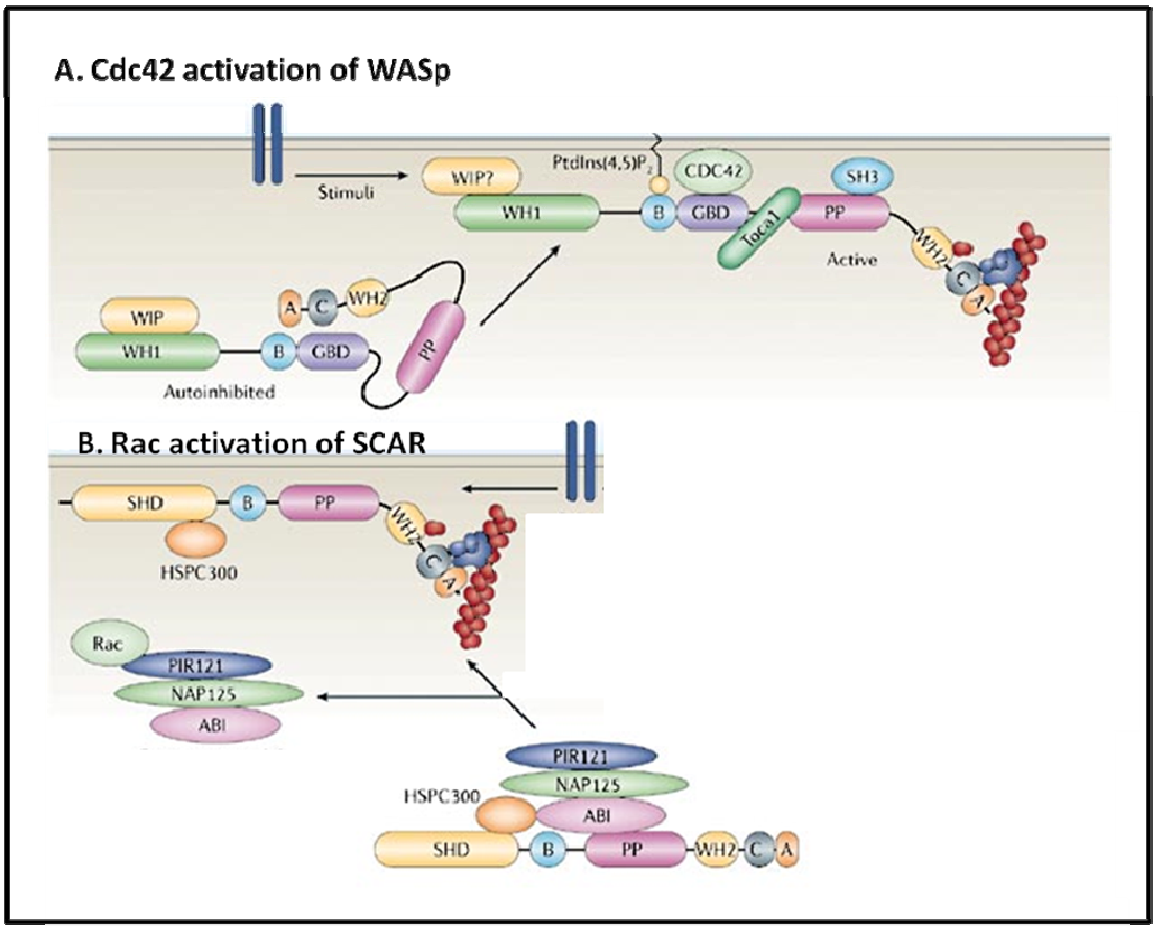

Figure 1.2. Activation of the Arp2/3 Complex Through WASp and SCAR/WAVE. (A) WASp exists in an autoinhibited state until activated by Cdc42. Activation of WASp leads to Arp2/3 complex activation and changes in actin. (B) Inactive SCAR/WAVE exists in a complex with PIR121, Nap125, ABI(Abi2) and HSPC300. When Rac binds to PIR121, SCAR/WAVE is released from this complex and activated. Activation of SCAR/WAVE leads to Arp2/3 activation and changes in actin. Adapted from Goley and Welch (Goley and Welch, 2006).

Small GTP-binding Proteins

The Ras superfamily of small GTP-binding proteins is a large group of proteins that participate in several key cell regulatory processes. They are found in a large variety of eukaryotic cells, from human to yeast and amoebae, and range in size from 20 to 40 kDa (Hattula, 2007). All of the GTPases act as molecular switches by cycling between active and inactive forms. GTPases are active when bound to GTP and inactive when bound to GDP (Figure 1.3). The Ras family proteins can be distinguished from other GTP-binding proteins by their five conserved domains, G1-G5. These domains are responsible for binding to effector proteins and nucleotides, which are necessary for the proper function of Ras family proteins (Bourne, Sanders, and McCormick, 1991).

The Ras superfamily proteins can be divided into five groups based on their structure and function. The five subgroups are Sar/Arf, Ran, Ras, Rho, and Rab GTPases. The Sar/Arf proteins are involved in vesicle formation. The Ran proteins have been shown to participate in nuclear trafficking and organization of microtubules during mitosis. The Ras family proteins function as key regulators for normal cell growth and differentiation. The Rho proteins play a primary role in cytoskeletal arrangement and have been implicated in gene expression. Finally, the largest group, the Rab family, is responsible for the regulation of vesicle trafficking (Hattula, 2007; Wennerberg, Rossman, and Der, 2005; Zerial and Huber, 1995).

Ras, Rho, Arf, and Rab GTPases contain a sequence that undergoes posttranslational lipid modification. This modification coordinates their binding to lipid membrane components, which must occur for these proteins to carry out their normal

functions (Zhang and Casey, 1996). Arf GTPases have an N-terminal myristoylation modification. Ras, Rho and Rab GTPases have one or two C-terminal cysteine residues which are prenylated. All of the Ras superfamily GTPases have the ability to bind and convert GTP to GDP. They bind GTP/GDP through a conserved amino acid sequence and have consensus sequences for binding downstream effectors as well (Bourne, Sanders, and McCormick, 1991).Within the GTP/GDP binding region of Ras, mutations were found which caused the GTPase to remain bound to GTP or GDP. This eliminated the switching ability of the GTPase, causing it to remain in the activated or inactivated state. Because the GTP/GDP binding sequence was conserved among the Ras superfamily members, this discovery allowed for the construction of constitutively active or dominant negative mutants of the GTPases, which have proven to be invaluable research tools (Hall, 2000).

The molecular switching of Ras superfamily GTPases (see Figure 1.3) is a highly regulated process. The GTPase protein binds to a single molecule of GTP. This activates the GTPase, causing a conformational change of the protein, which allows it to bind to its downstream effectors. Hydrolysis of the bound GTP to GDP and inorganic phosphate inactivates the GTPase. Three groups of proteins, including guanine nucleotide exchange factors (GEFs), GTPase activating proteins (GAPs) and, in Rho and Rab proteins, GDP dissociation inhibitors (GDIs), help to regulate the GTPase cycle. GEFs work to facilitate the exchange of GDP for GTP, thus playing a role in the activation of GTPases. GAPs are involved in the hydrolysis of GTP, thus playing a role in the deactivation of GTPases. In the case of Rho and Rab proteins, GDIs bind to the GDP-bound form of the GTPase and

inhibit its interaction with GEFs, thus holding the GTPase in an inactive state. GDIs also have the ability to remove GTPases from membranes and allow them to remain as soluble proteins in the cell cytoplasm. GEFs, GAPs, and GDIs help regulate the temporal and spatial activities of each GTPase, which enables them to regulate various downstream effectors and events (Hall, 2000; Jordens, Marsman, *et al.*, 2005; Stenmark and Olkkonen, 2001).

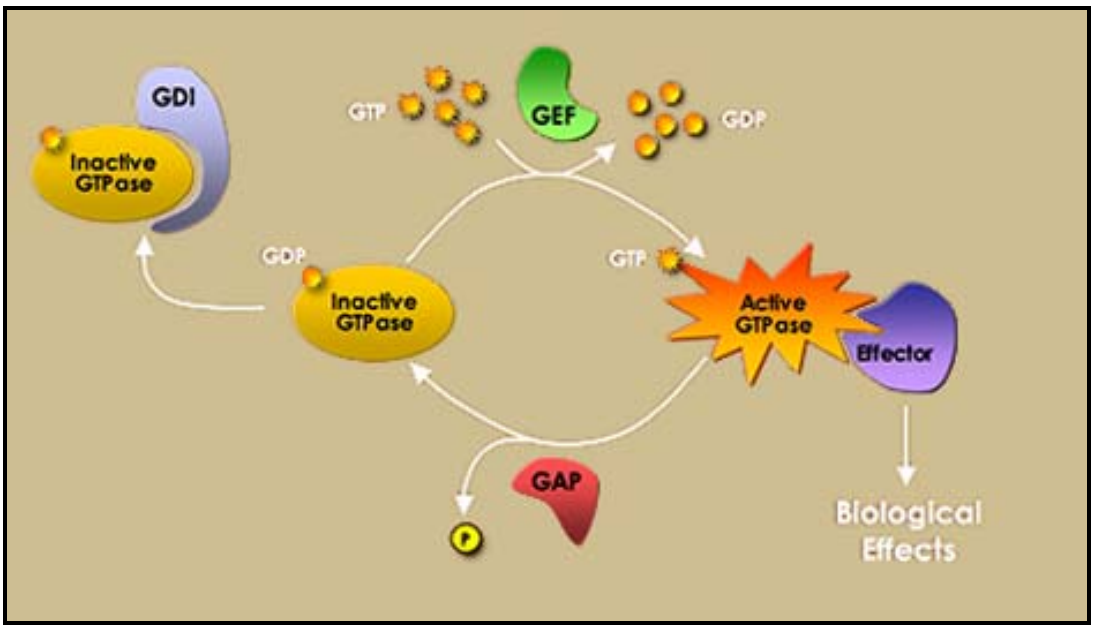

Figure 1.3. Ras Superfamily GTPase Molecular Switch Model. GTPases cycle between an active, GTP-bound state and an inactive, GDP-bound state. When active, GTPases bind to various effectors to mediate cellular effects. GEFs facilitate the exchange of GDP for GTP. GAPs aide in the hydrolysis of GTP. GDIs hold the GTPase in an inactive state by inhibiting its association with GEFs. Adopted from *Rho GTPases development, differentiation and physiopathology* (www.crbm.crns.fr/~fort/).

Sar/Arf GTPase Proteins

Sar (Secretion-associated and Ras-related protein) and Arf (ADP-ribosylation factor) GTPases belong to a group of monomeric GTPases referred to as the coat-recruitment GTPases (Pasqualato, Renault, and Cherfils, 2002). Sar1 was the first member of this group of proteins to be described. It was isolated from the yeast, *Saccharomyces cerevisiae* and was shown to be responsible for the assembly of COPII coats on vesicles originating at the endoplasmic reticulum and moving to the Golgi apparatus (Nakano and Muramatsu, 1989). Arf proteins are responsible for the assembly of COPI coats and clathrin coats on vesicles originating from the Golgi apparatus (Alberts, Johnson, *et al.*, 2008). There have been two Sar proteins (Sar1a, Sar1b) and six Arf proteins (Arf1-6) identified in mammals (Hattula, 2007). The six mammalian Arf proteins are divided into three classes. Class I Arfs (Arf 1, 2, 3) are redundant in their function and are responsible for COPI and clathrin coat assemblies at the Golgi. Class II Arfs (Arf 4, 5) have functional roles that are yet to be definitively determined. There is only a single Class III Arf, Arf6, which is involved in membrane trafficking and actin cytoskeletal dynamics at the plasma membrane (Hattula, 2007; Hu, Shi, *et al.*, 2009).

Ran GTPase Proteins

Ran (Ras-related nuclear protein) is a typical GTPase, in that it switches between active and inactive forms. However, it is unique, in that it does not bind to membranes, does not require lipids for its activation and has a nontraditional location for a GTPase within the cell (Moore, 1998; Rush, Drivas, and D'Eustachio, 1996). During interphase,

Ran is nuclear, while it appears to be dispersed throughout the cells during mitosis. It is one of the most abundant G-proteins and is highly evolutionarily conserved. It has been identified in every eukaryotic cell examined, and most cell types contain only a single Ran. It does not undergo posttranslational lipid modification, but all Ran homologues contain a conserved C-terminus acidic-DEDDDL sequence (Hattula, 2007; Moore and Blobel, 1993). Ran is responsible for providing the energy, by GTP hydrolysis, needed for the import of nuclear proteins through the nuclear pore complex (NPC). Ran is found both inside the nucleus and in the cytoplasm of the cell. Ran-GEF is located inside the nucleus and bound to chromatin while Ran-GAP is located outside the nucleus. Therefore, Ran inside the nucleus is mainly GTP-bound, while Ran in the cytoplasm is mainly GDP-bound. This gradient maintains the correct directionality of nuclear transport (Alberts, Johnson, *et al.*, 2008).

Ras GTPase Proteins

There are 13 members of the Ras GTPase family. The Ras GTPases act as signaling hubs by relaying signals from cell surface receptors to several downstream pathways. They are involved in the regulation of cellular functions including apoptosis, proliferation and differentiation (Bar-Sagi and Feramisco, 1985; Feramisco, Gross, *et al.*, 1984; Kauffmann-Zeh, Rodriguez-Viciana, *et al.*, 1997). In humans, there are three closely related Ras proteins, H-Ras, K-Ras and N-Ras, which are often referred to collectively as Ras. Point mutations that cause the constitutive activation of these GTPases have been shown to play a role in uncontrolled cell proliferation and tumor

formation (Brown, Marshall, *et al.*, 1984; Capon, Seeburg, *et al.*, 1983; Feramisco, Gross, *et al.*, 1984; McKay, Paterson, *et al.*, 1986; Stacey and Kung, 1984). It is estimated that Ras mutations may directly or indirectly cause up to 20-30% of all cancers (Barbacid, 1987; Bos, 1989).

Ras proteins are found on the cytoplasmic face of the plasma membrane where they are anchored through their C-terminal lipid groups (Alberts, Johnson, *et al.*, 2008; Choy, Chiu, *et al.*, 1999). From this position in the cell, the Ras GTPases are able to coordinate signaling from cell surface receptors to downstream effectors. For example, Ras relays the signal from cell surface RTKs (receptor tyrosine kinases) to the nucleus to induce cell proliferation or differentiation. A cell surface receptor with tyrosine kinase activity is first bound by a signaling molecule. This results in the activation of the kinase and phosphorylation of tyrosine residues near the catalytic site. Two cytosolic proteins, GRB2 and a Ras GEF, Sos (Son of Sevenless), bind to the activated receptor. The Sos GEF activates Ras by promoting the exchange of GDP for GTP. Activation of Ras allows it to interact with its downstream effectors. Raf kinase is one of the most well characterized downstream effectors of Ras. When Ras is activated, Raf is recruited to the membrane. Once Raf has been recruited, Ras hydrolyzes its bound GTP, which leads to the activation of Raf and its disassociation from Ras. Raf then binds to and phosphorylates MEK (a MAP kinase kinase), which, in turn, phosphorylates the MAP kinase, ERK. ERK translocates into the nucleus, where it is able to activate transcription factors that regulate the expression of cell proliferation and differentiation proteins (Lodish, Berk, *et al.*, 2000). Another well studied Ras effector is the catalytic domain of

PI3K, which leads to protection of the cell from apoptosis. Through the interaction of Ras with receptors at the cell surface, signaling complexes are assembled very quickly at the origin of the signal, which then, leads to changes in gene expression (Takai, Sasaki, and Matozaki, 2001).

Rho GTPase Proteins

Rho GTPases were first studied in yeast as contributors to the budding process. They were thought to be involved in the process by participating in actin cytoskeletal dynamics (Johnson and Pringle, 1990; Yamochi, Tanaka, *et al.*, 1994). It has since been demonstrated that the Rho GTPases are major contributors to the process of actin restructuring, which leads to cell shape changes, cell adhesion and cell motility (Roy, Kakinuma, and Kiyama, 2009). They are also involved in microtubule dynamics (Wittmann and Waterman-Storer, 2001), gene expression (Coso, Chiariello, *et al.*, 1995; Hill, Wynne, and Treisman, 1995; Perona, Montaner, *et al.*, 1997), and membrane transport (Brown, Marshall, *et al.*, 1984; Komuro, Sasaki, *et al.*, 1996; Lamaze, Chuang, *et al.*, 1996). To date, 18 Rho GTPases have been identified in mammalian cells (Govek, Newey, and Van Aelst, 2005; Schultz, Milpetz, *et al.*, 1998).

Actin rearrangement is triggered by a variety of cell surface receptors in response to environmental cues. However, they all initiate signaling that eventually converges on a group of proteins that are members of the Rho GTPase family: Cdc42, Rac1, and RhoA (Alberts, Johnson, *et al.*, 2008). These three proteins have been studied extensively, and have been found to play unique roles in the restructuring of the actin cytoskeleton (Figure

1.4). Cdc42 has been shown to promote the formation of short microspikes or filipodia, which are long, rod-like protrusions containing bundles of parallel actin fibers in the direction of the protrusion (Hattula, 2007; Kozma, Ahmed, *et al.*, 1995; Nobes and Hall, 1995a; Nobes and Hall, 1999). Rac1 works at the periphery of the cell to regulate the formation of lamellopodia, sheet-like formations at the leading edge of a cell, and membrane ruffles, which are actin-rich, dorsal projections of the cell membrane (Alberts, Johnson, *et al.*, 2008; Ridley, Schwartz, *et al.*, 2003). RhoA is instrumental in the formation of stress fibers from bundles of actin and myosin filaments as well as the formation of integrin-based focal adhesions (Alberts, Johnson, *et al.*, 2008; Nobes and Hall, 1995b).

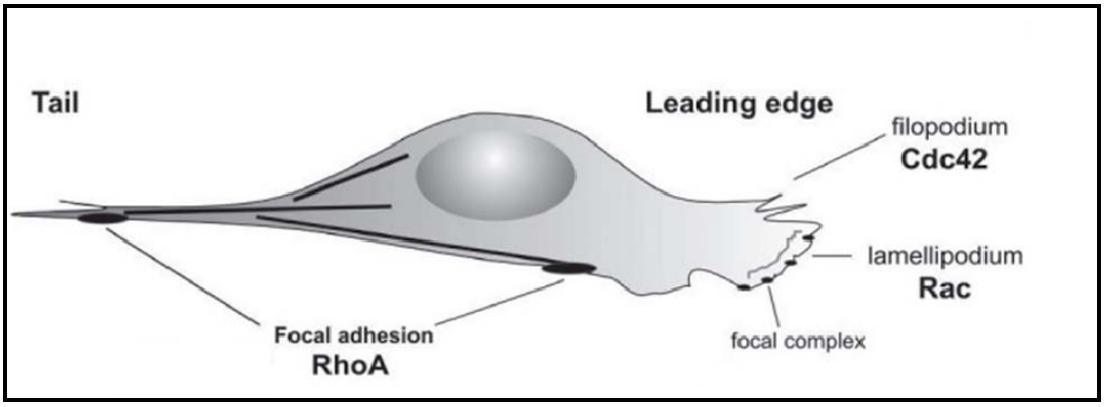

Figure 1.4. Rho GTPases and Actin-Based Cell Structures. Cdc42 functions in the formation of filipodia. Rac functions in the formation of lamellipodia, and RhoA functions in the formation of focal adhesions. Adapted from Hattula (Hattula, 2007)

Rho GTPase activity is regulated by GEFs and GAPs, as well as GDIs (GDP disassociation inhibitors). Rho GDIs bind to the Rho GTPase and hold it in an inactive

state in the cytosol of the cell. In order for the Rho GTPase to be activated by its GEF, it must first be released by the GDI. It is thought that ERM (ezrin/radixin/moesin) proteins may play a role in this release process, but the specifics of the process have not been established (Takahashi, Sasaki, *et al.*, 1997). The role of GDIs in Rho GTPase regulation is extremely important. The spatial and temporal activation of the Rho GTPases can be tightly regulated because of the ability of the GDIs to remove Rho GTPases from membranes and hold them in an inactive state within the cytosol. This is crucial for the proper targeting of the active Rho GTPases within the cell (Hall, 2000; Hattula, 2007).

Rho GTPases have a multitude of downstream effectors. However, the major targets for Rac and Cdc42 are the WASp family proteins, which are responsible for actin remodeling through the activation of the Arp2/3 complex. Rac has been shown to activate SCAR/WAVE through a pentaheteroprotein complex (Caracino, Jones, *et al.*, 2007; Eden, Rohatgi, *et al.*, 2002), and SCAR/WAVE2 through the insulin receptor substrate (IRS) p53 (Miki, Yamaguchi, *et al.*, 2000; Roy, Kakinuma, and Kiyama, 2009; Takenawa and Suetsugu, 2007). However, no evidence of direct activation of a WASp family protein alone by Rac has been found to date (Millard, Sharp, and Machesky, 2004). Cdc42 binds directly to and activates the WASp family proteins, WASp and N-WASp, through their CRIB domains. There is also evidence that demonstrates the ability of WASp family proteins to bind directly to Rho GTPase GEFs and GAPs, suggesting that they may be involved in a regulatory capacity in actin polymerization (Ridley, Schwartz, *et al.*, 2003).

Rab GTPase Proteins

The movement of protein transport vesicles, known as vesicle trafficking, is a highly regulated cellular process. Vesicles bud from their donor membrane compartment, move through the cytoplasm towards their target membrane, dock with their target membrane, and finally, fuse with that membrane (Novick and Zerial, 1997). Rab GTPases are key players in vesicle trafficking events within the eukaryotic cell. With more than 60 known members, the Rab protein group is the largest of the Rho GTPase family proteins (Bock, Matern, *et al.*, 2001; Hattula, 2007; Wang and Thurmond, 2009; Zerial and McBride, 2001). Rab GTPases and their effectors have been implicated in a number of diseases including retinal degeneration, mental retardation, Hermansky-Pudlak syndrome, polycystic kidney disease and Bardet-Beidel syndrome (Hattula, 2007; Nachury, Loktev, *et al.*, 2007; Seabra, Mules, and Hume, 2002).

Rabs, as all Rho family GTPases, function as molecular switches, alternating between a GTP-bound, active state and a GDP-bound, inactive state. It is believed that the rate of switching of the Rab has an effect on the timing of vesicle trafficking and fusion. Several proteins function to coordinate the Rab activation state. These proteins include specific GEFs, GAPs, GDFs and GDIs for each particular Rab. Rabs are distinguishable from other Rho GTPases through five Rab Family (RabF) and four Rab Subfamily (RabSF) conserved domains (Moore, Schell, and Palme, 1995). The sequence homologies of these conserved domains have been examined and used to group most, but not all, of the Rab GTPases into a number of Rab subfamilies (Rab1, Rab3, Rab4, Rab6,

Rab8, Rab11, Rab22, Rab27, Rab40) (Moore, Schell, and Palme, 1995; Pereira-Leal and Seabra, 2000).

Rab GTPases are soluble proteins that are manufactured in the cytosol. All Rab family proteins are post-transcriptionally modified by the addition of geranyl-geranyl lipid modifications to one or two cysteine residues at their C-termini. Most Rab GTPases have –XXCC, -XCXC, or –CCXX C-terminal prenylation sites. (Anant, Desnoyers, *et al.*, 1998; Casey and Seabra, 1996; Stenmark and Olkkonen, 2001). This lipid modification coordinates attachment of the Rab to its target membrane. REPs, or Rab escort proteins, aide in transporting newly formed Rabs to their particular site of action within the cell, and keep the hydrophobic, lipid prenylation group of the Rab soluble within the hydrophilic cytoplasm of the cell (Alexandrov, Horiuchi, *et al.*, 1994; Jordens, Marsman, *et al.*, 2005).

Rab GDIs, which are structurally similar to and more abundant than REPs (Schalk, Zeng, *et al.*, 1996; Ullrich, Stenmark, *et al.*, 1993; Ullrich, Horiuchi, *et al.*, 1994), hold Rabs within the cytosol in their GDP-bound, inactive state and play a role in escorting them back to their original target membrane for reactivation. Once the GDI-bound Rab is returned to its target membrane, it is believed that GDFs, GDI displacement factors, function to release the Rab from its GDI, although the specifics of this release process remain unknown (Soldati, Shapiro, *et al.*, 1994; Ullrich, Horiuchi, *et al.*, 1994). Once released, GEFs, or guanine nucleotide exchange factors, control the release of GDP and the binding of GTP and subsequent reactivation of the Rab. Following activation, the Rab is able to interact with downstream effectors and traffic vesicles to their appropriate

target locations within the cell. Downstream effectors of Rabs include a large number and variety of proteins such as motor complex components, which are responsible for vesicle movement (Hammer and Wu, 2002; Makioka, Kumagai, *et al.*, 2002), cytoskeletal interacting proteins, and proteins responsible for membrane tethering and fusion (Alberts, Johnson, *et al.*, 2008; Hammer and Wu, 2002; Zerial and McBride, 2001). After delivering a vesicle to its target location, the Rab interacts with GAPs, or GTPase activation proteins, which assist the Rab in the hydrolysis of GTP to GDP. The GDP-bound Rab is now inactive. It disassociates with the vesicle, binds to GDIs and is once again recycled back to its original membrane target (Alberts, Johnson, *et al.*, 2008; Hattula, 2007; Lodish, Berk, *et al.*, 2000; Pfeffer, 2005).

Targeted vesicle delivery is a complex process. Vesicles have the potential to come into contact with numerous membranes during their journey to their specific target membrane. In order to avoid mislocalization of vesicles, Rab GTPases and SNARE proteins (soluble N-ethylmaleimide sensitive factor attachment protein receptors) (Nickel and Tannich, 1994) work together to ensure the specificity of vesicle and target membrane interactions. It is believed that the subcellular localization of each Rab is dictated by its particular spatial role in vesicle trafficking (Figure 1.5) (Novick and Zerial, 1997; Nuoffer, Wu, *et al.*, 1997; Olkkonen and Stenmark, 1997; Takai, Sasaki, and Matozaki, 2001). Rabs are primarily responsible for directing the delivery of the vesicle to the proper membrane location, while SNAREs direct the fusion of the vesicle and target membrane lipid bilayers (Alberts, Johnson, *et al.*, 2008). According to the SNARE hypothesis, vesicle and target membranes are associated with SNARE proteins,

known respectively as v-SNAREs and t-SNAREs. Each vesicle has a specific v-SNARE, which selectively interacts with a specific t-SNARE found only on its correct target membrane. This coordinated SNARE system helps to safeguard against fusion of vesicles to incorrect target membranes. Rabs are known to bind directly to SNARE proteins, and are believed to play a role in ensuring the proper interaction between v-SNAREs and t-SNAREs. However, the exact mechanism by which Rabs may play a role in the process is still not known (Hattula, 2007; Seabra, Mules, and Hume, 2002; Sogaard, Tani, *et al.*, 1994; Takai, Sasaki, and Matozaki, 2001; Zerial and Huber, 1995).

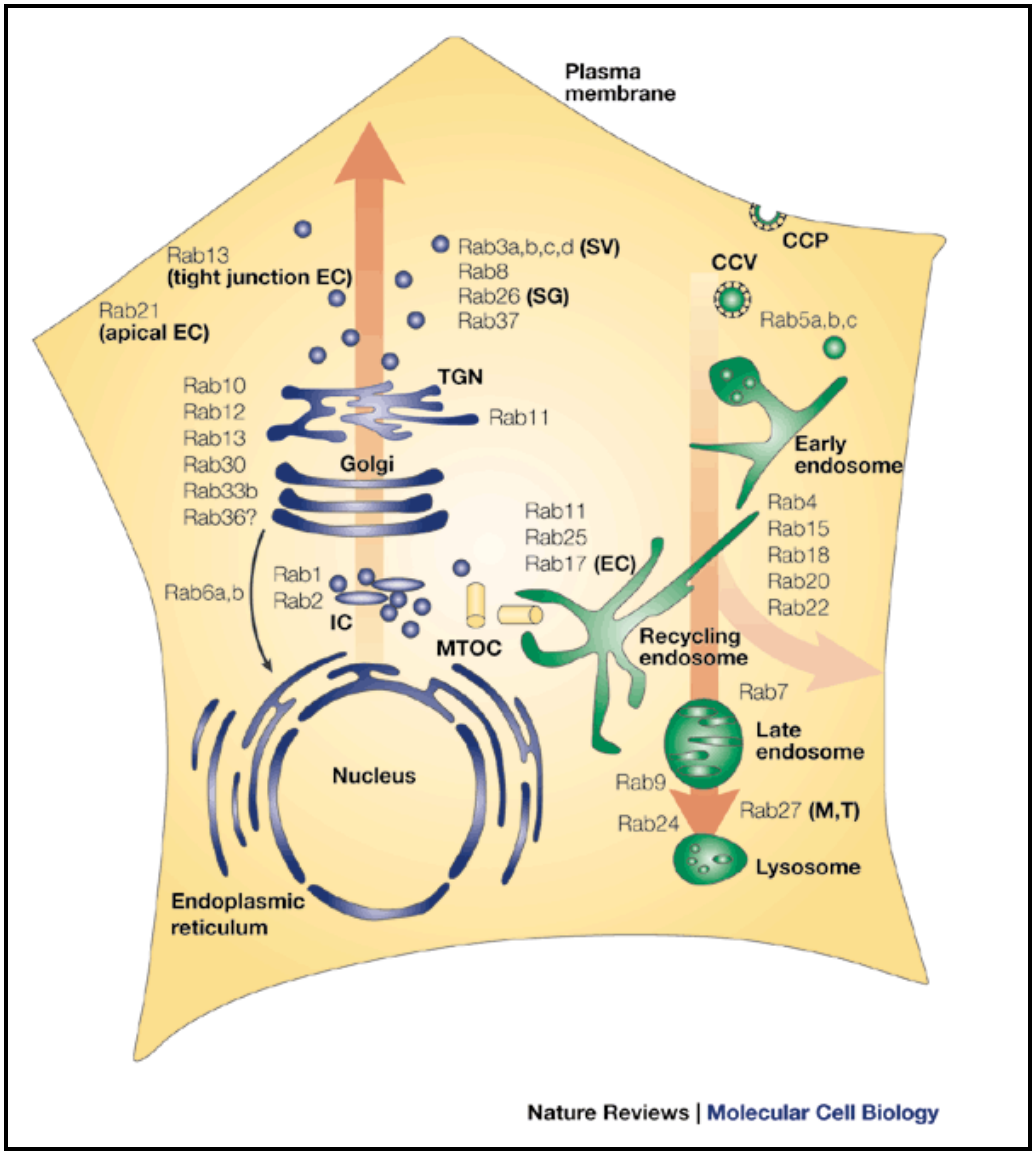

Figure 1.5. Overview of the Rab GTPase Pathways. There are more than 60 members of the Rab GTPase family. Rab GTPases are key regulators of vesicle trafficking events within the cell. Taken from Zerial and McBride (Zerial and McBride, 2001).

Rab8

Rab8 is a Rab GTPase that has been shown to play a role in vesicle trafficking and membrane recycling in mammalian cells. Most Rab GTPases have –XXCC, -XCXC, or –CCXX C-terminal prenylation sites. Therefore, most Rabs have two geranyl-geranyl lipid modifications. Rab8, however, has a –CAAL C-terminal prenylation site and a single geranyl-geranyl lipid modification (Casey and Seabra, 1996; Wilson, Erdman, *et al.*, 1998).

There are two Rab8 proteins in mammalian cells, Rab8a and Rab8b. The two proteins share a high degree of homology, but their expression patterns vary among different cell types. Rab8a is widely expressed in all cells, with the highest expression levels in the kidney, lungs and muscle. Rab8b is primarily expressed in the brain, testis and spleen. The two proteins differ only slightly at their C-termini, and no significant differences in their function have been ascertained (Armstrong, Thompson, *et al.*, 1996). When co-expressed in HeLa cells, Rab8a and Rab8b colocalized to vesicles indicating a shared trafficking pathway, and both proteins cause changes in actin distribution and cell morphology when constitutively activated or inactivated (Peranen and Furuhjelm, 2001). Rab8-like proteins with high levels of homology to mammalian Rab8 have been identified in *Saccharomyces cerevisiae* (Sec4), *Schizosaccharomyces pombe* (Ypt2p) and *D. discoideum* (Sas1 and Sas2) (Craighead, Bowden, *et al.*, 1993; Huber, Pimplikar, *et al.*, 1993; Saxe and Kimmel, 1990).

During a search for Rab proteins involved in polarized vesicle trafficking in MDCK (Madin Darby Canine Kidney) epithelial cells, Rab8 was identified as a vesicle

trafficking protein involved in the pathway from the trans-Golgi to the basolateral surface (Goud, Salminen, *et al.*, 1988; Huber, Pimplikar, *et al.*, 1993). It was also shown to be involved in the transport of vesicles from the trans-Golgi to nerve cell dendrites (Huber, Pimplikar, *et al.*, 1993). Later studies demonstrated that Rab8 had very little effect on the transport kinetics of the vesicle trafficking pathway from the trans-Golgi to the plasma membrane, suggesting that Rab8 might not be the primary trafficking protein in this pathway (Chen, Feng, *et al.*, 1998; Peranen, Auvinen, *et al.*, 1996). However, the importance of Rab8 in the transport of newly synthesized proteins from the trans-Golgi to the plasma membrane was substantiated by the findings of several further studies, which utilized constitutively active and dominant negative versions of Rab8. It was shown that the active form, but not the inactive form, of Rab8 led to missorting of VSV-G vesicles to the apical surface of polarized MDCK cells. Results of this study also suggested that Rab8 directed traffic may also involve recycling endosomes as an intermediate (Sato, Mushiake, *et al.*, 2007; Ang, Folsch, *et al.*, 2003). Linder *et al.* provided further evidence of this by demonstrating that Rab8 could rescue cholesterol removal in NPC (Niemann-Pick type C disease) cells, which are normally unable to traffic low-density lipoprotein effectively, suggesting that Rab8 may aide in directing cholesterol to recycling endosomes for trafficking to the plasma membrane (Linder, Uronen, *et al.*, 2007). A new twist in the story of Rab8 was recently added by Sato *et al.* All of the previous studies of Rab8 had been carried out *in vitro*; however, Sato *et al.* developed a conditional Rab8 knockout mouse line for *in vivo* studies. They showed that Rab8 was responsible for vesicle trafficking to the apical, not the basolateral, surface. In addition, they showed that

the test mice had defects in the structure of their intestinal microvilli and demonstrated symptoms similar to humans with microvillus inclusion disease (Sato, Mushiake, *et al.*, 2007). Therefore, although Rab8 seems to play a role in polarized vesicle transport, the exact location of Rab8 in this process is still unclear.

A role for Rab8 in the development of photoreceptors through polarized vesicle transport has been emerging over the past few years. Post-Golgi membranes isolated from *Xenopus*, which contained the photoreceptor, rhodopsin, were shown to be associated with Rab6 and Rab8 (Deretic, Huber, *et al.*, 1995). The involvement of Rab8 in trafficking rhodopsin from the trans-Golgi to the plasma membrane was subsequently confirmed when it was demonstrated that Rab8 mutations caused impairment of docking and fusion of rhodopsin vesicles to the plasma membrane (Moritz, Tam, *et al.*, 2001). Rab8 was also found to be associated with the transport of rhodopsin transport carriers (RTPs) from the trans-Golgi to the plasma membrane in frog photoreceptors (Deretic, Traverso, *et al.*, 2004). The investigation of the role of Rab8 in *Xenopus* photoreceptors showed that a dominant negative mutant version of Rab8 led to rhodopsin vesicle accumulation and cell death. Thus, by inhibiting vesicle trafficking via the connecting cilium in photoreceptors, Rab 8 may lead to retinal degeneration (Moritz, Tam, *et al.*, 2001). Additionally, optineurin was identified as a Rab8 effector, and was shown to lead to primary open-angle glaucoma when mutated (Rezaie, Child, *et al.*, 2002).

Most recently, Rab8 has been the focus of studies involving the primary cilium of mammalian cells. The primary cilium is a hairlike organelle with motile and sensory functions. A group of diseases known as ciliopathies are caused by dysfunction of the

primary cilium and include Bardet-Biedl syndrome (BBS), which is characterized by obesity, retinal degeneration, and polycystic kidney disorder (Leroux, 2007). The cilium organization depends on a complex of 12 proteins known as the BBSome and directed trafficking of vesicles into the structure. In 2007, Nachury *et al.* demonstrated a functional interaction between BBSome complex proteins and Rab8. This interaction is through the direct association of Rabin8, a Rab8 GEF, and one of the BBSome complex proteins, BBS1. Rabin8 helps recruit the BBSome to the base of the primary cilium, and participates in the activation of Rab8, which then, helps promote vesicle docking and fusion at the membrane of the primary cilium (Nachury, Loktev, *et al.*, 2007).

While it has been established that Rab8 plays a role in polarized vesicle trafficking, later studies demonstrate an intriguing "moonlighting" capability of Rab8. The small GTPase has the ability to effect changes in the cytoskeletal elements, actin filaments and microtubules. When Peranen *et al.* expressed constitutively activate Rab8 in BHK (Baby Hamster Kidney) cells, it caused dramatic changes in cell morphology. Cells expressing constitutively activate Rab8 developed long, actin-rich protrusions similar to neuronal dendritic extensions (Peranen, Auvinen, *et al.*, 1996). Chen *et al.* also showed that constitutively active Rab8 localized to actin-rich membrane ruffles in CHO (Chinese Hamster Ovary) cells (Chen, Holcomb, and Moore, 1993). This role for Rab8 appears to be evolutionarily conserved, as Powell and Temesvari demonstrated that constitutively active Rab8 expression led to the appearance of polarized actin caps and an increase in filipodia in the social amoebae, *D. discoideum* (Powell and Temesvari, 2004). However, to date, it is still unknown how Rab8 effects changes in the actin cytoskeleton.

Rab8 Interacting Proteins

To date, very few proteins have been shown to interact with Rab8. The proteins that have been identified include Rab8ip, Trip8b, Mss4, FIP-2, Rabin8, JFC1, AS160 and JRAB/MICAL-L2. Rab8ip is a GCK-like (germinal center kinase) protein that interacts only with GTP-bound Rab8. GCK is a kinase that is implicated in the stress response (Ren, Zeng, *et al.*, 1996). FIP-2, like Rab8ip, only interacts with the GTP-bound form of Rab8. FIP-2, also known as optineurin (Rezaie, Child, *et al.*, 2002), is induced by TNF-α, and is related to the NEMO protein. It provides a link between activated Rab8 and huntingtin, a membrane protein, which is implicated in Huntington's disease (Hattula and Peranen, 2000; Hattula, Furuhjelm, *et al.*, 2002).

JRAB/MICAL-L2 interacts directly with the GTP-bound form of Rab8 and the GTP-bound form of Rab13. This is a unique type of Rab effector, as most are very specific with regards to Rab binding. It interacts with active Rab8 at the perinuclear recycling compartment and with active Rab13 at the plasma membrane. The Rab8-JRAB/MICAL-L2 complex and the Rab13-JRAB/MICAL-L2 complex appear to play a role in the formation of adherens junctions and tight junctions by regulating Rab8-dependent E-cadherin transport and Rab13-dependent claudins/occludin transport (Yamamura, Nishimura, *et al.*, 2008). Another Rab8 effector protein, JFC1, was also shown to bind to another Rab, Rab27a. Like JRAB/MICAL-L2, JFC1 only interacts with active Rab8. In the case of JFC1, Rab8 is coupled with Rab27a in the actin-based movement of melanosomes (Chabrillat, Wilhelm, *et al.*, 2005; Fukuda, Kuroda, and Mikoshiba, 2002).

Trip8b is able to interact with Rab8, whether it is bound to GDP or GTP. It is a membrane bound protein that can interact with Rab8 even if it is not prenylated (Chen, Liang, *et al.*, 2001). Mss4, which is a zinc binding protein, has the ability to bind to several Rabs. While it has the ability to aide in disassociation of GDP from Rabs (Horiuchi, Lippe, *et al.*, 1997), it is not considered a true GEF because does not participate in the binding of GTP (Nuoffer, Wu, *et al.*, 1997). Hattula *et al.* have identified a Rab8-specific GEF, Rabin8. This GEF ties Rab8 to vesicle trafficking to the primary cilium in mammalian cells (Hattula, Furuhjelm, *et al.*, 2002; Hattula and Peranen, 2005). The first Rab8 GAP, AS160 (Akt substrates of 160 kDa) was identified by Miinea *et al.* AS160 also functions as a GAP for Rabs 2A, 10 and 14 (Miinea, Sano, *et al.*, 2005).

Dictyostelium discoideum Rab8

Two Rab8 homologues have been identified in the social amoebae, *Dictyostelium discoideum*. The two Rab8-like proteins, originally referred to as Sas1 and Sas2, are now referred to as Rab8 and Rab8b, and share 90% sequence identity, with differences primarily at their C-termini (Saxe and Kimmel, 1990), which is reminiscent of mammalian Rab8a and Rab8b (Peranen and Furuhjelm, 2001). The proteins are expressed at low to moderate levels during the vegetative stage and early development. However, their expression levels increase following aggregation. Rab8 is expressed at higher levels than Rab8b throughout the vegetative stage and early development. The expression of Rab8 is highest at approximately 15 hours of development, after which, the

Rab8 expression levels drop. Rab8b expression levels begin to increase after 15 hours of development as Rab8 levels begin to decrease. This suggests that each protein may play a specific role at varying stages of development (Saxe and Kimmel, 1990).

In studies conducted by Powell and Temesvari, the constitutively active and dominant negative versions of Rab8 and Rab8b were examined for their function in *D. discoideum*. Interestingly, the overexpression of the active form of Rab8 led to the formation of actin-rich membrane extensions, inhibition of aggregation, reduction in the level of the calcium-dependent early adhesion molecule, gp24, increase in the extracellular levels of countin, a subunit of cell-counting factor, which helps regulate aggregate size, and oversecretion of acid phosphatase under starvation conditions. The same results were not seen in Rab8b or in wildtype and dominant negative forms of Rab8. Cells expressing dominant negative Rab8 did demonstrate enhanced aggregation and an increase in gp24 levels. Rab8b mutations did not adversely affect early development (Powell and Temesvari, 2004). As with mammalian Rab8, *D. discoideum* Rab8 seems to be involved in the formation of actin-rich protrusions in addition to the trafficking of calcium-dependent adherence proteins important for adherens junctions. The study of Rab8 seems to indicate that the “moonlighting” role of Rab8 in actin remodeling, as well as the traditional role of Rab8 in vesicle trafficking, may be evolutionarily conserved.

Summary

The small GTPase, Rab8, is involved in vesicle trafficking and cell-cell adhesion, but also unexpectedly "moonlights" as an actin cytoskeleton regulator. Recently, Rab8 has been linked to the human genetic diseases, microvillus inclusion disease and Bardet-Biedl syndrome (BBS), which both involve malformation of actin based structures (Hattula, 2007; Leroux, 2007; Nachury, Loktev, *et al.*, 2007; Seabra, Mules, and Hume, 2002). Rab8 was first identified in melanoma cells and is homologous to the *mel* transforming oncogene (Nimmo, Sanders, *et al.*, 1991), suggesting its role in malignant tumor formation. In this study, we have utilized the model eukaryote, *Dictyostelium discoideum*, to attempt to elucidate the pathway by which Rab8 can elicit changes in the actin cytoskeleton. In addition, we have designed a Rab8 activation assay for use in mammalian cell studies of the small GTPase. Specific objectives include:

1. Determining the interaction of Rab8 and the WASp family protein, SCAR, in *D. discoideum.*
2. Determining the interaction of Rab8 and the Rac GTPase, RacF2, in *D. discoideum*.
3. Generating EGFP (enhanced green fluorescent protein) chimeras of constitutively active or dominant negative mutant forms of Rab8 for expression in mammalian cells.
4. Generation of a Rab8 activation assay for use in mammalian system studies.

This is the first report of a functional interaction between Rab8 and a WASp family protein, SCAR, in any cell system.

References

Alberts, B., Johnson, A., Lewis, J., Raff, M., Roberts, K., and Walter, P. (2008). *Molecular Biology of the Cell*. (New York, Garland Science, Taylor & Francis Group, LLC).

Alexandrov, K., Horiuchi, H., Steele-Mortimer, O., Seabra, M.C., and Zerial, M. (1994). Rab escort protein-1 is a multifunctional protein that accompanies newly prenylated rab proteins to their target membranes. *EMBO J. 13*, 5262-5273.

Anant, J.S., Desnoyers, L., Machius, M., Demeler, B., Hansen, J.C., Westover, K.D., Deisenhofer, J., and Seabra, M.C. (1998). Mechanism of Rab geranylgeranylation: formation of the catalytic ternary complex. *Biochemistry 37*, 12559-12568.

Ang, A.L., Folsch, H., Koivisto, U.M., Pypaert, M., and Mellman, I. (2003). The Rab8 GTPase selectively regulates AP-1B-dependent basolateral transport in polarized Madin-Darby canine kidney cells. *J. Cell Biol. 163*, 339-350.

Armstrong, J., Thompson, N., Squire, J.H., Smith, J., Hayes, B., and Solari, R. (1996). Identification of a novel member of the Rab8 family from the rat basophilic leukaemia cell line, RBL.2H3. *J. Cell. Sci. 109 (Pt 6)*, 1265-1274.

Aspenstrom, P., Lindberg, U., and Hall, A. (1996). Two GTPases, Cdc42 and Rac, bind directly to a protein implicated in the immunodeficiency disorder Wiskott-Aldrich syndrome. *Curr. Biol. 6*, 70-75.

Barbacid, M. (1987). Ras Genes. *Annu. Rev. Biochem. 56*, 779-827.

Bar-Sagi, D., and Feramisco, J.R. (1985). Microinjection of the ras oncogene protein into PC12 cells induces morphological differentiation. *Cell 42*, 841-848.

Bear, J.E., Rawls, J.F., and Saxe, C.L.,3rd. (1998). SCAR, a WASP-related protein, isolated as a suppressor of receptor defects in late *Dictyostelium* development. *J. Cell Biol. 142*, 1325-1335.

Ben-Yaacov, S., Le Borgne, R., Abramson, I., Schweisguth, F., and Schejter, E.D. (2001). Wasp, the Drosophila Wiskott-Aldrich syndrome gene homologue, is required for cell fate decisions mediated by Notch signaling. *J. Cell Biol. 152*, 1-13.

Blagg, S.L., and Insall, R.H. (2004). Control of SCAR activity in *Dictyostelium discoideum*. *Biochem. Soc. Trans. 32*, 1113-1114.

Blagg, S.L., Stewart, M., Sambles, C., and Insall, R.H. (2003). PIR121 regulates pseudopod dynamics and SCAR activity in *Dictyostelium*. *Curr. Biol. 13*, 1480-1487.

Bock, J.B., Matern, H.T., Peden, A.A., and Scheller, R.H. (2001). A genomic perspective on membrane compartment organization. *Nature 409,* 839-841.

Bos, J.L. (1989). Ras Oncogenes in Human Cancer: a Review. Cancer Res. *49,* 4682-4689.

Bourne, H.R., Sanders, D.A., and McCormick, F. (1991). The GTPase superfamily: conserved structure and molecular mechanism. *Nature 349,* 117-127.

Brown, R., Marshall, C.J., Pennie, S.G., and Hall, A. (1984). Mechanism of activation of an N-ras gene in the human fibrosarcoma cell line HT1080. *EMBO J. 3,* 1321-1326.

Capon, D.J., Seeburg, P.H., McGrath, J.P., Hayflick, J.S., Edman, U., Levinson, A.D., and Goeddel, D.V. (1983). Activation of Ki-ras2 gene in human colon and lung carcinomas by two different point mutations. *Nature 304,* 507-513.

Caracino, D., Jones, C., Compton, M., and Saxe, C.L.,3rd. (2007). The N-terminus of *Dictyostelium* Scar interacts with Abi and HSPC300 and is essential for proper regulation and function. *Mol. Biol. Cell 18,* 1609-1620.

Carlier, M.F. (1998). Control of actin dynamics. *Curr. Opin. Cell Biol. 10,* 45-51.

Casey, P.J., and Seabra, M.C. (1996). Protein prenyltransferases. *J. Biol. Chem. 271,* 5289-5292.

Chabrillat, M.L., Wilhelm, C., Wasmeier, C., Sviderskaya, E.V., Louvard, D., and Coudrier, E. (2005). Rab8 regulates the actin-based movement of melanosomes. *Mol. Biol. Cell 16,* 1640-1650.

Chan, A.Y., Bailly, M., Zebda, N., Segall, J.E., and Condeelis, J.S. (2000). Role of cofilin in epidermal growth factor-stimulated actin polymerization and lamellipod protrusion. *J. Cell Biol. 148,* 531-542.

Chen, L., Iijima, M., Tang, M., Landree, M.A., Huang, Y.E., Xiong, Y., Iglesias, P.A., and Devreotes, P.N. (2007). PLA2 and PI3K/PTEN pathways act in parallel to mediate chemotaxis. *Dev. Cell. 12,* 603-614.

Chen, S., Liang, M.C., Chia, J.N., Ngsee, J.K., and Ting, A.E. (2001). Rab8b and its interacting partner TRIP8b are involved in regulated secretion in AtT20 cells. *J. Biol. Chem. 276,* 13209-13216.

Chen, W., Feng, Y., Chen, D., and Wandinger-Ness, A. (1998). Rab11 is required for trans-golgi network-to-plasma membrane transport and a preferential target for GDP dissociation inhibitor. *Mol. Biol. Cell 9,* 3241-3257.

Chen, Y.T., Holcomb, C., and Moore, H.P. (1993). Expression and localization of two low molecular weight GTP-binding proteins, Rab8 and Rab10, by epitope tag. *Proc. Natl. Acad. Sci. U. S. A. 90*, 6508-6512.

Choy, E., Chiu, V.K., Silletti, J., Feoktistov, M., Morimoto, T., Michaelson, D., Ivanov, I.E., and Philips, M.R. (1999). Endomembrane trafficking of ras: the CAAX motif targets proteins to the ER and Golgi. *Cell 98,* 69-80.

Condeelis, J. (1993). Life at the leading edge: the formation of cell protrusions. *Annu. Rev. Cell Biol. 9,* 411-444.

Coso, O.A., Chiariello, M., Yu, J.C., Teramoto, H., Crespo, P., Xu, N., Miki, T., and Gutkind, J.S. (1995). The small GTP-binding proteins Rac1 and Cdc42 regulate the activity of the JNK/SAPK signaling pathway. *Cell 81,* 1137-1146.

Craighead, M.W., Bowden, S., Watson, R., and Armstrong, J. (1993). Function of the ypt2 gene in the exocytic pathway of *Schizosaccharomyces pombe*. Mol. Biol. *Cell 4,* 1069-1076.

Deretic, D., Huber, L.A., Ransom, N., Mancini, M., Simons, K., and Papermaster, D.S. (1995). Rab8 in Retinal Photoreceptors may Participate in Rhodopsin Transport and in Rod Outer Segment Disk Morphogenesis. *J. Cell. Sci. 108 (Pt 1),* 215-224.

Deretic, D., Traverso, V., Parkins, N., Jackson, F., Rodriguez de Turco, E.B., and Ransom, N. (2004). Phosphoinositides, ezrin/moesin, and rac1 regulate fusion of rhodopsin transport carriers in retinal photoreceptors. *Mol. Biol. Cell 15*, 359-370.

Derry, J.M., Ochs, H.D., and Francke, U. (1994). Isolation of a novel gene mutated in Wiskott-Aldrich syndrome. *Cell 78,* 635-644.

Dormann, D., and Weijer, C.J. (2006). Visualizing signaling and cell movement during the multicellular stages of *Dictyostelium* development. *Methods Mol. Biol. 346,* 297-309.

Dormann, D., Weijer, G., Dowler, S., and Weijer, C.J. (2004). In vivo analysis of 3-phosphoinositide dynamics during *Dictyostelium* phagocytosis and chemotaxis. *J. Cell. Sci. 117,* 6497-6509.

Eden, S., Rohatgi, R., Podtelejnikov, A.V., Mann, M., and Kirschner, M.W. (2002). Mechanism of regulation of WAVE1-induced actin nucleation by Rac1 and Nck. *Nature 418,* 790-793.

Eichinger, L., and Rivero, F. (2006). *Dictyostelium discoideum Protocols.* (Totowa, Humana Press).

Eichinger, L., and Noegel, A.A. (2003). Crawling into a new era-the *Dictyostelium* genome project. *EMBO J. 22*, 1941-1946.

Feramisco, J.R., Gross, M., Kamata, T., Rosenberg, M., and Sweet, R.W. (1984). Microinjection of the oncogene form of the human H-ras (T-24) protein results in rapid proliferation of quiescent cells. *Cell 38*, 109-117.

Fuchs, E., and Yang, Y. (1999). Crossroads on cytoskeletal highways. *Cell 98*, 547-550.

Fukuda, M., Kuroda, T.S., and Mikoshiba, K. (2002). Slac2-a/melanophilin, the missing link between Rab27 and myosin Va: implications of a tripartite protein complex for melanosome transport. *J. Biol. Chem. 277*, 12432-12436.

Gilbert, S.F. (2003). *Developmental Biology* (Sunderland, Massachusetts: Sinauer Associates, Inc.).

Ginsburg, G.T., and Kimmel, A.R. (1997). Autonomous and nonautonomous regulation of axis formation by antagonistic signaling via 7-span cAMP receptors and GSK3 in *Dictyostelium*. *Genes Dev. 11*, 2112-2123.

Goley, E.D., and Welch, M.D. (2006). The ARP2/3 complex: an actin nucleator comes of age. *Nat. Rev. Mol. Cell Biol. 7*, 713-726.

Goud, B., Salminen, A., Walworth, N.C., and Novick, P.J. (1988). A GTP-binding protein required for secretion rapidly associates with secretory vesicles and the plasma membrane in yeast. *Cell 53*, 753-768.

Govek, E.E., Newey, S.E., and Van Aelst, L. (2005). The role of the Rho GTPases in neuronal development. *Genes Dev. 19*, 1-49.

Hall, A. (2000). *GTPases.* (Oxford: Oxford University Press).

Hammer, J.A.,3rd, and Wu, X.S. (2002). Rabs grab motors: defining the connections between Rab GTPases and motor proteins. *Curr. Opin. Cell Biol. 14*, 69-75.

Hattula, K. (2007). *Rab8 and Rab8-interacting proteins as players in cell polarization.*

Hattula, K., Furuhjelm, J., Arffman, A., and Peranen, J. (2002). A Rab8-specific GDP/GTP exchange factor is involved in actin remodeling and polarized membrane transport. *Mol. Biol. Cell 13*, 3268-3280.

Hattula, K., and Peranen, J. (2005). Purification and functional properties of a Rab8-specific GEF (Rabin3) in action remodeling and polarized transport. *Methods Enzymol. 403*, 284-295.

Hattula, K., and Peranen, J. (2000). FIP-2, a coiled-coil protein, links Huntingtin to Rab8 and modulates cellular morphogenesis. *Curr. Biol. 10,* 1603-1606.

Hill, C.S., Wynne, J., and Treisman, R. (1995). The Rho family GTPases RhoA, Rac1, and CDC42Hs regulate transcriptional activation by SRF. *Cell 81,* 1159-1170.

Ho, H.Y., Rohatgi, R., Lebensohn, A.M., Le, M., Li, J., Gygi, S.P., and Kirschner, M.W. (2004). Toca-1 mediates Cdc42-dependent actin nucleation by activating the N-WASP-WIP complex. *Cell 118,* 203-216.

Horiuchi, H., Lippe, R., McBride, H.M., Rubino, M., Woodman, P., Stenmark, H., Rybin, V., Wilm, M., Ashman, K., Mann, M., and Zerial, M. (1997). A novel Rab5 GDP/GTP exchange factor complexed to Rabaptin-5 links nucleotide exchange to effector recruitment and function. *Cell 90,* 1149-1159.

Hu, B., Shi, B., Jarzynka, M.J., Yiin, J.J., D'Souza-Schorey, C., and Cheng, S.Y. (2009). ADP-ribosylation factor 6 regulates glioma cell invasion through the IQ-domain GTPase-activating protein 1-Rac1-mediated pathway. *Cancer Res. 69,* 794-801.

Huber, L.A., Pimplikar, S., Parton, R.G., Virta, H., Zerial, M., and Simons, K. (1993). Rab8, a small GTPase involved in vesicular traffic between the TGN and the basolateral plasma membrane. *J. Cell Biol. 123,* 35-45.

Ichetovkin, I., Grant, W., and Condeelis, J. (2002). Cofilin produces newly polymerized actin filaments that are preferred for dendritic nucleation by the Arp2/3 complex. *Curr. Biol. 12,* 79-84.

Insall, R., Muller-Taubenberger, A., Machesky, L., Kohler, J., Simmeth, E., Atkinson, S.J., Weber, I., and Gerisch, G. (2001). Dynamics of the *Dictyostelium* Arp2/3 complex in endocytosis, cytokinesis, and chemotaxis. Cell Motil. *Cytoskeleton 50,* 115-128.

Iqbal, K., Liu, F., Gong, C.X., Alonso, A.D., and Grundke-Iqbal, I. (2009). Mechanisms of tau-induced neurodegeneration. *Acta Neuropathol.*

Johnson, D.I., and Pringle, J.R. (1990). Molecular characterization of CDC42, a *Saccharomyces cerevisiae* gene involved in the development of cell polarity. *J. Cell Biol. 111,* 143-152.

Johnson, R.L., Van Haastert, P.J., Kimmel, A.R., Saxe, C.L.,3rd, Jastorff, B., and Devreotes, P.N. (1992). The cyclic nucleotide specificity of three cAMP receptors in *Dictyostelium*. *J. Biol. Chem. 267,* 4600-4607.

Jordens, I., Marsman, M., Kuijl, C., and Neefjes, J. (2005). Rab proteins, connecting transport and vesicle fusion. *Traffic 6,* 1070-1077.

Kauffmann-Zeh, A., Rodriguez-Viciana, P., Ulrich, E., Gilbert, C., Coffer, P., Downward, J., and Evan, G. (1997). Suppression of c-Myc-induced apoptosis by Ras signalling through PI(3)K and PKB. *Nature 385,* 544-548.

Keizer-Gunnink, I., Kortholt, A., and Van Haastert, P.J. (2007). Chemoattractants and chemorepellents act by inducing opposite polarity in phospholipase C and PI3-kinase signaling. *J. Cell Biol. 177,* 579-585.

Klein, P.S., Sun, T.J., Saxe, C.L.,3rd, Kimmel, A.R., Johnson, R.L., and Devreotes, P.N. (1988). A chemoattractant receptor controls development in *Dictyostelium discoideum*. *Science 241,* 1467-1472.

Komuro, R., Sasaki, T., Takaishi, K., Orita, S., and Takai, Y. (1996). Involvement of Rho and Rac small G proteins and Rho GDI in Ca2+-dependent exocytosis from PC12 cells. *Genes Cells 1,* 943-951.

Kozma, R., Ahmed, S., Best, A., and Lim, L. (1995). The Ras-related protein Cdc42Hs and bradykinin promote formation of peripheral actin microspikes and filopodia in Swiss 3T3 fibroblasts. *Mol. Cell. Biol. 15,* 1942-1952.

Kriebel, P.W., Barr, V.A., Rericha, E.C., Zhang, G., and Parent, C.A. (2008). Collective cell migration requires vesicular trafficking for chemoattractant delivery at the trailing edge. *J. Cell Biol. 183,* 949-961.

Lamaze, C., Chuang, T.H., Terlecky, L.J., Bokoch, G.M., and Schmid, S.L. (1996). Regulation of receptor-mediated endocytosis by Rho and Rac. *Nature 382,* 177-179.

Legg, J.A., Bompard, G., Dawson, J., Morris, H.L., Andrew, N., Cooper, L., Johnston, S.A., Tramountanis, G., and Machesky, L.M. (2007). N-WASP involvement in dorsal ruffle formation in mouse embryonic fibroblasts. *Mol. Biol. Cell 18,* 678-687.

Leroux, M.R. (2007). Taking vesicular transport to the cilium. *Cell 129,* 1041-1043.

Linder, M.D., Uronen, R.L., Holtta-Vuori, M., van der Sluijs, P., Peranen, J., and Ikonen, E. (2007). Rab8-dependent recycling promotes endosomal cholesterol removal in normal and sphingolipidosis cells. Mol. Biol. *Cell 18,* 47-56.

Lodish, H., Berk, A., Zipursky, S.L., Matsudaira, P., Baltimore, D., and Darnell, J. (2000). *Molecular Cell Biology* (New York, W. H. Freeman and Company).

Loomis, W.F. (1975). *Dictyostelium discoideum: a Developmental System.* (New York: Academic Press).

Loovers, H.M., Postma, M., Keizer-Gunnink, I., Huang, Y.E., Devreotes, P.N., and van Haastert, P.J. (2006). Distinct roles of PI(3,4,5)P3 during chemoattractant signaling in *Dictyostelium*: a quantitative in vivo analysis by inhibition of PI3-kinase. *Mol. Biol. Cell 17,* 1503-1513.

Louis, J.M., Ginsburg, G.T., and Kimmel, A.R. (1994). The cAMP receptor CAR4 regulates axial patterning and cellular differentiation during late development of *Dictyostelium*. *Genes Dev. 8,* 2086-2096.

Machesky, L.M., and Insall, R.H. (1998). Scar1 and the related Wiskott-Aldrich syndrome protein, WASP, regulate the actin cytoskeleton through the Arp2/3 complex. *Curr. Biol. 8,* 1347-1356.

Makioka, A., Kumagai, M., Ohtomo, H., Kobayashi, S., and Takeuchi, T. (2002). Effect of proteasome inhibitors on the growth, encystation, and excystation of *Entamoeba histolytica* and *Entamoeba invadens*. *Parasitol. Res. 88,* 454-459.

May, R.C., Caron, E., Hall, A., and Machesky, L.M. (2000). Involvement of the Arp2/3 complex in phagocytosis mediated by Fc gammaR or CR3. *Nat. Cell Biol. 2,* 246-248.

McKay, I.A., Paterson, H., Brown, R., Toksoz, D., Marshall, C.J., and Hall, A. (1986). N-ras and human cancer. *Anticancer Res. 6,* 483-490.

Miinea, C.P., Sano, H., Kane, S., Sano, E., Fukuda, M., Peranen, J., Lane, W.S., and Lienhard, G.E. (2005). AS160, the Akt substrate regulating GLUT4 translocation, has a functional Rab GTPase-activating protein domain. *Biochem. J. 391,* 87-93.

Miki, H., Miura, K., and Takenawa, T. (1996). N-WASP, a novel actin-depolymerizing protein, regulates the cortical cytoskeletal rearrangement in a PIP2-dependent manner downstream of tyrosine kinases. *EMBO J. 15,* 5326-5335.

Miki, H., Sasaki, T., Takai, Y., and Takenawa, T. (1998). Induction of filopodium formation by a WASP-related actin-depolymerizing protein N-WASP. *Nature 391,* 93-96.

Miki, H., Suetsugu, S., and Takenawa, T. (1998). WAVE, a novel WASP-family protein involved in actin reorganization induced by Rac. *EMBO J. 17,* 6932-6941.

Miki, H., and Takenawa, T. (2002). WAVE2 serves a functional partner of IRSp53 by regulating its interaction with Rac. *Biochem. Biophys. Res. Commun. 293,* 93-99.

Miki, H., Yamaguchi, H., Suetsugu, S., and Takenawa, T. (2000). IRSp53 is an essential intermediate between Rac and WAVE in the regulation of membrane ruffling. *Nature 408,* 732-735.

Millard, T.H., Sharp, S.J., and Machesky, L.M. (2004). Signalling to actin assembly via the WASP (Wiskott-Aldrich syndrome protein)-family proteins and the Arp2/3 complex. *Biochem. J. 380,* 1-17.

Moore, I., Schell, J., and Palme, K. (1995). Subclass-specific sequence motifs identified in Rab GTPases. *Trends Biochem. Sci. 20,* 10-12.

Moore, M.S. (1998). Ran and nuclear transport. *J. Biol. Chem. 273,* 22857-22860.

Moore, M.S., and Blobel, G. (1993). The GTP-binding protein Ran/TC4 is required for protein import into the nucleus. *Nature 365,* 661-663.

Moritz, O.L., Tam, B.M., Hurd, L.L., Peranen, J., Deretic, D., and Papermaster, D.S. (2001). Mutant rab8 Impairs docking and fusion of rhodopsin-bearing post-Golgi membranes and causes cell death of transgenic *Xenopus* rods. *Mol. Biol. Cell 12,* 2341-2351.

Myers, S.A., Han, J.W., Lee, Y., Firtel, R.A., and Chung, C.Y. (2005). A *Dictyostelium* homologue of WASP is required for polarized F-actin assembly during chemotaxis. *Mol. Biol. Cell 16,* 2191-2206.

Nachury, M.V., Loktev, A.V., Zhang, Q., Westlake, C.J., Peranen, J., Merdes, A., Slusarski, D.C., Scheller, R.H., Bazan, J.F., Sheffield, V.C., and Jackson, P.K. (2007). A core complex of BBS proteins cooperates with the GTPase Rab8 to promote ciliary membrane biogenesis. *Cell 129,* 1201-1213.

Nakano, A., and Muramatsu, M. (1989). A novel GTP-binding protein, Sar1p, is involved in transport from the endoplasmic reticulum to the Golgi apparatus. *J. Cell Biol. 109,* 2677-2691.

Nefsky, B., and Bretscher, A. (1992). Yeast actin is relatively well behaved. *Eur. J. Biochem. 206,* 949-955.

Nickel, R., and Tannich, E. (1994). Transfection and transient expression of chloramphenicol acetyltransferase gene in the protozoan parasite *Entamoeba histolytica*. *Proc. Natl. Acad. Sci. U. S. A. 91,* 7095-7098.

Nimmo, E.R., Sanders, P.G., Padua, R.A., Hughes, D., Williamson, R., and Johnson, K.J. (1991). The MEL gene: a new member of the RAB/YPT class of RAS-related genes. *Oncogene 6,* 1347-1351.

Nobes, C.D., and Hall, A. (1999). Rho GTPases control polarity, protrusion, and adhesion during cell movement. *J. Cell Biol. 144,* 1235-1244.

Nobes, C.D., and Hall, A. (1995a). Rho, rac and cdc42 GTPases: regulators of actin structures, cell adhesion and motility. *Biochem. Soc. Trans. 23,* 456-459.

Nobes, C.D., and Hall, A. (1995b). Rho, rac, and cdc42 GTPases regulate the assembly of multimolecular focal complexes associated with actin stress fibers, lamellipodia, and filopodia. *Cell 81,* 53-62.

Noegel, A.A., and Schleicher, M. (2000). The actin cytoskeleton of *Dictyostelium*: a story told by mutants. *J. Cell. Sci. 113 (Pt 5),* 759-766.

Novick, P., and Zerial, M. (1997). The diversity of Rab proteins in vesicle transport. *Curr. Opin. Cell Biol. 9,* 496-504.

Nuoffer, C., Wu, S.K., Dascher, C., and Balch, W.E. (1997). Mss4 does not function as an exchange factor for Rab in endoplasmic reticulum to Golgi transport. *Mol. Biol. Cell 8,* 1305-1316.

Oikawa, T., Yamaguchi, H., Itoh, T., Kato, M., Ijuin, T., Yamazaki, D., Suetsugu, S., and Takenawa, T. (2004). PtdIns(3,4,5)P3 binding is necessary for WAVE2-induced formation of lamellipodia. *Nat. Cell Biol. 6,* 420-426.

Olkkonen, V.M., and Stenmark, H. (1997). Role of Rab GTPases in membrane traffic. *Int. Rev. Cytol. 176,* 1-85.

Parent, C.A., Blacklock, B.J., Froehlich, W.M., Murphy, D.B., and Devreotes, P.N. (1998). G protein signaling events are activated at the leading edge of chemotactic cells. *Cell 95,* 81-91.

Pasqualato, S., Renault, L., and Cherfils, J. (2002). Arf, Arl, Arp and Sar proteins: a family of GTP-binding proteins with a structural device for 'front-back' communication. *EMBO Rep. 3,* 1035-1041.

Peranen, J., Auvinen, P., Virta, H., Wepf, R., and Simons, K. (1996). Rab8 promotes polarized membrane transport through reorganization of actin and microtubules in fibroblasts. *J. Cell Biol. 135,* 153-167.

Peranen, J., and Furuhjelm, J. (2001). Expression, purification, and properties of Rab8 function in actin cortical skeleton organization and polarized transport. *Methods Enzymol. 329,* 188-196.

Pereira-Leal, J.B., and Seabra, M.C. (2000). The mammalian Rab family of small GTPases: definition of family and subfamily sequence motifs suggests a mechanism for functional specificity in the Ras superfamily. *J. Mol. Biol. 301,* 1077-1087.

Perona, R., Montaner, S., Saniger, L., Sanchez-Perez, I., Bravo, R., and Lacal, J.C. (1997). Activation of the nuclear factor-kappaB by Rho, CDC42, and Rac-1 proteins. *Genes Dev. 11,* 463-475.

Pfeffer, S. (2005). A model for Rab GTPase localization. *Biochem. Soc. Trans. 33,* 627-630.

Pinyol, R., Haeckel, A., Ritter, A., Qualmann, B., and Kessels, M.M. (2007). Regulation of N-WASP and the Arp2/3 complex by Abp1 controls neuronal morphology. *PLoS ONE 2,* e400.

Postma, M., Roelofs, J., Goedhart, J., Loovers, H.M., Visser, A.J., and Van Haastert, P.J. (2004). Sensitization of *Dictyostelium* chemotaxis by phosphoinositide-3-kinase-mediated self-organizing signalling patches. *J. Cell. Sci. 117,* 2925-2935.

Powell, R.R., and Temesvari, L.A. (2004). Involvement of a Rab8-like protein of *Dictyostelium discoideum*, Sas1, in the formation of membrane extensions, secretion and adhesion during development. *Microbiology 150,* 2513-2525.

Ren, M., Zeng, J., De Lemos-Chiarandini, C., Rosenfeld, M., Adesnik, M., and Sabatini, D.D. (1996). In its active form, the GTP-binding protein rab8 interacts with a stress-activated protein kinase. *Proc. Natl. Acad. Sci. U. S. A. 93,* 5151-5155.

Ren, Y., Jiang, H., Yang, F., Nakaso, K., and Feng, J. (2009). Parkin Protects Dopaminergic Neurons against Microtubule-depolymerizing Toxins by Attenuating Microtubule-associated Protein Kinase Activation. *J. Biol. Chem. 284,* 4009-4017.

Rezaie, T., Child, A., Hitchings, R., Brice, G., Miller, L., Coca-Prados, M., Heon, E., Krupin, T., Ritch, R., Kreutzer, D., Crick, R.P., and Sarfarazi, M. (2002). Adult-onset primary open-angle glaucoma caused by mutations in optineurin. *Science 295,* 1077-1079.

Ridley, A.J., Schwartz, M.A., Burridge, K., Firtel, R.A., Ginsberg, M.H., Borisy, G., Parsons, J.T., and Horwitz, A.R. (2003). Cell migration: integrating signals from front to back. *Science 302,* 1704-1709.

Roy, B.C., Kakinuma, N., and Kiyama, R. (2009). Kank attenuates actin remodeling by preventing interaction between IRSp53 and Rac1. *The Journal of Cell Biology 184,* 253.

Rozelle, A.L., Machesky, L.M., Yamamoto, M., Driessens, M.H., Insall, R.H., Roth, M.G., Luby-Phelps, K., Marriott, G., Hall, A., and Yin, H.L. (2000). Phosphatidylinositol 4,5-bisphosphate induces actin-based movement of raft-enriched vesicles through WASP-Arp2/3. *Curr. Biol. 10,* 311-320.

Rush, M.G., Drivas, G., and D'Eustachio, P. (1996). The small nuclear GTPase Ran: how much does it run? *Bioessays 18,* 103-112.

Sato, T., Mushiake, S., Kato, Y., Sato, K., Sato, M., Takeda, N., Ozono, K., Miki, K., Kubo, Y., Tsuji, A., Harada, R., and Harada, A. (2007). The Rab8 GTPase regulates apical protein localization in intestinal cells. *Nature 448,* 366-369.

Sawa, M., Suetsugu, S., Sugimoto, A., Miki, H., Yamamoto, M., and Takenawa, T. (2003). Essential role of the C. elegans Arp2/3 complex in cell migration during ventral enclosure. *J. Cell. Sci. 116,* 1505-1518.

Saxe, C.L.,3rd, Ginsburg, G.T., Louis, J.M., Johnson, R., Devreotes, P.N., and Kimmel, A.R. (1993). CAR2, a prestalk cAMP receptor required for normal tip formation and late development of *Dictyostelium discoideum*. *Genes Dev. 7,* 262-272.

Saxe, S.A., and Kimmel, A.R. (1990). SAS1 and SAS2, GTP-binding protein genes in *Dictyostelium discoideum* with sequence similarities to essential genes in *Saccharomyces cerevisiae. Mol. Cell. Biol. 10,* 2367-2378.

Schalk, I., Zeng, K., Wu, S.K., Stura, E.A., Matteson, J., Huang, M., Tandon, A., Wilson, I.A., and Balch, W.E. (1996). Structure and mutational analysis of Rab GDP-dissociation inhibitor. *Nature 381,* 42-48.

Schultz, J., Milpetz, F., Bork, P., and Ponting, C.P. (1998). SMART, a simple modular architecture research tool: identification of signaling domains. *Proc. Natl. Acad. Sci. U. S. A. 95,* 5857-5864.

Seabra, M.C., Mules, E.H., and Hume, A.N. (2002). Rab GTPases, intracellular traffic and disease. *Trends Mol. Med. 8,* 23-30.

Seastone, D.J., Harris, E., Temesvari, L.A., Bear, J.E., Saxe, C.L., and Cardelli, J. (2001). The WASp-like protein scar regulates macropinocytosis, phagocytosis and endosomal membrane flow in *Dictyostelium. J. Cell. Sci. 114,* 2673-2683.

Silacci, P., Mazzolai, L., Gauci, C., Stergiopulos, N., Yin, H.L., and Hayoz, D. (2004). Gelsolin superfamily proteins: key regulators of cellular functions. *Cell Mol. Life Sci. 61,* 2614-2623.

Sogaard, M., Tani, K., Ye, R.R., Geromanos, S., Tempst, P., Kirchhausen, T., Rothman, J.E., and Sollner, T. (1994). A rab protein is required for the assembly of SNARE complexes in the docking of transport vesicles. *Cell 78,* 937-948.

Soldati, T., Shapiro, A.D., Svejstrup, A.B., and Pfeffer, S.R. (1994). Membrane targeting of the small GTPase Rab9 is accompanied by nucleotide exchange. *Nature 369,* 76-78.

Stacey, D.W., and Kung, H.F. (1984). Transformation of NIH 3T3 cells by microinjection of Ha-ras p21 protein. *Nature 310,* 508-511.

Stenmark, H., and Olkkonen, V.M. (2001). The Rab GTPase family. *Genome Biol. Reviews 3*, 2007.

Suetsugu, S., Miki, H., and Takenawa, T. (1999). Identification of two human WAVE/SCAR homologues as general actin regulatory molecules which associate with the Arp2/3 complex. *Biochem. Biophys. Res. Commun. 260,* 296-302.

Sun, T.J., and Devreotes, P.N. (1991). Gene targeting of the aggregation stage cAMP receptor cAR1 in *Dictyostelium*. *Genes Dev. 5,* 572-582.

Symons, M., Derry, J.M., Karlak, B., Jiang, S., Lemahieu, V., Mccormick, F., Francke, U., and Abo, A. (1996). Wiskott-Aldrich syndrome protein, a novel effector for the GTPase CDC42Hs, is implicated in actin polymerization. *Cell 84,* 723-734.

Takahashi, K., Sasaki, T., Mammoto, A., Takaishi, K., Kameyama, T., Tsukita, S., and Takai, Y. (1997). Direct interaction of the Rho GDP dissociation inhibitor with ezrin/radixin/moesin initiates the activation of the Rho small G protein. *J. Biol. Chem. 272,* 23371-23375.

Takai, Y., Sasaki, T., and Matozaki, T. (2001). Small GTP-binding proteins. *Physiol. Rev. 81,* 153-208.

Takenawa, T., and Suetsugu, S. (2007). The WASP-WAVE protein network: connecting the membrane to the cytoskeleton. *Nat. Rev. Mol. Cell Biol. 8,* 37-48.

Ullrich, O., Horiuchi, H., Bucci, C., and Zerial, M. (1994). Membrane association of Rab5 mediated by GDP-dissociation inhibitor and accompanied by GDP/GTP exchange. *Nature 368,* 157-160.

Ullrich, O., Stenmark, H., Alexandrov, K., Huber, L.A., Kaibuchi, K., Sasaki, T., Takai, Y., and Zerial, M. (1993). Rab GDP dissociation inhibitor as a general regulator for the membrane association of rab proteins. *J. Biol. Chem. 268,* 18143-18150.

van Haastert, P.J., Keizer-Gunnink, I., and Kortholt, A. (2007). Essential role of PI3-kinase and phospholipase A2 in *Dictyostelium discoideum* chemotaxis. *J. Cell Biol. 177,* 809-816.

Vicker, M.G., and Grutsch, J.F. (2008). Dual chemotaxis signalling regulates *Dictyostelium* development: intercellular cyclic AMP pulses and intracellular F-actin disassembly waves induce each other. *Eur. J. Cell Biol. 87,* 845-861.

Wang, Z., and Thurmond, D.C. (2009). Mechanisms of biphasic insulin-granule exocytosis - roles of the cytoskeleton, small GTPases and SNARE proteins. *J. Cell. Sci. 122,* 893-903.

Ward, M.E., Wu, J.Y., and Rao, Y. (2004). Visualization of spatially and temporally regulated N-WASP activity during cytoskeletal reorganization in living cells. *Proc. Natl. Acad. Sci. U. S. A. 101,* 970-974.

Welch, M.D., Iwamatsu, A., and Mitchison, T.J. (1997). Actin polymerization is induced by Arp2/3 protein complex at the surface of *Listeria monocytogenes*. *Nature 385,* 265-269.

Wennerberg, K., Rossman, K.L., and Der, C.J. (2005). The Ras superfamily at a glance. *J. Cell. Sci. 118,* 843-846.

Westphal, M., Jungbluth, A., Heidecker, M., Muhlbauer, B., Heizer, C., Schwartz, J.M., Marriott, G., and Gerisch, G. (1997). Microfilament dynamics during cell movement and chemotaxis monitored using a GFP-actin fusion protein. *Curr. Biol. 7,* 176-183.

Wilson, A.L., Erdman, R.A., Castellano, F., and Maltese, W.A. (1998). Prenylation of Rab8 GTPase by type I and type II geranylgeranyl transferases. *Biochem. J. 333 (Pt 3),* 497-504.

Wittmann, T., and Waterman-Storer, C.M. (2001). Cell motility: can Rho GTPases and microtubules point the way? *J. Cell. Sci. 114,* 3795-3803.

Xu, X., Meier-Schellersheim, M., Jiao, X., Nelson, L.E., and Jin, T. (2005). Quantitative imaging of single live cells reveals spatiotemporal dynamics of multistep signaling events of chemoattractant gradient sensing in *Dictyostelium*. *Mol. Biol. Cell 16,* 676-688.

Yamamura, R., Nishimura, N., Nakatsuji, H., Arase, S., and Sasaki, T. (2008). The interaction of JRAB/MICAL-L2 with Rab8 and Rab13 coordinates the assembly of tight junctions and adherens junctions. *Mol. Biol. Cell 19,* 971-983.

Yamochi, W., Tanaka, K., Nonaka, H., Maeda, A., Musha, T., and Takai, Y. (1994). Growth site localization of Rho1 small GTP-binding protein and its involvement in bud formation in *Saccharomyces cerevisiae*. *J. Cell Biol. 125,* 1077-1093.

Zallen, J.A., Cohen, Y., Hudson, A.M., Cooley, L., Wieschaus, E., and Schejter, E.D. (2002). SCAR is a primary regulator of Arp2/3-dependent morphological events in *Drosophila*. *J. Cell Biol. 156,* 689-701.

Zerial, M., and Huber, L.A. (1995). *Guidebook to the small GTPases* (Oxford: Oxford University Press).

Zerial, M., and McBride, H. (2001). Rab proteins as membrane organizers. *Nat. Rev. Mol. Cell Biol. 2,* 107-117.

Zhang, F.L., and Casey, P.J. (1996). Protein prenylation: molecular mechanisms and functional consequences. *Annu. Rev. Biochem. 65,* 241-269.

CHAPTER TWO

FUNCTIONAL INTERACTION OF RACF2 AND SCAR IN THE RAB8 SIGNALING PATHWAY IN *DICTYOSTELIUM DISCOIDEUM*

Abstract

The small GTPase, Rab8, has been shown to play a role in cell-cell adhesion and restructuring of the actin cytoskeleton in both mammalian cells and the lower eukaryote, *Dictyostelium discoideum*. In *D. discoideum*, cells expressing constitutively activate Rab8 (Rab8CA) display reduced cell-cell adhesion and increased actin-rich protrusions, as well as delayed aggregation. In other systems, actin-rich membrane extension formation is regulated by WASp family proteins, including SCAR. To elucidate the mechanism by which Rab8 influences actin dynamics, Rab8CA was expressed in a SCAR-knockout *D. discoideum* cell line. Interestingly, aggregation was normal in this double mutant, suggesting that the defect was a result of aberrant signaling through SCAR, and that Rab8 may be upstream of SCAR in a signaling cascade. This provides the first genetic evidence in any cell system of a functional interaction between Rab8 and a WASp family protein.

Cdc42 and Rac (Cdc42/Rac) have been shown to be important activators of WASp-family proteins, including SCAR. It has been shown that Rac interacts directly with SCAR; thus, it was hypothesized that Rab8 functions upstream of Rac. Our recent results indicate that expression of an inactive form of *D. discoideum* RacF2, which shares 71% homology with human Rac1, leads to rescue of the adhesion defect in the Rab8CA mutant, supporting the idea that Rab8 may lie upstream of Rac.

Introduction

Rab8 is a small GTPase that has been implicated in polarized vesicle trafficking events in eukaryotic cells. Like all small molecular weight GTPases of the Rab family, Rab8 acts as a molecular switch by cycling between an active, GTP-bound form, and an inactive, GDP-bound form, and has a C-terminal lipid modification, which allows it to interact with the lipid membranes of transport vesicles (Hall, 2000; Jordens, Marsman, *et al.*, 2005; Stenmark and Olkkonen, 2001). While it has been established that Rab8 plays a role in vesicle trafficking, Rab8 has also been shown to effect changes in actin and microtubule cytoskeletal elements. This "moonlighting" capability of Rab8 has been studied primarily in mammalian cells. When constitutively activated Rab8 was expressed in BHK (Baby Hamster Kidney) cells, it caused dramatic changes in cell morphology, including the development of actin-rich protrusions similar to neuronal dendritic extensions (Peranen, Auvinen, *et al.*, 1996). Additionally, expression of constitutively active Rab8 caused membrane ruffling when expressed in CHO (Chinese Hamster Ovary) cells (Chen, Holcomb, and Moore, 1993). This role for Rab8 appears to be evolutionarily conserved, as the expression of constitutively activate Rab8 leads to the appearance of polarized actin caps and an increase in filipodia in the social amoeba, *D. discoideum* (Powell and Temesvari, 2004). However, to date, it is still not known how Rab8 effects changes in the actin cytoskeleton.

D. discoideum is a non-pathogenic, eukaryotic amoeba that is normally found in the soil or leaf litter of deciduous forest environments. The life cycle of the organism involves both a single cell, vegetative stage and a multi-cellular stage. When resources,

including food, light and water, are plentiful, the cells exist as free living, single cell amoebae. However, when resources become limited, the organism has the ability to trigger a developmental program that leads to the formation of aggregates of cells, which eventually undergo differentiation to form a multicellular structure for the formation and storage of spores for long term survival (Eichinger and Rivero, 2006; Loomis, 1975)

When food resources become scarce, the ensuing starvation induces changes in gene expression in the amoebae. As a result, a number of adhesion molecules, cAMP generating protein machinery and cAMP receptor molecules are produced. After approximately 5 hours of starvation, founder cells begin to secrete cAMP, which induces cAMP secretion and chemotaxis towards the cAMP source in surrounding cells. As cells chemotax, they move collectively, as streams of cells, towards the central founder cell and begin to adhere to one another. Initial cell-cell adhesion is mediated by a 24-kilodalton glycoprotein adhesion molecule, gp24 (DdCAD-1). This process culminates in the formation of aggregates of approximately 100,000 cells (Gilbert, 2003).

Two Rab8 homologues have been identified in *D. discoideum*. Originally termed Sas1 and Sas2, these homologues are now referred to as Rab8 and Rab8b, respectively. The proteins are expressed at low to moderate levels during the vegetative stage through early development, and increase to higher levels of expression following aggregation. Rab8 is expressed at higher levels than Rab8b throughout the vegetative stage and early development, and is expressed at its highest level at approximately 15 hours of development. After this point, Rab8 levels decrease and Rab8b levels increase,

suggesting that each protein may play a specific role during development (Saxe and Kimmel, 1990).

In studies conducted by Powell and Temesvari (Powell and Temesvari, 2004), the constitutively active (GTP-bound) and dominant negative (GDP-bound) versions of Rab8 and Rab8b were examined for their function in *D. discoideum*. Interestingly, the overexpression of the active form of Rab8 led to the formation of actin-rich membrane extensions, inhibition of aggregation, reduction in the level of the calcium-dependent early adhesion molecule, gp24, increase in the extracellular levels of countin, a subunit of cell-counting factor, which helps regulate aggregate size, and oversecretion of acid phosphatase under starvation conditions. No changes to the actin cytoskeleton were seen in cells expressing dominant negative Rab8 or wildtype Rab8, or in cells expressing dominant negative or constitutively active Rab8b. Cells expressing dominant negative Rab8 did demonstrate enhanced aggregation and an increase in gp24 levels, while Rab8b mutations did not adversely affect early development (Powell and Temesvari, 2004). As with mammalian Rab8, *D. discoideum* Rab8 seems to be involved in the formation of actin-rich protrusions, in addition to the regulation of calcium-dependent adherence proteins important for adherens junctions.

Actin filament assembly is vital for a multitude of cellular functions, including chemotaxis, endocytosis, and changes in cellular morphology (Blagg and Insall, 2004; Pinyol, Haeckel, *et al.*, 2007). Actin filaments are assembled from globular actin monomers (Millard, Sharp, and Machesky, 2004). However, the assembly of actin monomers is energetically unfavorable, and dimers and trimers of actin monomers are

inherently unstable. Therefore, a number of accessory proteins are required to regulate the process of actin filament formation. One of the key accessory proteins in this process is the Arp2/3 complex, which functions as a nucleating agent for the formation of new actin filaments (Chan, Bailly, *et al.*, 2000; Ichetovkin, Grant, and Condeelis, 2002; Millard, Sharp, and Machesky, 2004).

The Arp2/3 complex may be activated by a number of proteins to effect changes in the actin cytoskeleton. One group of Arp2/3 activator proteins is the WASp (Wiskott-Aldrich Syndrome protein) family proteins. WASp family proteins have been implicated in actin-based processes, including the generation of lamellipodia, filipodia and membrane ruffling (Legg, Bompard, *et al.*, 2007), as well as cell migration, extension of neurites, and vesicle trafficking (Suetsugu, Miki, and Takenawa, 1999; Ward, Wu, and Rao, 2004). Rho-GTPases are believed to be linked to actin cytoskeletal dynamics through WASp family proteins (Blagg, Stewart, *et al.*, 2003; Blagg and Insall, 2004; Oikawa, Yamaguchi, *et al.*, 2004). Members of the WASp family include WASp, N-WASp, SCAR/WAVE1, SCAR/WAVE2, and SCAR/WAVE3 (Millard, Sharp, and Machesky, 2004; Suetsugu, Miki, and Takenawa, 1999).

SCAR, or suppressor of cAMP receptor, was identified as a WASp- related protein during a genetic screen in *D. discoideum*. SCAR acts as a suppressor of the defect caused by the loss of the *D. discoideum* cAMP receptor, cAR2. The absence of cAR2 causes disruption of tip formation during development. By disrupting SCAR in cAR2 null cells, normal tip formation was restored (Bear, Rawls, and Saxe, 1998).

SCAR/WAVE exists as a complex of proteins, including PIR121 (p53-inducible mRNA 121), Nap125 (Nck-associated protein 1), Abi2 (Abl-interactor 2) and HSPC300 (Blagg, Stewart, *et al.*, 2003; Eden, Rohatgi, *et al.*, 2002). SCAR/WAVE is inactive when associated with the complex. When activated Rac binds to the complex, SCAR/WAVE and HSPC300 disassociates from the complex, and SCAR/WAVE is subsequently activated. Thus, Rac functions as an upstream activator of SCAR/WAVE (Caracino, Jones, *et al.*, 2007; Eden, Rohatgi, *et al.*, 2002).

There are 15 known and 3 putative Rac GTPases in *D. discoideum*. One of these Rac GTPases, RacF2, shares 71% homology with human Rac1, and has been implicated in sexual cell fusion and in the regulation of EDTA-sensitive cell-cell adhesion during early development (Muramoto and Urushihara, 2006). Like the expression of the dominant negative form of Rab8 (Powell and Temesvari, 2004), expression of the dominant negative form of RacF2 leads to increased EDTA-sensitive cell-cell adhesion (Muramoto and Urushihara, 2006).

Cell-cell adhesion is a crucial aspect of *D. discoideum* development and is mediated by a number of sequentially expressed cell adhesion molecules, or CAMs. The first cell-cell adhesion molecule that is expressed during development is a calcium dependent protein called DdCAD-1, also known as contact sites B (csB), or gp24. This CAM is initially expressed in the cytoplasm of cells within one hour of entering starvation. As development proceeds, gp24 is secreted; however, a large percentage of the adhesion molecule remains associated with the external surface of the plasma

membrane. This plasma membrane association is sensitive to EDTA (Coates and Harwood, 2001).

In this study, we demonstrate the first functional interaction between a WASp family protein, SCAR, and Rab8. We have also shown that Rab8 and RacF2 interact directly, perhaps in the control of cellular levels of the EDTA-sensitive, cell-cell adhesion molecule, gp24.

Materials and Methods

Cell and culture conditions

D. discoideum parental AX2 and mutant cell lines were grown axenically in HL5 medium (10 g Oxoid Proteose Peptone (Oxoid Ltd., Hampshire, England), 10 g glucose, 5 g yeast extract, 0.19 g Na_2HPO_4, 0.35 g KH_2PO_4) supplemented with 100 μg/ml ampicillin at room temperature in 25 cm^2 culture flasks. The GFP-Rab8DN (dominant negative), SCAR-null/ GFP-Rab8CA (constitutively active), and HA-RacF2DN (dominant negative) mutant cell lines were maintained with the addition of 20 μg/ml neomycin (G418) (Mediatech, Inc., Manassas, VA). The GFP-Rab8CA (constitutively active) cell line was maintained with the addition of 75 μg/ml hygromycin B (Invitrogen, Carlsbad, CA). The GFP-Rab8CA/ HA-RacF2DN and GFP-Rab8CA/HA- RacF2WT (wild type) cell lines were maintained with the addition of 75 μg/ml hygromycin and 20 μg/ml G418.

Constructs

The GFP-Rab8CA and GFP-Rab8DN constructs are as described previously by Powell and Temesvari (Powell and Temesvari, 2004). Briefly, Rab8, formerly referred to as Sas1, was mutated using the QuickChange Kit (Stratagene, La Jolla, CA), a PCR-based site-directed mutagenesis kit. In order to create the constitutively active Rab8 (Rab8CA) mutant, an encoded glutamine (Q) residue at amino acid position 74 was changed to a leucine (L) residue (Rab8Q67L). To create the dominant negative Rab8 (Rab8DN) mutant, an encoded asparagine (N) residue at amino acid position 128 was changed to an isoleucine (I) residue (Rab8N128I). The wildtype and mutant Rab8 cDNAs were subsequently subcloned into the pDJS expression vector (gift of Dr. James Cardelli, LSU Health Sciences Center, Shreveport, LA, USA), in order to produce GFP-Rab8 chimeric proteins under the control of the folate-repressible *discoidin I* promoter. The resulting constructs were used to transfect parental AX2 *D. discoideum* cells by electroporation. The pDJS expression vector confers neomycin (G418) resistance; therefore, clones were selected using 20 μg/ml G418. The clones were sorted using fluorescence activated cell sorting (FACS).

To create the SCAR-null/ GFP-Rab8CA mutant, the SCAR-null cell line (gift of Dr. Karl Saxe, American Cancer Society, Atlanta, GA) was transfected with the GFP-Rab8CA vector using electroporation as described by Kuspa and Loomis (Kuspa and Loomis, 1992). Clones were selected using 20 μg/ml G418.

In order to create the HA-tagged dominant negative RacF2 (HA-RacF2DN) cell line, the pRacF2-WT (wildtype) plasmid was obtained from DictyBase

(www.dictybase.org). PCR was used to add EcoRI cutsites to both ends of the RacF2 coding region. The following primers were used:

Forward: 5'- CCG AAT TCC AAA ATA TTA AAT G -3'

Reverse: 5'-CCG AAT TCT TAC ATT ATT GTA C-3'

The resulting ~750 bp PCR product was subcloned into the TOPO-TA vector, pCR2.1 (Invitrogen, Carlsbad, CA).

The QuickChange Kit (Stratagene, La Jolla, CA) was used to create the RacF2DN mutant, by changing an encoded threonine (T) residue at amino acid position 17 to an asparagine (N) residue (RacF2 T17N). The mutagenesis primers used were as follows:

Sense: 5'-GTT GGT GAT GGT GCA GTT GTG TAA AA**A** TTG TAT GTT AAT T – 3'

AntiSense: 5'-GAA ATT AAC ATA CAA **T**TT TTA CCA ACT GCA CCA TCA CCA AC – 3'

The RacF2WT and RacF2DN cDNAs were subcloned behind and in frame with the DNA element encoding the HA epitope tag in the pAD80HA vector (gift of Dr.

Arturo De Lozanne, Duke University Medical Center, Durham, NC, USA) (Burns, Reedy, *et al.*, 1995). This vector confers G418 resistance.

The GFP-Rab8CA and HA-RacF2DN plasmids both conferred G418 resistance. Therefore, in order to obtain double mutants, which expressed both the GFP-Rab8CA and either HA-RacF2DN or HA-RacF2WT, it was necessary to rebuild one of the constructs in an expression vector which would confer resistance to a selection agent other than G418. The GFP-Rab8CA was rebuilt in an expression vector which confers hygromycin resistance, pDHGFP (gift of Dr. David Knecht, University of Connecticut, Storrs, CT, USA). PCR was used to add BglII cutsites to the GFP-Rab8CA coding region. The following primers were used:

Forward: 5'- CCA GAT CTA CTT CTC CAG CAA C -3'

Reverse: 5'-CCA GAT CTC CCA ATT TAA CAA C-3'

The resulting ~700 bp PCR product was subcloned into the TOPO-TA vector, pCR2.1 (Invitrogen, Carlsbad, CA). The pCR2.1 – GFP-Rab8CA plasmid and the pDHGFP plasmid were digested with BglII. The GFP-Rab8CA sequences were ligated into pDHGFP according to the manufacturer's instructions using the Epicentre Biotechnologies Fast-LinkTM DNA Ligation Kit (Epicentre Biotechnologies, Madison, WI). This resulted in a plasmid encoding GFP-Rab8CA and hygromycin resistance.

XL-2 Blue Ultracompetent cells (Stratagene, Agilent Technologies, Santa Clara, CA) were transformed with the GFP-Rab8CA plasmid, which conferred hygromycin

resistance, and either the HA-RacF2DN plasmid or the HA-RacF2WT plasmid, which conferred G418 resistance, according to the manufacturer's protocol. Cells were grown in 1 ml of Luria Broth for 1 hour at 37^{o}C and 200 rpm shaking. Cells were plated onto agarose plates with ampicillin selection and incubated overnight at 37^{o}C. The resulting clones were screened by restriction enzyme analysis and PCR colony screening. Positive clones were sequenced to verify that the GFP and Rab8CA or HA and RacF2WT or RacF2DN were in frame, and that the correct cut sites and point mutations had been maintained throughout the cloning process. Sequences were verified using NCBI BLAST.

Transfection

For transfections, *D. discoideum* were grown axenically in HL5 medium overnight in 75 cm^2 culture flasks. Transfections were performed using electroporation as described by Pang *et al.* (Pang, Lynes, and Knecht, 1999). Log phase cells were washed twice, counted, and resuspended at a concentration of 2 x 10^7 cells per ml in ice cold H50 buffer (20 mM HEPES, 50 mM KCl, 10 mM NaCl, 1 mM $MgSO_4$, 5 mM $NaHCO_3$, 1 mM NaH_2PO_4, pH 7.0). A total of 40 μg of plasmid DNA was added to a chilled, 1 mm electroporation cuvette. For transfection of the parental AX2 strain with the hygromycin resistance conferring GFP-Rab8CA construct, 20 μg of the GFP-Rab8CA plasmid DNA was cotransfected with 20 μg of a hygromycin resistance conferring vector, pHygTm(plus)/pG7 (gift of Dr. David Knecht, University of Connecticut, Storrs, CT, USA). After addition of the DNA, 100 μl of the cell suspension was added to the chilled

cuvette. The cells and DNA were mixed and incubated on ice for 5 minutes. Two consecutive pulses (0.85 kV, 25 μF) were applied to the cuvette with a 5 second recovery period between the pulses. The cuvettes were immediately placed on ice and incubated for 5 minutes. The cells were then plated onto a 100-mm culture dish with 10 ml of HL5 medium supplemented with 100 μg/ml ampicillin. After 24 hours, selection was added. The G418 selection level was 20 μg/ml, and the hygromycin selection level was 75 μg/ml. Clones were subsequently subjected to limited dilution cloning and FACS sorting.

Immunofluorescence Microscopy

Cells were washed twice in HL5 (nutrient media) or Developmental Buffer (DB) (5 mM $Na_2HPO_4{\cdot}7H_2O$, 5mM KH_2PO_4, 2 mM $MgSO_4$, 0.2 mM $CaCl_2$, pH 6.2). The cells were then counted, and 1 x 10^5 cells were plated onto coverslips or Lab-Tek coverglass chamber wells (Nalge Nunc International, Rochester, NY) and allowed to adhere for 1 hour. Cells in developmental media were starved for 5 hours prior to fixation.

Cells were fixed in 4% paraformaldehyde in media for 10 minutes at room temperature. Cells were permeabilized with 0.1 % Triton-X-100 for 4 minutes at room temperature. Nonspecific binding sites were blocked by incubating with 3%BSA/ 10% goat serum in PBS for 20 minutes at room temperature. The blocking solution was removed and replaced with 200 μl of 1% BSA in PBS. Following blocking, 10 μl of a 20μM solution of AlexaFluor-594 conjugated phalloidin (Molecular Probes, Eugene, OR) were added, and the cells were incubated for 20 minutes at room temperature. The stained cells were washed twice with 1% BSA, washed with 1X PBS, mounted in 50%

PBS/glycerol and observed using a Zeiss LSM 510 confocal microscope (Carl Zeiss, Thornwood, NY)(Powell, Welter, *et al.*, 2006).

Aggregations

For timed aggregation studies, cells were grown axenically in HL5 medium overnight in 75 cm^2 culture flasks. The cells were resuspended in DB. Cells were washed twice in DB and counted. Next, 5.5 x 10^5 cells were centrifuged and resuspended in 1 ml of DB. The cells were dispensed into a 96- well plate by pipetting 200 μl of the cell suspension into 5 wells of the plate. Therefore, there were approximately 1.1 x 10^5 cells per well. For timed aggregations, one plate was set up for each time point. The plates were covered with aluminum foil and left in the dark to stimulate development. Plates were removed at the appropriate time and examined for the presence of aggregation using a Carl Zeiss (Thornwood, NY) Axiovert 135 fluorescence microscope. Images were captured using a Canon PC 1192 camera (Lake Success, NY).

Time-Lapse Video Microscopy and Cell Tracking

For time lapse videos, cells were grown axenically in HL5 medium overnight in 75 cm^2 culture flasks. The cells were resuspended in DB. Cells were washed twice in DB and counted. Next, 2.5 x 10^5 cells were centrifuged and resuspended in 800 μl of DB. The cells were dispensed into Lab-Tek coverglass chamber wells (Nalge Nunc International, Rochester, NY), and placed in the dark for 5 hours. Time lapse video was captured using a Nikon Eclipse TI-E Confocal Microscope (Nikon, Lewisville, TX) at a

rate of 1 frame every 5 seconds for 10 minutes. Images were analyzed using the Nikon NIS Elements Software (Nikon, Lewisville, TX). Cells were manually tracked, and the motility index was calculated as (distance moved from origin)/(total path distance).

Cell-Cell Contact Index

Time lapse videos were analyzed to determine the cell-cell contact indices. Every 50^{th} frame was analyzed by counting the number of cells in contact with another cell as well as the number of cells not in contact with another cell. The contact index (%) was calculated as (number of cells in contact with another cell)/ (total number of cells).

Chemotaxis Assays

Chemotaxis assays were performed as described by Woznica and Knecht (Eichinger and Rivero, 2006). A 1.5% agarose gel in DB was prepared. Approximately 8 ml of the agarose gel were dispensed into a cover glass bottom, 35 mm petri dish (WillCo wells, Amsterdam, The Netherlands). The agarose gel was allowed to cool and set overnight. Three wells were cut into the agarose using a razor blade. The wells were approximately 2 mm wide, 39 mm long, and were placed approximately 5 mm apart (see Figure 2.14 C)

Cells were washed, counted, and resuspended at a concentration of 7×10^6 cells per ml in 5 ml of Developmental Buffer. The cells were shaken at room temperature at a speed of 180 rpm for 8 hours to allow expression of the cAR1 cAMP receptor. cAMP (Sigma, St. Louis, MO) was prepared in DB at a concentration of 5 mM. The cAMP

chemoattractant (200 μl) was added to the middle well. The cells (200 μl) were added to the outer wells. The plates were incubated in the dark at room temperature for 1 hour. The cells were observed using a Carl Zeiss (Thornwood, NY) LSM 510 confocal microscope. The distance from the trough to the leading cell in each field of view was measured using Carl Zeiss (Thornwood, NY) LSM Image Software.

RacF2-HA Pulldown Assays

One 25 cm^2 flask of cells was used to inoculate a 75 cm^2 flask. The cells were grown axenically at room temperature overnight in HL5 medium. The cells were resuspended and washed in 1X PBS (phosphate buffered saline). The cells were counted and 1 x 10^6 cells were pelleted by centrifugation. The supernatants were removed and the pellets were frozen at -80^oC for 1 hour to aide lysis. The pellets were thawed and resuspended in 500 μl of B-PER Bacterial Protein Extraction Reagent (Pierce, Rockford, IL) supplemented with 5 μl of 100X Pierce Protease Inhibitor Cocktail (HALT) (Pierce, Rockford, IL). The pellets were vortex mixed for approximately 10 seconds. The samples were incubated for 10 minutes at room temperature with rotation. A 25 μl sample of the cell lysate was mixed with 25 μl of LDS buffer (50% LDS (Invitrogen, Carlsbad, CA), 40% water, 10% 2-mercaptoethanol (Bio-Rad Laboratories, Hercules, CA) and frozen. The remaining lysate was added to a Handee Spin Column (Pierce, Rockford, IL). The Profound^{TM} HA Tag IP/Co-IP Kit was used to pulldown RacF2-HA and any interacting proteins. The manufacturer provided HA-antibody linked agarose bead slurry (6 μl) was

added to the cell lysates. The cell lysates were incubated with the HA-antibody linked beads at 4^{o}C for 18 hours with rotation.

A wash solution was prepared by adding 1% Tween-20 to the manufacturer provided BupH TBS (Tris Buffered Saline), for a final concentration of 0.05% Tween-20. The caps on the Handee Spin Columns were loosened, the bottom plugs were removed, and the columns were placed into 2 ml collection tubes. The columns were centrifuged for 30 seconds and the flow through was discarded. The bottom plugs were replaced, 500 µl of wash buffer were added, and the caps were tightened on each column. The beads were washed by inverting the column 4-5 times. The caps were reloosened, the bottom plugs removed, and the columns were placed into 2 ml collection tubes. The columns were centrifuged for 30 seconds, and the flow through was discarded. The columns were washed twice more in this manner for a total of 3 washes.

The spin columns were placed into clean collection tubes. Next, 25 µl of the manufacturer provided 2X Non-Reducing Sample Buffer was added to the HA-antibody linked agarose beads. The cap was loosely screwed on and the column was gently tapped to resuspend the beads. The column and collection tube assembly was heated on a heat block at 95-100^{o}C for 5 minutes. The samples were centrifuged for 1 minute. To prepare the samples for SDS-PAGE, 2.5 µl of 2-mercaptoethanol (Bio-Rad Laboratories, Hercules, CA) were added. The frozen cell lysate samples were thawed, and along with the pulldown samples, were incubated in a water bath at 70^{o}C for 10 minutes. SDS-PAGE was performed as described below, by loading 20 µl samples onto a NuPage Gel (10% Bis-Tris) (Invitrogen, Carlsbad, CA). Western blot analysis was performed as

described below using a primary rabbit-anti-Rab8 (1:1000) (Sas1) (Zymed, San Francisco, CA) (Powell and Temesvari, 2004), or rabbit anti-WAVE/Scar (1:500) (Millipore, Billerica, MA) antibody and a secondary horseradish peroxidase-conjugated goat anti-rabbit (1:5000) IgG antibody (Cappel, ICN Pharmaceuticals, Costa Mesa, CA).

SDS-PAGE and Western Blot Analysis

SDS-PAGE and Western blot analyses were carried out as previously described by Welter *et al*. (Welter, Laughlin, and Temesvari, 2002). Cells were washed twice with PBS. Cells were counted, and 1 x 10^6 cells were pelleted by centrifugation. The pellet was resuspended in 30 µl LDS sample buffer with 2-mercaptoethanol (2% v/v) and heated at 70^{o}C for 10 minutes. Next, 15 µl of each sample were loaded onto a NuPage Gel (10% Bis-Tris) (Invitrogen, Carlsbad, CA). Samples were electrophoresed at 200 V for 1 hour and transferred to a PVDF (polyvinylidene difluoride) membrane (Invitrogen, Carlsbad, CA) in Towbin buffer at 100 V for 90 minutes. Blotted membranes were blocked in 5% powdered milk / 0.5% Tween 20/TBS (Tris Buffered Saline) for 2 hours at room temperature. After rinsing with 0.5%Tween 20/TBS, the membrane was incubated overnight at 4^{o}C with primary antibody (1:500 mouse anti-GFP, 1:125 rabbit anti-HA, 1:1500 rabbit anti-Rab8 (Sas1) (Zymed, San Francisco, CA)(Powell and Temesvari, 2004), 1:1000 rabbit anti-cAR2 (gift of Dr. Karl Saxe, American Cancer Society, Atlanta, GA, USA), or 1:500 rabbit anti-WAVE/Scar (Millipore, Billerica, MA). The membrane was washed and incubated with a secondary horseradish peroxidase-conjugated goat anti-rabbit (1:5000) or goat anti-mouse (1:2000) IgG antibody (Cappel,

ICN Pharmaceuticals, Costa Mesa, CA) for 1 hour at room temperature. After washing, proteins were detected with the Enhanced Chemi Luminescence (ECL) Western blotting detection system (Pierce, Rockland, IL), according to the manufacturer's instructions.

FACS sorting

GFP-Rab8 expressing cells were washed and resuspended in 1 X PBS at a concentration of 1x 10^6 cells/ml. 5 mls of cells were filtered through a 40 micron sterile filter (Millipore, Danvers, MA). FACS sorting was carried out using a Cytopeia Influx FACS sorter (BD Biosciences, San Jose, CA) capable of high-speed analysis and cell-sorting. The gating was set to capture the highest 1% of GFP expressing cells. Cells were sorted into a media tube containing HL5 media supplemented with 100 μg/ml ampicillin and 75 μg/ml hygromycin, and in the case of clones also expressing HA-RacF2DN or HA-RacF2WT, 20 ug/ml G418. Single cells were dispensed into each well of a sterile 96-well plate to obtain single clones.

Statistical Analysis

All values, unless otherwise stated, are reported as a mean ± SD. Statistical analyses were performed using GraphPad Instat V.3 with One Way ANOVA and a Dunnett Multiple Comparison test. *P* values less than 0.01 were considered highly statistically significant, and *P* values between 0.01 and 0.05 were considered statistically significant (Powell and Temesvari, 2004).

Results

Establishment and verification of GFP-Rab8CA mutant cell lines

Parental AX2 *D. discoideum* cells were transfected with an N-terminal green fluorescent protein (GFP) fusion of constitutively active Rab8. Stable clones were selected with 75 μg/ml of hygromycin, and isolated by limited dilution cloning. Each clone was examined using fluorescence microscopy (Figure 2.1, A-B) for expression of the GFP-Rab8CA chimeric protein. The cells display dendritic-like extensions. Expression was verified by Western blot analysis (Figure 2.1 C) using primary antibodies to GFP and Rab8. The GFP-Rab8CA expressing clones showed a number of long, thin extensions (Figure 2.1 A).

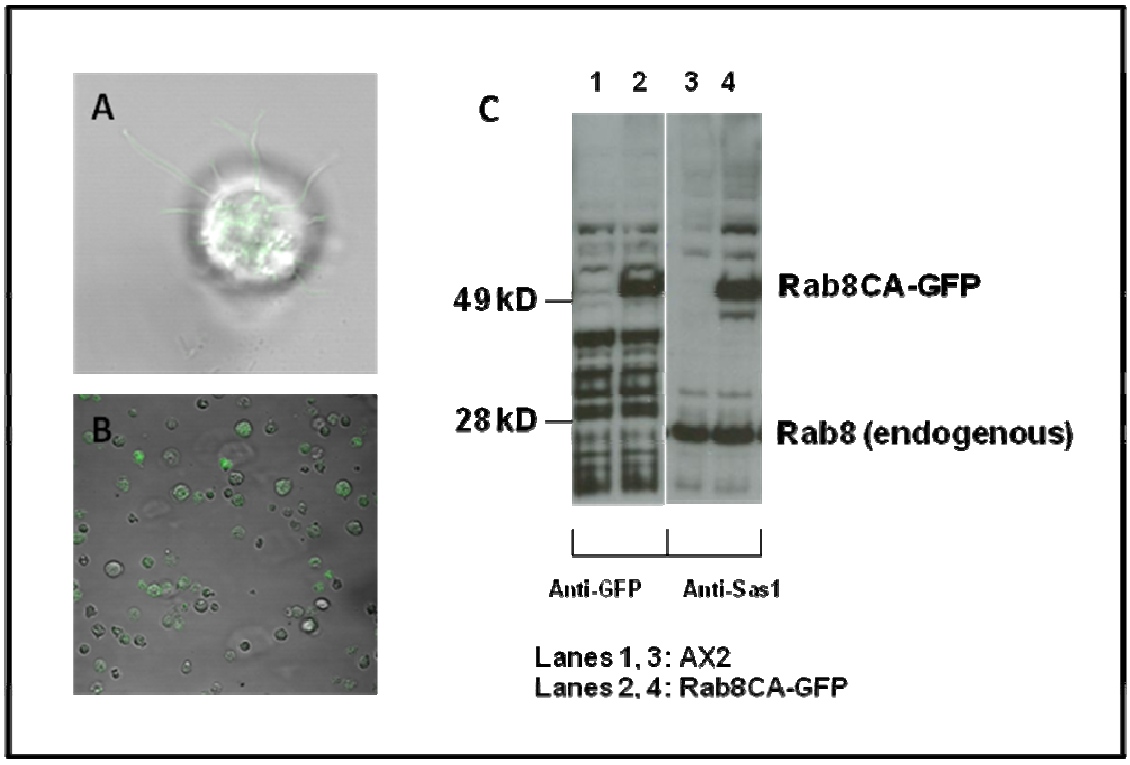

Figure 2.1. Expression of GFP-Rab8CA in AX2 Cells. The GFP-Rab8CA cDNA was subcloned into the expression vector, pHyg39, which confers hygromycin resistance. (A-B) Fluorescence microscopy using a Zeiss LSM 510 confocal microscope was used to confirm GFP-Rab8CA expression. Cells display dendritic-like extensions. (C) Western blot analysis with antibodies to Rab8 and GFP were used to confirm expression of the chimeric GFP-Rab8CA protein.

SCAR-null AX2 *D. discoideum* cells were transfected with an N-terminal green fluorescent protein (GFP) fusion of constitutively active Rab8. Stable clones were selected with 20 μg/ml of G418, and isolated by limited dilution cloning. Each clone was examined using fluorescence microscopy (Figure 2.2, A-B) for expression of the GFP-Rab8CA chimeric protein. Cells no longer displayed dendritic-like extensions. Expression was verified by Western blot analysis (Figure 2.2 C) using primary antibodies

to GFP and Rab8. Western blot analysis was also used to verify that SCAR had been knocked out in the mutant cell line. (Figure 2.2 D).

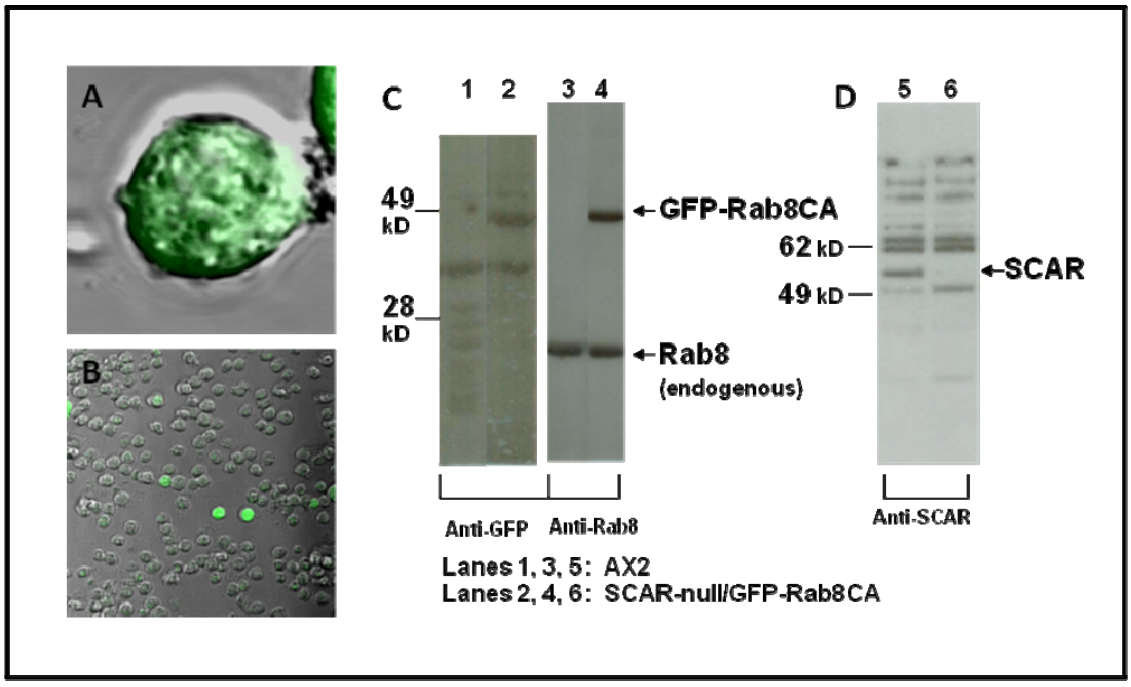

Figure 2.2. Expression of GFP-Rab8CA in SCAR-null Cells. The GFP-Rab8CA cDNA conferring G418 resistance was transfected into SCAR-null cells. (A-B) Fluorescence microscopy using a Zeiss LSM 510 confocal microscope was used to confirm GFP-Rab8CA expression. Cells do not display dendritic-like extensions. (C)Western blot analysis with antibodies to Rab8 and GFP were used to confirm expression of the chimeric GFP-Rab8CA protein. (D) Western blot analysis with an antibody to SCAR/WAVE was used to confirm knockout of SCAR.

AX2 cells were transfected with N-terminal HA epitope tagged dominant negative RacF2. Stable clones were selected with 20 μg/ml of G418. Clones were obtained and subjected to limited dilution cloning. The resulting HA-RacF2DN cell line was then transfected with an N-terminal green fluorescent protein (GFP) fusion of constitutively active Rab8. Stable clones that expressed both HA-RacF2DN and GFP-Rab8CA were

selected with 20 μg/ml G418 and 75 μg/ml of hygromycin, and isolated by limited dilution cloning. Each clone was examined using fluorescence microscopy (Figure 2.3, A-B) for expression of the GFP-Rab8CA chimeric protein. Cells did not display dendritic-like extensions. Expression was verified by Western blot analysis (Figure 2.3 C) using primary antibodies to GFP and Rab8. Expression of the HA-tagged RacF2DN protein was confirmed by Western blot analysis using a primary antibody to the HA epitope (Figure 2.3 D).

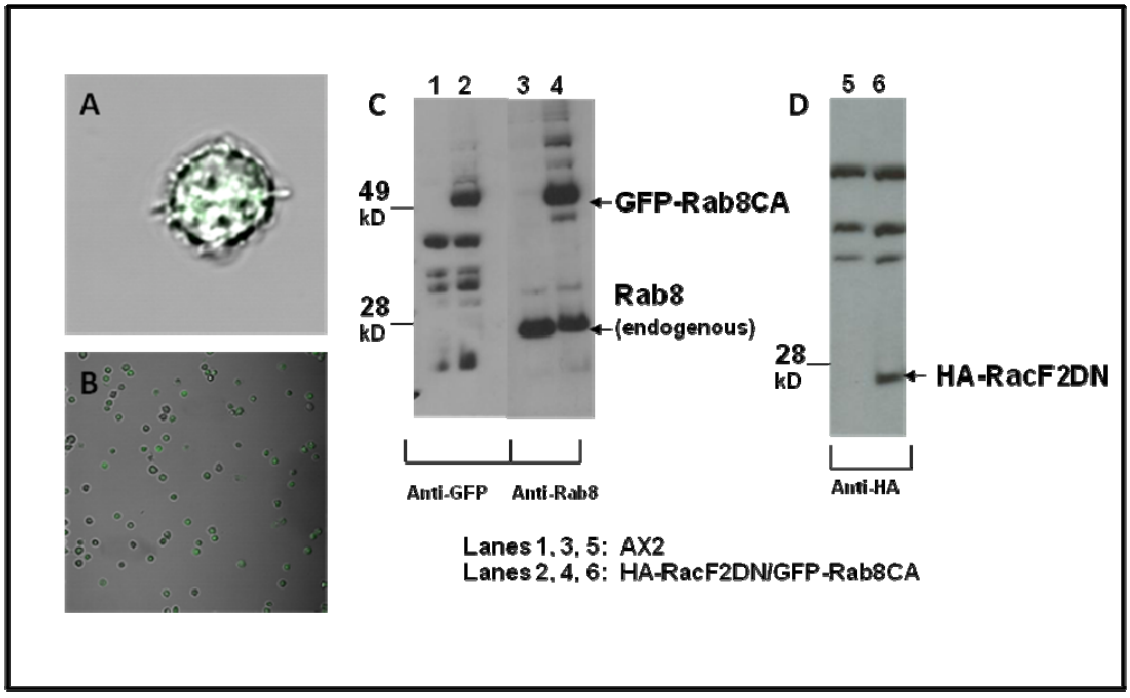

Figure 2.3. Expression of HA-RacF2DN/GFP-Rab8CA. (A-B) Fluorescence microscopy using a Zeiss LSM 510 confocal microscope was used to confirm GFP-Rab8CA expression. Cells do not display dendritic-like extensions. (C)Western blot analysis with antibodies to Rab8 and GFP was used to confirm expression of the chimeric GFP-Rab8CA protein. (D) Western blot analysis with an antibody to HA was used to confirm expression of the HA-tagged RacF2DN protein.

Cells expressing GFP-RabCA were transfected with N-terminal HA epitope tagged wildtype RacF2. Stable clones that expressed both HA- RacF2WT and GFP-Rab8CA were selected with 20 μg/ml G418 and 75 μg/ml of hygromycin, and isolated by limited dilution cloning. Each clone was examined using fluorescence microscopy (Figure 2.4, A-B) for expression of the GFP-Rab8CA chimeric protein. Cells do not display dendritic-like extensions. Expression was verified by Western blot analysis (Figure 2.4 C) using primary antibodies to GFP and Rab8. Expression of the HA-tagged RacF2WT protein was confirmed by Western blot analysis using a primary antibody to the HA epitope (Figure 2.4 D).

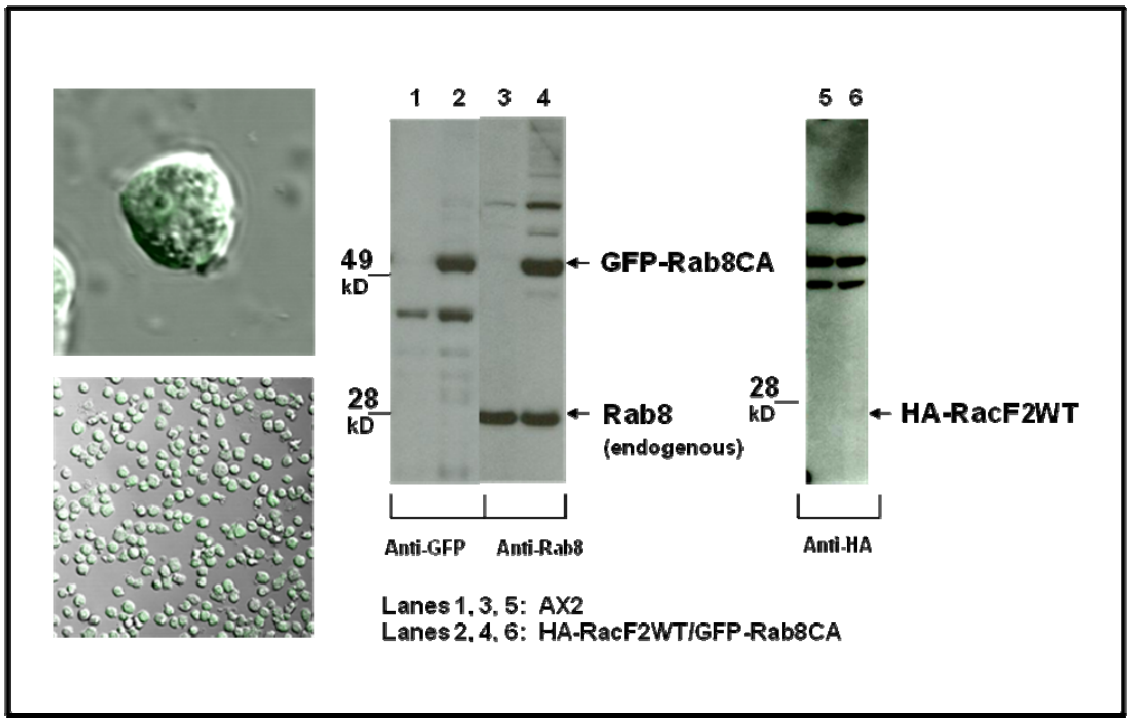

Figure 2.4. Expression of HA-RacF2WT/GFP-Rab8CA. (A-B) Fluorescence microscopy using a Zeiss LSM 510 confocal microscope was used to confirm GFP-Rab8CA expression. Cells do not display dendritic-like extensions. (C)Western blot analysis with antibodies to Rab8 and GFP was used to confirm expression of the chimeric GFP-Rab8CA protein. (D) Western blot analysis with an antibody to HA was used to confirm expression of the HA-tagged RacF2WT protein.

Disruption of SCAR rescues Rab8CA aggregation defect

As previously reported, the GFP-Rab8CA expressing cells have an aggregation defect. Powell and Temesvari reported that cells expressing Rab8CA do not aggregate by 15 hours of development (Figure 2.5 A-B) (Powell and Temesvari, 2004). It was hypothesized that the formation of actin-rich protrusions in the Rab8CA expressing cells could be the reason for this defect in aggregation. Therefore, we expressed GFP-Rab8CA in a SCAR-null background AX2 strain of *D. discoideum*. SCAR is known to participate in restructuring of the actin cytoskeleton (Suetsugu, Miki, and Takenawa, 1999; Ward,

Wu, and Rao, 2004). Interestingly, when we expressed GFP-Rab8CA in the SCAR null cells, the ability to aggregate was restored (Figure 2.5 C-D), suggesting a functional interaction between SCAR and Rab8.

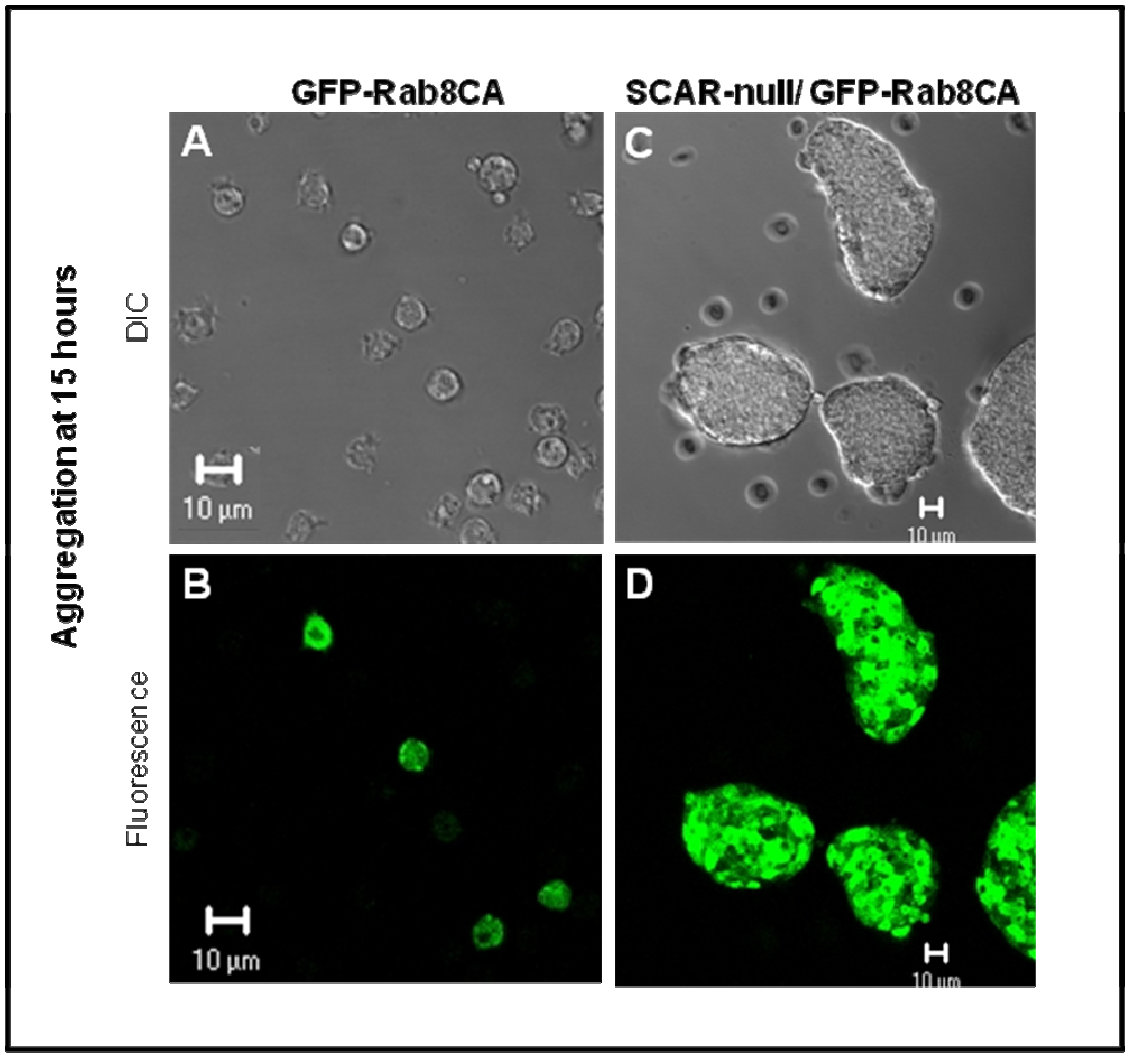

Figure 2.5. Disruption of SCAR Rescues GFP-Rab8CA Aggregation Defect. AX2 cells expressing GFP-Rab8CA and SCAR-null cells expressing GFP-Rab8CA were developed for 15 hours and examined for aggregation. The GFP-Rab8CA expressing cells failed to aggregate (A-B); however, this aggregation defect was rescued when GFP-Rab8CA was expressed in a SCAR-null background strain of AX2 (C-D).

RacF2DN rescues Rab8CA aggregation defect

Rac has been shown to activate SCAR/WAVE through a pentaheteroprotein complex. Inactive SCAR/WAVE exists in a complex with PIR121, Abi2, and HSPC300. Activated Rac1 leads to the disassociation from the complex and the subsequent

activation of SCAR/WAVE (Caracino, Jones, *et al.*, 2007; Eden, Rohatgi, *et al.*, 2002). Therefore, it was hypothesized that Rab8 may lie upstream of Rac in a signaling pathway. Because the SCAR-null cells expressing GFP-Rab8CA restored the ability to aggregate, we hypothesized that the cause of the aggregation defect in the GFP-Rab8CA expressing cells could be the presence of excessive actin protrusions due to aberrant signaling through SCAR. Since Rac1 has been shown to lie directly upstream of activated SCAR/WAVE, we further hypothesized that Rab8 may lie upstream of Rac1 (Figure 2.6).

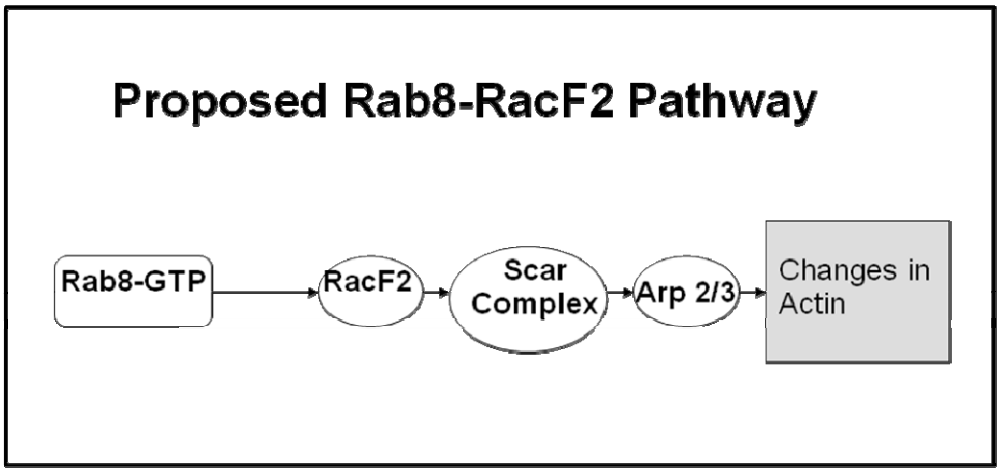

Figure 2.6. Proposed Rab8-RacF2 Pathway. The changes in actin associated with the expression of GFP-Rab8CA may be the result of aberrant signaling through SCAR. SCAR is most likely activated through a Rac protein, such as RacF2. Therefore, Rab8 may lie upstream of RacF2.

Based on this hypothesis, we decided to examine if the expression of a dominant negative version of Rac could also rescue the aggregation defect in cells expressing GFP-Rab8CA. There are 15 described, and 3 additional putative, Rac homologues in *D. discoideum* (Muramoto and Urushihara, 2006). As such, we examined the developmental

phenotypes of several Racs to identify a candidate Rac homologue. According to the study conducted by Muramoto and Urushihara (Muramoto and Urushihara, 2006), RacF2DN expressing mutants display a developmental phenotype very similar to that of cells expressing GFP-Rab8DN. During development, cells expressing either RacF2DN or Rab8DN display EDTA-sensitive aggregation and increased levels of adhesion. In addition, cells expressing these proteins first form large aggregates, which subsequently break apart into smaller aggregates as development progresses (Muramoto and Urushihara, 2006; Powell and Temesvari, 2004). Based on this, we selected RacF2 as the candidate Rac homologue for this study. When we expressed HA-RacF2DN and GFP-Rab8CA together, aggregation was restored (Figure 2.7). This suggests a functional interaction between RacF2 and Rab8.

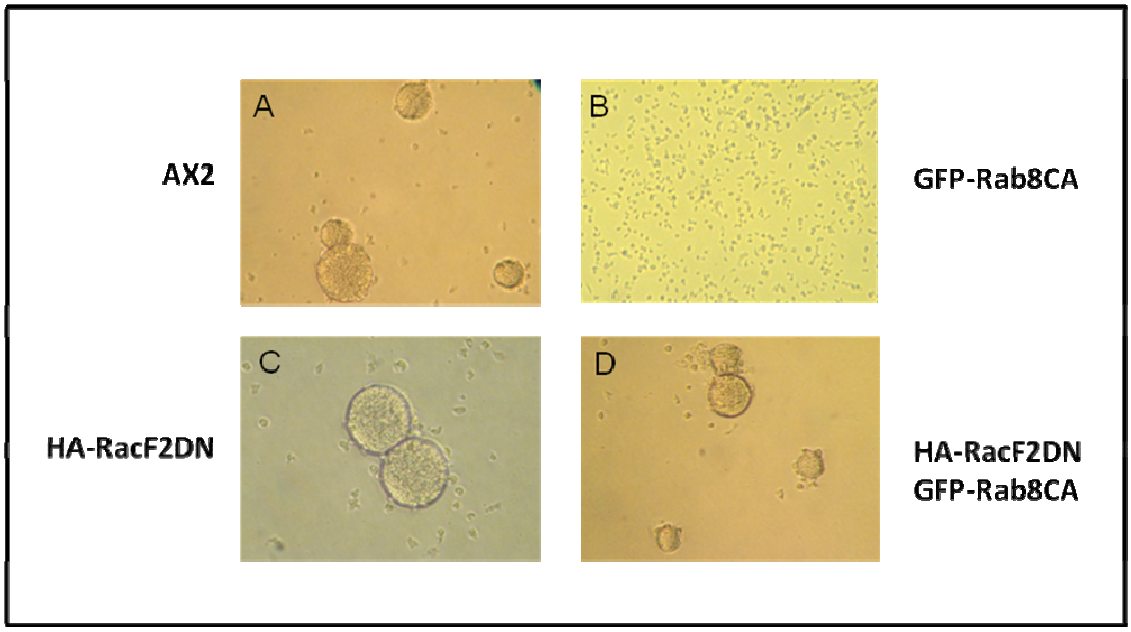

Figure 2.7. Expression of HA-RacF2DN Rescues GFP-Rab8CA Aggregation Defect. Parental AX2 cells, AX2 cells expressing GFP-Rab8CA, AX2 cells expressing HA-RacF2DN and AX2 cells expressing both HA-RacF2DN and GFP-Rab8CA were developed for 15 hours and examined for aggregation. The AX2 cells (A) and the AX2 cells expressing HA-RacF2DN (C) aggregated normally. The GFP-Rab8CA expressing cells failed to aggregate (B); however, this aggregation defect was rescued when GFP-Rab8CA was expressed with HA-RacF2DN (D).

Timed aggregation series demonstrates Rab8CA delayed aggregation phenotype

We observed that cells expressing GFP-Rab8CA displayed an aggregation defect when allowed to develop for 15 hours. However, if allowed to develop for 24 hours, the GFP-Rab8CA expressing cells were able to complete aggregation. Therefore, we performed a timed series of aggregations in order to determine the amount of time that the GFP-Rab8CA expressing cells were delayed in aggregating. A series of aggregations were set up and examined every two hours from 12 hours of development to 20 hours of development (Figure 2.8). The parental AX2 cell line, as well as cells expressing HA-

RacF2DN, HA-RacF2DN and GFP-Rab8CA, and SCAR null cells expressing GFP-Rab8CA, all formed aggregates by 12 hours of development. The GFP-Rab8CA expressing cells did not form aggregates until 18 hours of development, indicating an aggregation delay of approximately 6 hours.

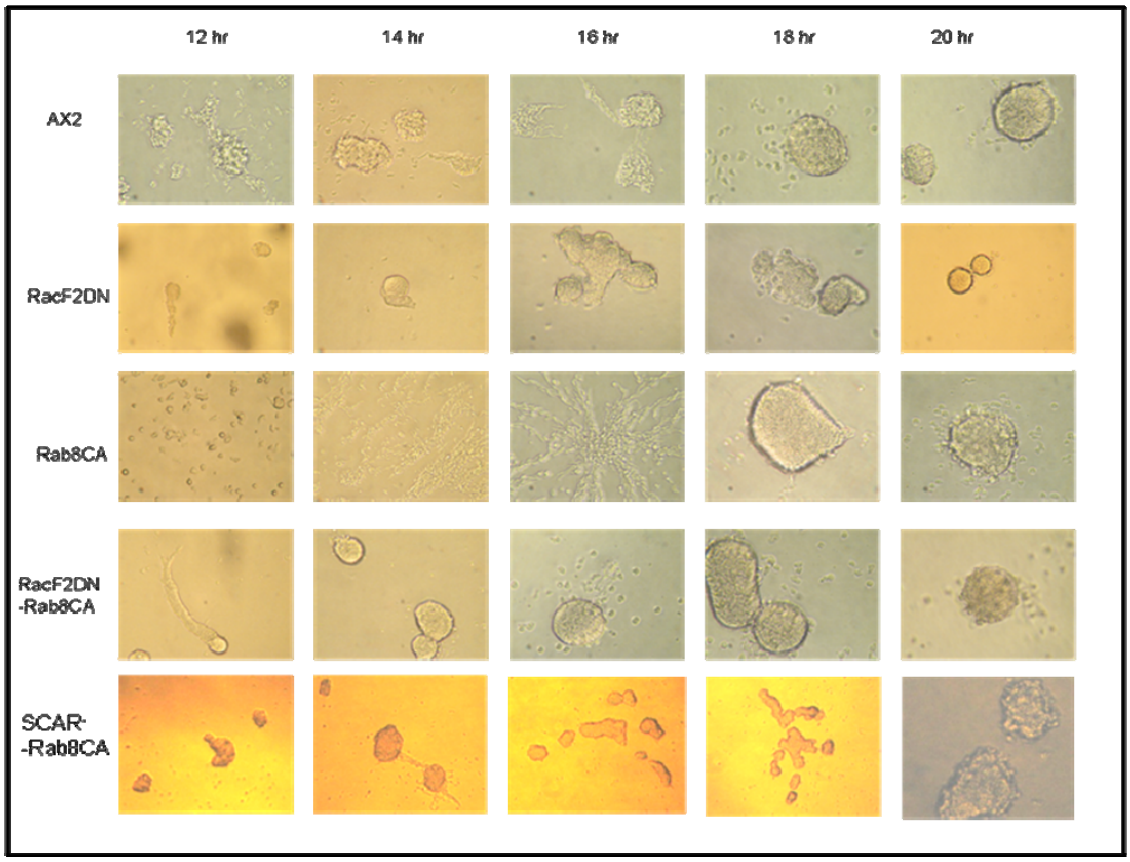

Figure 2.8. Timed Aggregation Series from 12 to 20 Hours of Development. The parental AX2 cell line, as well as cells expressing HA-RacF2DN, HA-RacF2DN and GFP-Rab8CA, and SCAR null cells expressing GFP-Rab8CA, all formed aggregates by 12 hours of development. The GFP-Rab8CA expressing cells did not form aggregates until 18 hours of development, indicating an aggregation delay of approximately 6 hours.

Timed aggregation series demonstrates Rab8DN, RacF2DN and RacF2DN/Rab8CA precocious aggregation phenotype

The AX2 cells formed loose aggregates by 12 hours of development (Figure 2.8). The SCAR null, GFP-Rab8CA expressing cells had formed tight aggregates by 12 hours of development. However, the cells expressing RacF2DN had formed tight aggregates with thick, tail-like streams of cells. We next examined several mutant strains for precocious development, or aggregation occurring sooner than 12 hours as seen in the parental AX2 cell line (Figure 2.9). The SCAR null cells expressing GFP-Rab8CA aggregated after 10 hours of development, only slightly ahead of the parental AX2 cells, which aggregated by 12 hours. The cells expressing HA-RacF2DN, both alone and with GFP-Rab8CA, aggregated by 8 hours of development, approximately 4 hours sooner than the parental AX2 cells. Meanwhile, the GFP-Rab8DN expressing cells were completely aggregated after only 6 hours of development. Powell and Temesvari demonstrated that cells expressing GFP-Rab8DN have higher levels of the calcium-dependent adhesion molecule, gp24 (Powell and Temesvari, 2004). Adhesion studies of cells expressing RacF2DN suggest that RacF2 interacts with gp24 (Muramoto and Urushihara, 2006). Therefore, it is possible that Rab8 interacts with RacF2 to mediate calcium dependent cell-cell adhesion through gp24.

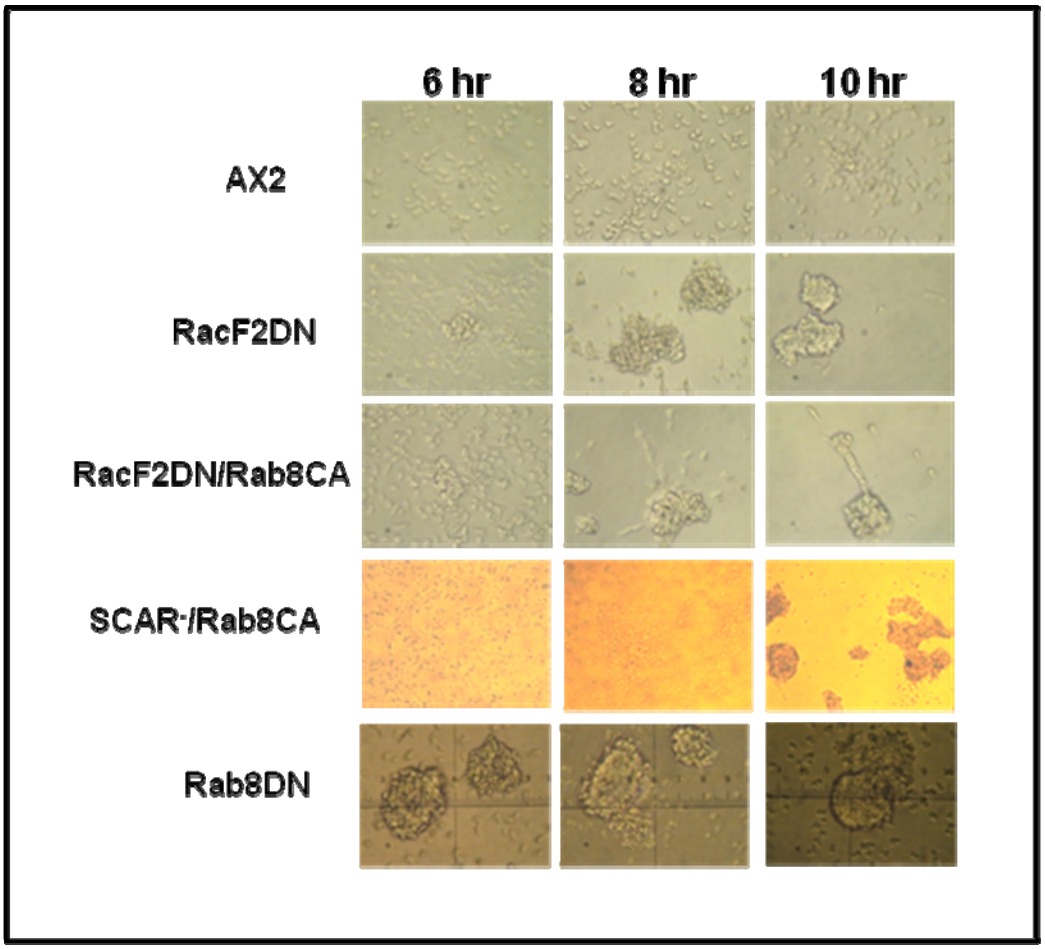

Figure 2.9. Timed Aggregation Series from 6 to 10 Hours of Development. The parental AX2 cell line showed no aggregation by 10 hours of development. By 10 hours of development, the SCAR null cells expressing GFP-Rab8CA had formed aggregates. The cells expressing HA-RacF2DN, and the cells expressing HA-RacF2DN and GFP-Rab8CA together, formed aggregates by 8 hours of development. The cells expressing GFP-Rab8DN formed aggregates by 6 hours of development.

Rab8CA and RacF2 interaction

In order to determine if Rab8CA and RacF2 interact, we performed HA-RacF2 pulldown assays using commercially available HA-antibody linked agarose beads. Cell lysates from parental AX2 cells, and cells expressing GFP-Rab8CA, HA-RacF2DN, HA-RacF2DN/GFP-Rab8CA, and HA-RacF2WT/GFP-Rab8CA, were incubated with the

HA-antibody linked agarose beads. The proteins eluted from the beads were resolved using SDS-PAGE and examined by Western blot analysis with a primary antibody to Rab8 (Figure 2.10). Control cell lysate from cells expressing GFP-Rab8CA demonstrated that GFP-Rab8CA and endogenous Rab8 were present; however, neither was present in the pulldown sample. Control cell lysates from cells expressing HA-RacF2DN showed that endogenous Rab8 was present; however, endogenous Rab8 was not present in the pulldown sample. In cell lysates and pulldowns from cells expressing HA-RacF2DN or HA-RacF2WT with GFP-Rab8CA, both GFP-Rab8CA and endogenous Rab8 were present. These results indicate that RacF2DN and RacF2WT interact with GFP-Rab8CA. This may indicate that Rab8 and RacF2 function in a complex, perhaps in association with transport vesicles, for the delivery of gp24 to the cell surface. Further studies to identify cellular localization of Rab8 and RacF2 and their association with gp24 will be necessary to elucidate this potential gp24 trafficking pathway.

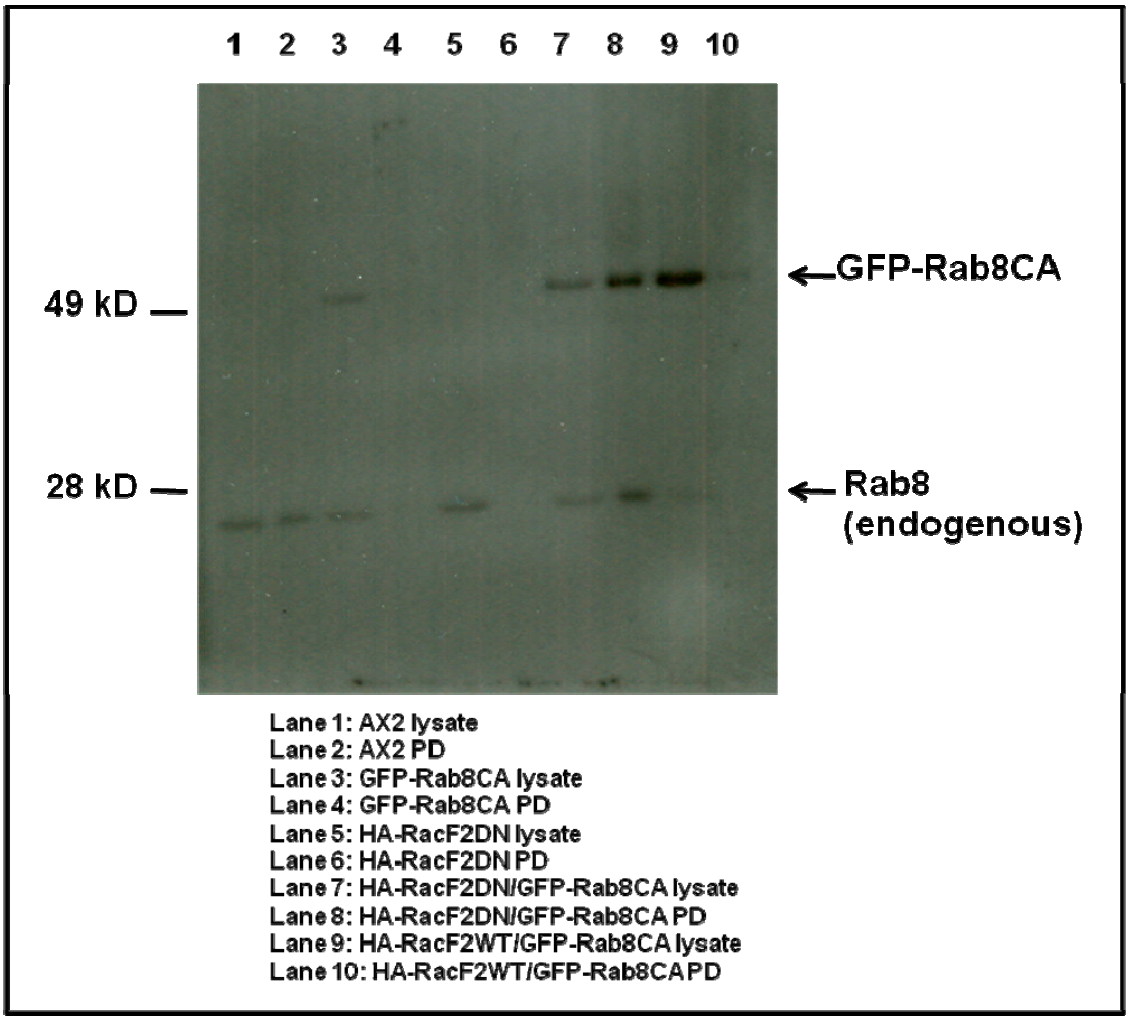

Figure 2.10. HA-RacF2 Pulldown Assay with Rab8 Antibody. Cell lysates were incubated with HA antibody-linked agarose beads. Western blot analysis was performed with a primary antibody to Rab8 in order to determine if HA-RacF2 and GFP-Rab8CA interact. Endogenous Rab8 is present in all of the lysates. GFP-Rab8CA is present in cell lysates from cells expressing GFP-Rab8 alone or with HA-RacF2DN or HA-RacF2WT. Pulldown samples show the presence of GFP-Rab8CA in cells expressing GFP-RabCA with HA-RacF2DN or HA-RacF2WT, but not in the parental AX2 cells or in cells expressing GFP-Rab8CA alone or HA-RacF2DN alone.

In addition, to determine if RacF2 and SCAR interact, lysates and eluted proteins from parental AX2 cells, and cells expressing GFP-Rab8CA, HA-RacF2DN, HA-RacF2DN/GFP-Rab8CA, and HA-RacF2WT/GFP-Rab8CA were resolved by SDS-PAGE and examined by Western blot analysis using a primary antibody to SCAR (Figure 2.11). While SCAR was present in the cell lysates (faint bands), none was present in the eluted protein samples from the HA-antibody pulldown. Therefore, it is unlikely that RacF2 interacts with SCAR.

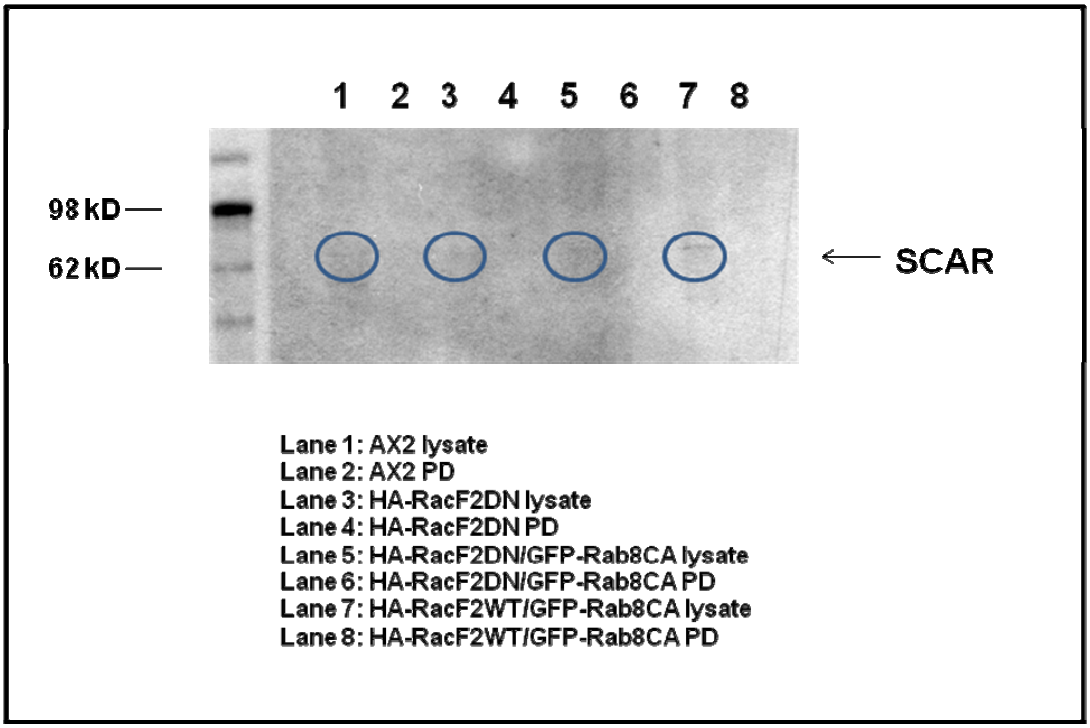

Figure 2.11. HA-RacF2 Pulldown Assay with SCAR Antibody. Cell lysates were incubated with HA antibody-linked agarose beads. Western blot analysis was performed with a primary antibody to SCAR in order to determine if HA-RacF2 and SCAR interact. SCAR is present in all of the lysates (circles indicate the positions of very faint bands). However, SCAR is not seen in any of the pulldown samples.

SCAR null rescues actin protrusion formation in Rab8CA expressing cells under starvation conditions

The disruption of SCAR is able to rescue the aggregation delay seen in cells expressing GFP-Rab8CA. Because SCAR directly mediates changes in actin organization through the Arp2/3 complex, it most likely mediates its developmental effects in cells expressing GFP-Rab8CA through this process. Expression of GFP-Rab8CA induces the formation of membrane extensions that are concentrated in one or several locations on the cells. This is accompanied by concentration of most of the F-actin in polarized cellular protrusions (Figure 2.12 C,D) under both nutrient (Figure 2.12 C) and starvation (Figure 2.12 D) conditions. SCAR null/GFP-Rab8CA and HA- RacF2DN/GFP-Rab8CA cells showed the persistence of these F-actin-rich, polarized protrusions under nutrient conditions (Figure 2.12 E, G). However, under starvation conditions, HA-RacF2DN/GFP-Rab8CA cells showed the persistence of F-actin-rich, polarized protrusions, while, SCAR null/GFP-Rab8CA cells showed cortical actin localized at the cell periphery (Figure 2.12 F,H), as seen in the AX2 parental cell line (Figure 2.12 B). These results suggest that Rab8 and SCAR may functionally interact during early development to coordinate changes in actin.

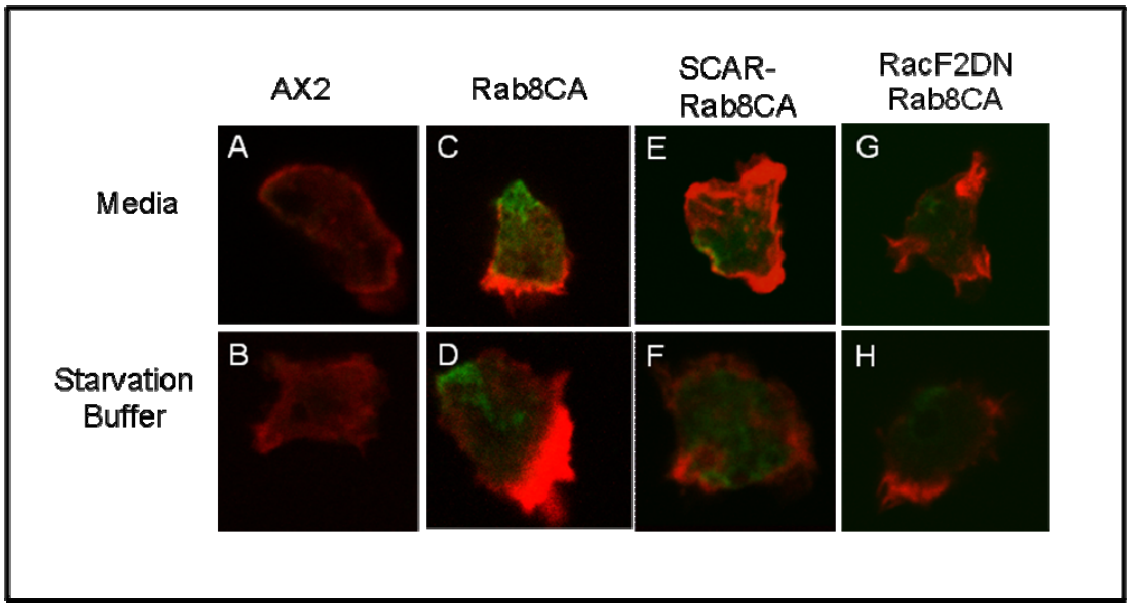

Figure 2.12. Comparison of Actin-rich Protrusions in Cells Incubated in Media and Starvation Buffer. Cells expressing GFP-Rab8CA show polarized, actin-rich protrusions in media and in starvation buffer. These protrusions are not present in the parental AX2 cells. SCAR- null cells expressing GFP-Rab8CA show actin-rich protrusions at several locations when in nutrient media; however, these protrusions are not present when cells are incubated in starvation buffer. Cells expressing both HA-RacF2DN and GFP-Rab8CA show actin-rich protrusions at several locations both in nutrient media and in starvation buffer.

cAR2 Expression is normal in Rab8CA mutants

SCAR, or suppressor of cAMP receptor, was first identified in *D. discoideum* during a genetic screening. The identified WASp-related protein acts as a suppressor of the defect caused by the loss of the *D. discoideum* cAMP receptor, cAR2. The absence of cAR2 causes disruption of tip formation during development. By disrupting SCAR in cAR2 null cells, normal tip formation was restored (Bear, Rawls, and Saxe, 1998). Because the disruption of SCAR rescues the aggregation defect seen in cells expressing GFP-Rab8CA, we examined the levels of the cAR2 receptor in the parental AX2 cells and cells expressing GFP-Rab8CA. Western blot analysis was performed with a primary

antibody to cAR2 (gift of Dr. Karl Saxe, American Cancer Society, Atlanta, GA, USA) in order to examine cellular cAR2 levels (Figure 2.13). A non-specific band at ~27 kD serves as an internal load control. There were no apparent differences in the overall cellular levels of cAR2 seen between the two cell lines, indicating that cAR2 levels most likely do not play a role in the aggregation defect seen the cells expressing GFP-Rab8CA.

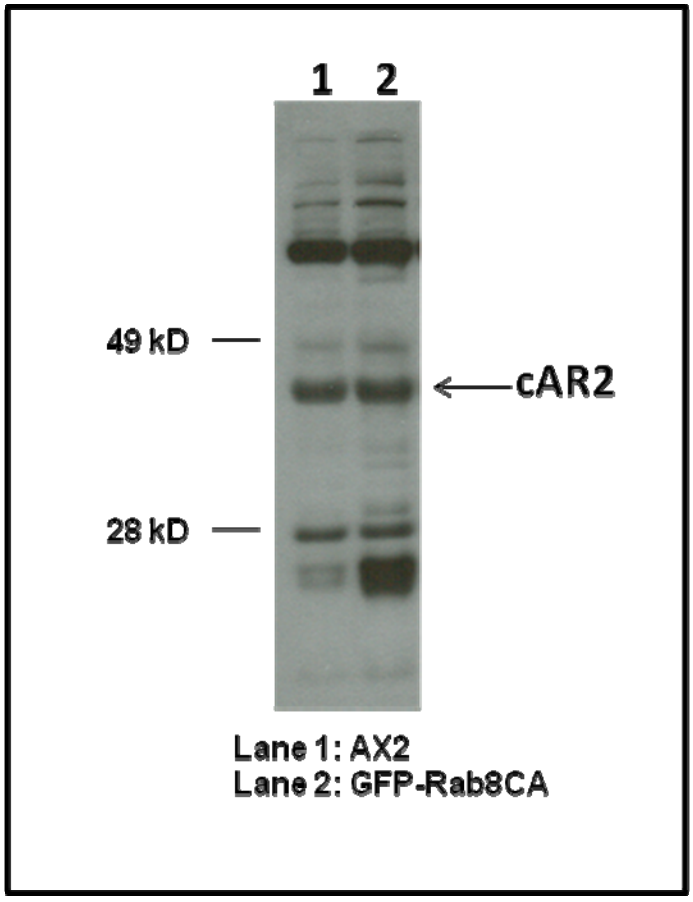

Figure 2.13. cAR2 levels in AX2 and Rab8CA cells. Western blot analysis with an antibody to cAR2 was performed to examine cAR2 levels in AX2 cells and cells expressing GFP-Rab8CA. A non-specific band at ~ 27 kD acts as an internal load control. No difference was detectable in cAR2 levels.

Rab8 mutant cell lines do not demonstrate defects in general motility

Because the expression of Rab8CA has such dramatic effects on the actin cytoskeleton, we wondered if the delayed aggregation phenotype seen in GFP-RabCA expressing cells was due to a motility impairment. In order to determine if the cells expressing GFP-Rab8CA or GFP-Rab8DN had a general motility defect, we examined time lapse video of cells. Time lapse videos were generated using a Nikon Eclipse Ti-E Confocal Microscope (Nikon, Lewisville, TX) by taking one frame every 5 seconds for 10 minutes. The resulting videos were analyzed using Nikon NIS Elements Software 2-D Tracking (Nikon, Lewisville, TX) (Figure 2.14 A-C). Ten cells were randomly chosen from each field for tracking analysis. The motility index of each cell was calculated as the distance the cell moved from its origin divided by the total path length of the cell (Figure 2.14 D). Based on this index, there were no significant differences in general motility of cells expressing either GFP-Rab8CA or GFP-Rab8DN from the AX2 parental cells. This indicates that Rab8 does not affect general motility of the cells.

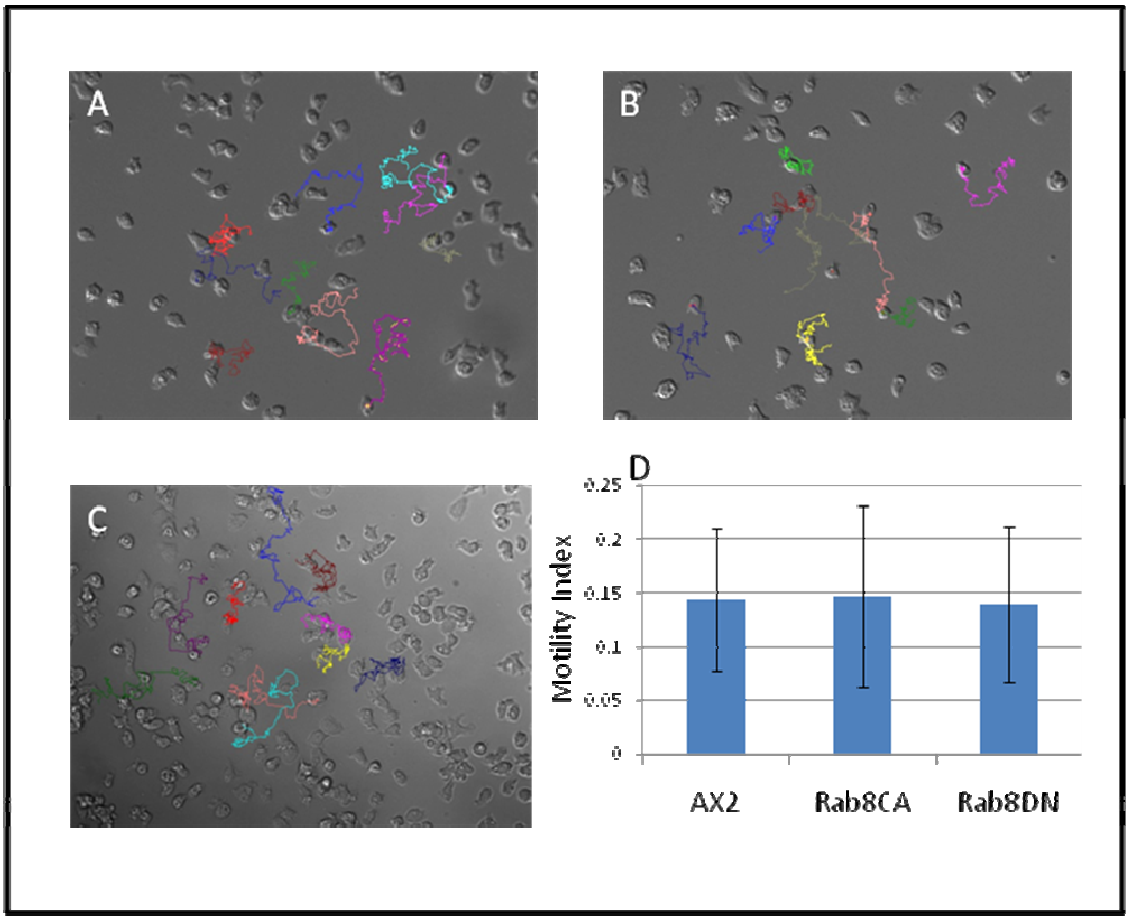

Figure 2.14. Cell Motility Index. Time lapse videos of parental AX2 cells (A) and cells expressing GFP-Rab8CA(B) or GFP-Rab8DN(C) were analyzed by 2-D tracking of individual cells. The motility index (D) was calculated as the (distance from the origin)/(total path length). Values presented are the mean (± SD) of ten cells.

Rab8DN, RacF2, and RacF2/Rab8CA cells demonstrate enhanced cell-cell contact

While examining the time lapse videos for general cell motility, we noticed an interesting difference in the cells expressing GFP-Rab8CA as compared to the other cell lines used in this study. The cells expressing GFP-Rab8CA appeared to be in contact with each other less frequently than the other cell types. Therefore, we examined AX2 parental cells, as well as cells expressing GFP-Rab8CA, GFP-Rab8DN, HA-RacF2DN,

HA-RacF2DN and GFP-Rab8CA, and SCAR-null cells expressing GFP-Rab8CA, for cell-cell contact levels. We examined every 50^{th} frame of the 10 minute time lapse videos and scored cells as making no contact with another cell or as contacting another cell. We then calculated the contact index of the cell lines as number of cells in contact with another cell(s)/total number of cells. Our preliminary results (Figure 2.15) indicate that cells expressing GFP-Rab8CA show significantly decreased cell-cell contact as compared to the parental AX2 cells. SCAR-null cells expressing GFP-Rab8CA demonstrate higher cell-cell contact levels than cells expressing GFP-Rab8 alone; however, these cells show a slight decrease in cell-cell contact as compared to the parental AX2 cells. Cells expressing both GFP-Rab8CA and HA-RacF2DN demonstrate significantly increased cell-cell contact compared to the parental AX2 cells. In order for adhesion to occur, cells must first make contact with one another. These results indicate that cells expressing GFP-Rab8CA are less likely to make contact with one another than the other cell lines. This may be a contributing factor to their delay in aggregation. Further studies will be necessary to establish the basis for this phenomenon.

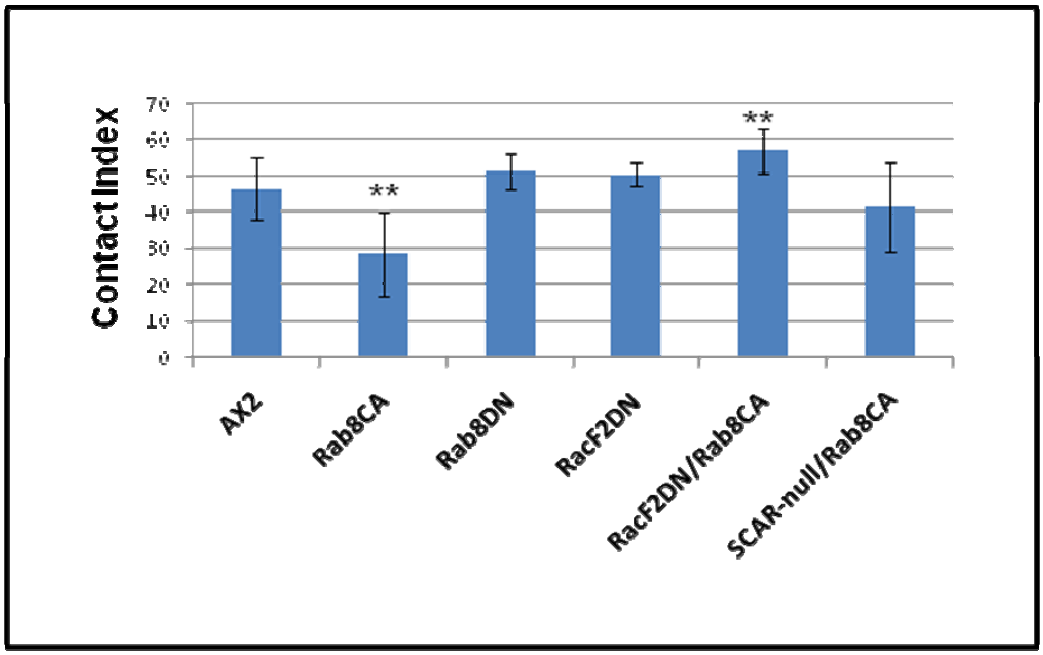

Figure 2.15. Contact Index. Cells expressing GFP-Rab8CA demonstrate significantly reduced cell-cell contact (**P<0.01). Disruption of SCAR in cells expressing GFP-Rab8CA partially rescues cell-cell contact levels. Cells expressing both GFP-Rab8CA and HA-RacF2DN demonstrate significantly enhanced cell-cell contact compared to parental AX2 levels (**P<0.01). Values presented are the mean (± SD) of 25 frames.

Rab8CA expressing Cells Demonstrate Enhanced Chemotaxis

Because general motility of cells expressing mutant versions of Rab8 was not affected, we wondered if cells expressing GFP-Rab8CA or GFP-Rab8DN could sense a cAMP gradient and carry out chemotaxis efficiently. If chemotaxis was negatively impacted by expression of GFP-Rab8CA or GFP-Rab8DN, this could affect the ability of the cells to aggregate. Chemotaxis towards cAMP is the first stage in development in *D. discoideum*, so if this process is negatively affected, aggregation may be slowed or abrogated. In order to determine if the aggregation delay in the GFP-Rab8CA expressing cells was due to a defect in chemotaxis, we performed under-agarose cAMP chemotaxis

assays as described by Woznica and Knecht (Eichinger and Rivero, 2006). Petri dishes with 1.5% agarose in developmental buffer were used for the assays. The cells were placed in two wells on either side of a third well filled with 5mM cAMP (Figure 2.16 C). The plates were placed in the dark and incubated at room temperature for 1 hour. Images were taken and analyzed to determine the distance of chemotaxis. Measurements were made from the edge of the well to the leading edge of cells. The leading edge cells are measured because as these cells move, they alter the environment behind them (Eichinger and Rivero, 2006). Therefore, cells behind the leading edge do not necessarily encounter the same cAMP gradient as the leading edge cells.

Remarkably, the cells expressing GFP-Rab8CA chemotaxed significantly further (Figure 2.16 A, Figure 2.17) than the parental AX2 cells in one hour (Figure 2.16 B, Figure 2.17), while the cells expressing GFP-Rab8DN chemotaxed nearly the same distance as the parental AX2 cells (Figure 2.17) in one hour. These results indicate that expression of constitutively active Rab8, but not dominant negative Rab8, results in enhanced chemotaxis. Therefore, the aggregation delay in cells expressing GFP-Rab8CA is likely not due to a defect in their ability to sense and chemotax towards cAMP. Interestingly, we also observed that GFP-Rab8CA localizes to the lagging edge of the chemotaxing cells (Figure 2.16 D).

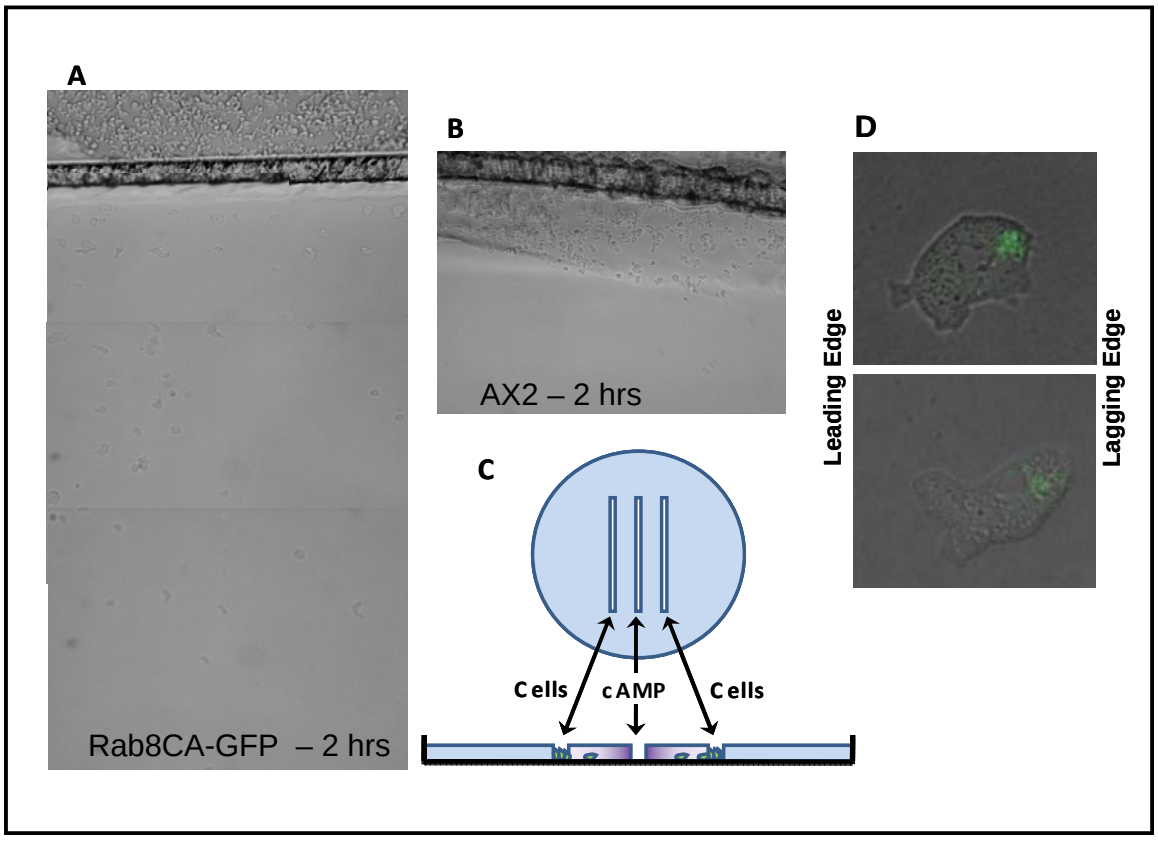

Figure 2.16. cAMP Chemotaxis Assay. Cells expressing GFP-Rab8CA (A) chemotaxed further than parental AX2 cells (B) in a one hour period. Under-agarose chemotaxis was measured by plating cells in two wells on either side of a well containing 5 mM cAMP (C). GFP-Rab8CA localizes to the lagging edge of the cell during chemotaxis towards cAMP (D).

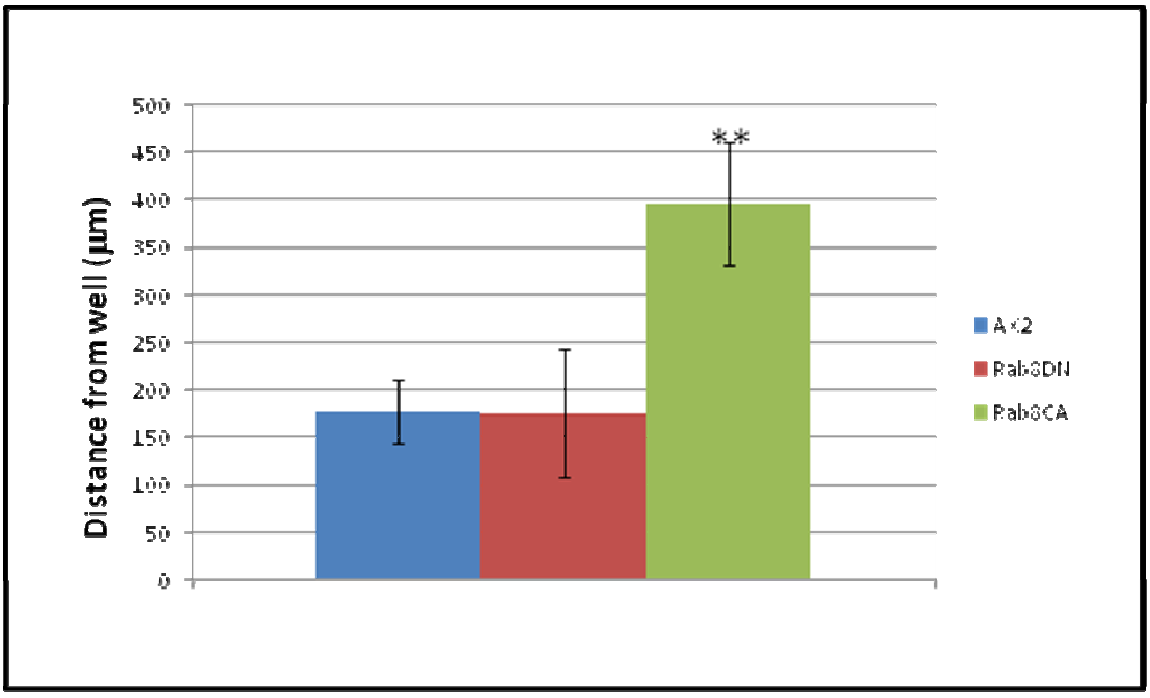

Figure 2.17. cAMP Chemotaxis Distances. Cells expressing GFP-Rab8CA chemotaxed a distance towards 5 mM cAMP that was significantly further than parental AX2 cells or cells expressing GFP-Rab8DN (**P<0.01). Values presented are the mean (± SD) of three experiments.

Discussion

We hypothesized that Rab8 may act upstream of Rac to control SCAR activity, leading to changes in the actin cytoskeleton. To this end, we have demonstrated a direct interaction between Rab8 and RacF2, which may be involved in the regulation of cellular levels of the adhesion molecule, gp24. In this study, we have also established the first genetic evidence in any cell system of a functional interaction between Rab8 and a WASp family protein, SCAR.

The expression of GFP-Rab8CA leads to the formation of polarized actin-rich protrusions and a delay in aggregation. Because the reorganization of the actin cytoskeleton is often the result of signaling through the Arp2/3 complex (Ichetovkin, Grant, and Condeelis, 2002; Millard, Sharp, and Machesky, 2004), we decided to express GFP-Rab8CA in cells with disrupted expression of SCAR. SCAR is a WASp family protein that was first identified in *D. discoideum* (Bear, Rawls, and Saxe, 1998), and is a regulator of the Arp2/3 complex (Millard, Sharp, and Machesky, 2004; Takenawa and Suetsugu, 2007). We postulated that if GFP-Rab8CA was leading to aberrant signaling through SCAR, then changes in the actin cytoskeleton would likely be the result. Additionally, if the aggregation delay in cells expressing GFP-Rab8CA was due to errant formation of actin protrusions, then, the disruption of SCAR in these cells could rescue aggregation. When we expressed GFP-Rab8CA in a SCAR-null cell line, aggregation was, in fact, restored. Therefore, the actin-rich protrusions caused by the expression of GFP-Rab8CA likely contribute to the aggregation defect seen in these cells.

Cdc42 and Rac (Cdc42/Rac) have been shown to be important activators of WASp-family proteins, including SCAR. Because Rac has been shown to be an activator of SCAR (Caracino, Jones, *et al.*, 2007; Eden, Rohatgi, *et al.*, 2002), we surmised that Rab8 would likely lie upstream of Rac in a signaling cascade leading to SCAR activation. We decided to test this idea by expressing a dominant negative version of Rac in cells expressing GFP-Rab8CA. In mammalian cells, Rac1 is responsible for the activation of SCAR (Caracino, Jones, *et al.*, 2007; Eden, Rohatgi, *et al.*, 2002). However, in *D. discoideum*, there are 15 described and 3 putative Rac homologues (Muramoto and

Urushihara, 2006). We chose to investigate the effect of expressing the dominant version of RacF2. This Rac homologue was chosen because cells expressing a dominant negative version of RacF2 (Muramoto and Urushihara, 2006) demonstrated a developmental phenotype similar to that seen in cells expressing a dominant negative version of Rab8 (Powell and Temesvari, 2004). In both cell lines, an increase in the level of the EDTA-sensitive adhesion molecule, gp24, was seen. These cells formed large aggregates, which broke apart into smaller aggregates as development progressed (Muramoto, Takeda, *et al.*, 2005; Powell and Temesvari, 2004). When we expressed the dominant negative version of RacF2 in cells expressing the constitutively active version of Rab8, aggregation was restored in these cells.

Our previous studies indicated that cells expressing GFP-Rab8CA failed to aggregate by 15 hours of development (Powell and Temesvari, 2004). We were able to rescue this aggregation defect by either disrupting SCAR or by expressing a dominant negative version of RacF2 in these cells. However, we also observed that if cells expressing GFP-Rab8CA were allowed to develop for longer than 15 hours, approximately 24 hours, they were able to form aggregates without the disruption of SCAR or the expression of the dominant negative version of RacF2. This led us to investigate the developmental timing of the mutant cell lines. By examining development over a period of time from 12 to 20 hours, we were able to determine that cells expressing GFP-Rab8CA had an aggregation delay of approximately 6 hours. In addition, we noticed that while the parental AX2 cells had developed loose aggregates by 12 hours of development, cells expressing dominant negative RacF2 had formed very tight

aggregates with thick streaming tails. This led us to investigate the developmental timing of the mutant cell lines over a period of time from 6 to 10 hours. Remarkably, cells expressing dominant negative Rab8 and dominant negative RacF2 aggregated approximately 6 to 4 hours sooner than the parental AX2 cells.

We believed that the precocious development seen in the cell lines expressing dominant negative Rab8 and dominant negative RacF2 was most likely due to an increase in cell-cell adhesion. If cells are more adherent, then, they should be able to adhere and form aggregates quicker. We have shown previously that cells expressing constitutively active Rab8 have a decreased level of cell-cell adhesion and cells expressing dominant negative Rab8 have an increased level of cell-cell adhesion as compared to the parental AX2 cell line. We have further demonstrated that cells expressing constitutively active Rab8 have lower levels of cellular and secreted gp24, while cells expressing dominant negative Rab8 have higher levels of cellular and secreted gp24 than the parental AX2 cells (Powell and Temesvari, 2004). Since cells expressing dominant negative RacF2 have been shown to have increased levels of EDTA-sensitive adherence, likely due to higher levels of gp24, it is reasonable to assume that the expression of dominant negative RacF2 rescues GFP-Rab8CA expressing cell aggregation by increasing gp24 levels. Further tests, including cell-cell adhesion assays with EDTA-treated and untreated cells, as well as Western blot analysis for intracellular and extracellular gp24 levels, to confirm that gp24 levels are higher in the HA-RacF2/GFP-Rab8CA cell line are ongoing. If these tests show that gp24 levels are restored in the GFP-RabCA expressing cells by the

expression of HA-RacF2DN, then, it is likely that RacF2 and Rab8 function together in a pathway leading to the expression and/or transport of the gp24 adhesion molecule.

As RacF2 and Rab8 clearly interact functionally, we next investigated whether or not the two proteins interacted physically. By performing pulldown assays, we have demonstrated that RacF2 and Rab8 do interact. In order to determine if the two proteins interact directly, further studies will be required. Future studies, including yeast-2-hybrid studies, are planned to determine if the interaction between RacF2 and Rab8 is direct. In mammalian cells, Rac has been shown to be involved in the recycling of cadherins to cell adherens and tight junctions (Izumi, Sakisaka, *et al.*, 2004). Rab8 has also recently been implicated in this process (Yamamura, Nishimura, *et al.*, 2008). Therefore, it is not surprising that Rab8 and the Rac homologue, RacF2, may function together to control cell-cell adherence in *D. discoideum* through the adhesion molecule, gp24.

The RacF2 interacting protein pulldown assays were also analyzed for interaction with SCAR. There was no evidence of interaction between RacF2 and SCAR. Therefore, while there is interaction between RacF2 and Rab8, it is unlikely that Rab8 and SCAR interact through a pathway that includes RacF2. Even so, the functional interaction between Rab8 and SCAR is intriguing. By disrupting SCAR in cells expressing GFP-Rab8CA, aggregation occurs by 10 hours, which is similar to the parental AX2 cells, which aggregate by 12 hours. To investigate if disrupting SCAR abrogated the formation of polarized, actin-rich protrusions seen in GFP-Rab8CA expressing cells, we used AlexaFluor 594-conjugated phalloidin to stain filamentous actin. We initially stained cells in nutrient medium. In the cells expressing GFP-Rab8CA, regardless of SCAR

disruption, the actin-rich protrusions persisted. However, SCAR activation has been shown to differ in fed, vegetative cells compared to starved, developing cells (Pollitt, Blagg, *et al.*, 2006). Therefore, we decided to stain cells that had been starved for 5 hours. While the cells expressing GFP-Rab8CA alone or with HA-RacF2DN continue to show actin-rich protrusions, the SCAR null cells expressing Rab8CA show only cortical actin staining, as seen in the parental AX2 cells. Therefore, it is likely that Rab8 and SCAR functionally interact in the control of actin dynamics during early development. The exact mechanism for this interaction is still to be determined. Even so, this is the first time that Rab8 has been functionally linked to a WASp family protein in any cell system. Further studies involving the expression of dominant negative versions of additional Rac homologues may lead to the elucidation of this potential pathway.

Our initial hypothesis was that Rab8 may work upstream of RacF2 to activate the WASp family protein, SCAR, in order to cause changes in the actin cytoskeleton (Figure 2.18, 1A). Our results indicate that Rab8 interacts directly with RacF2 to effect changes in cell-cell adhesion, likely through the cell-cell adhesion molecule, gp24; however, RacF2 does not interact directly with SCAR (Figure 2.18, 2A, B). Even so, our results indicate that actin-rich protrusions are likely a result of Rab8-GTP causing aberrant signaling through SCAR. Therefore, Rab8 may function upstream of a different Rac to effect changes in SCAR activation, which may lead to the formation of actin-rich protrusions (Figure 2.18, 2B). We also cannot rule out that Rab8 may be involved in the vesicle trafficking of a signaling molecule, which could, in turn, activate Rac (Figure 2.18, 1B). In addition, Rab8 may interact directly with SCAR, or may interact directly

with the Arp2/3 complex, independent of SCAR. Further studies including pulldown assays and spent media exchange development assays will be necessary to evaluate these possible pathways.

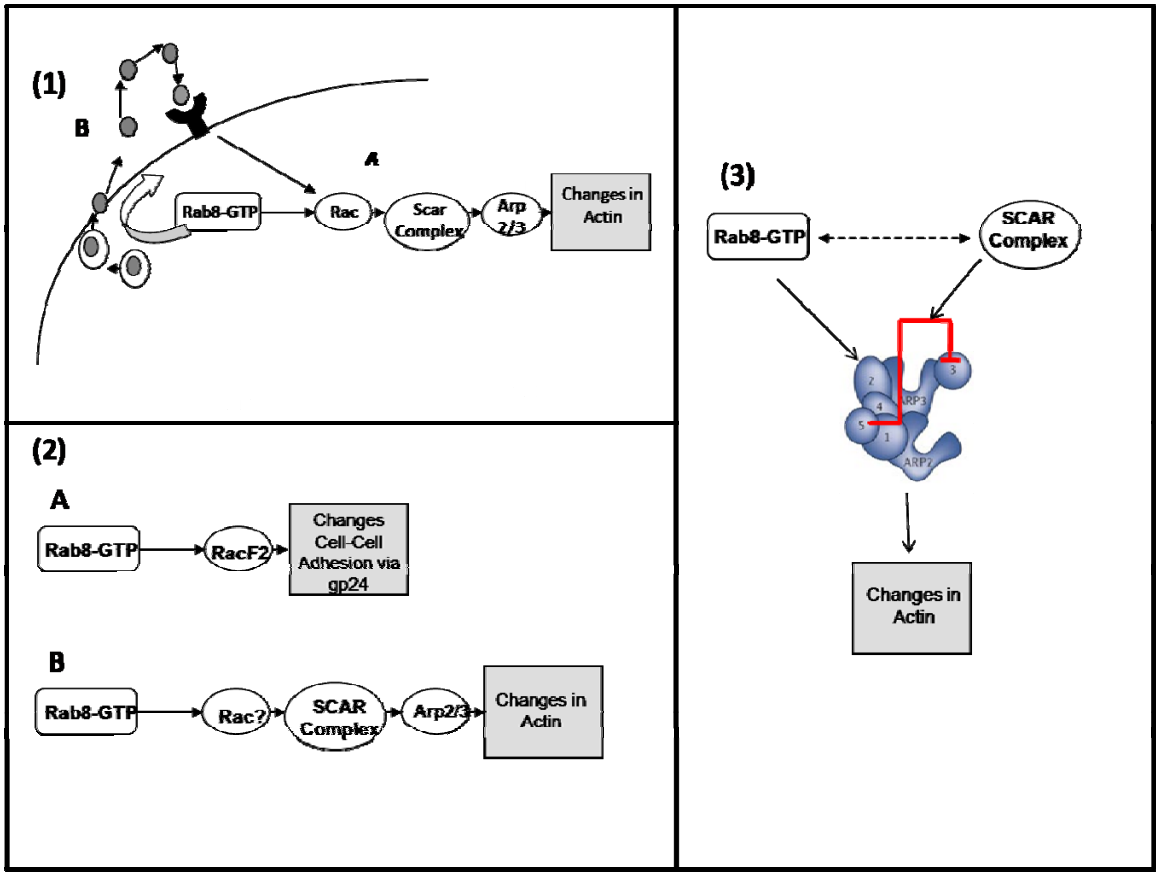

Figure 2.18. Possible Rab8-GTP Signaling Pathways in *Dictyostelium discoideum*. (1A) Rab8-GTP may act directly upstream of Rac to activate the WASp family protein, SCAR, which activates the Arp2/3 complex, causing changes in actin . (1B) Alternatively, Rab8-GTP may enhance the vesicle trafficking and secretion of a signaling molecule that binds to cell surface receptors, which, in turn, activate Rac. (2A) The results of this study indicate that Rab8-GTP binds directly to RacF2, which may lead to increased cell-cell adhesion through the regulation of the EDTA-sensitive, cell-cell adhesion molecule, gp24. (2B) The results of this study do not provide clear evidence that RacF2 acts directly to activate SCAR. However, results do indicate that actin-rich protrusions are likely a result of Rab8-GTP causing aberrant signaling through SCAR. Therefore, Rab8-GTP may act upstream of a different *Dictyostelium discoideum* Rac to activate SCAR and effect changes in actin. (3) We also cannot rule out the fact that Rab8-GTP may interact directly with SCAR. We also cannot rule that Rab8-GTP may interact directly, independent of SCAR, with the Arp2/3 complex to effect changes in actin. Arp2/3 complex adapted from Goley & Welch, 2006.

Because the disruption of SCAR leads to the disappearance of actin-rich protrusions in cells expressing GFP-Rab8CA during early development, we began to question how these actin-rich protrusions might contribute to the aggregation delay seen in these cells. We postulated that changes in actin could hinder aggregation by altering general motility or directed chemotactic movement towards cAMP. From our analysis of general motility using time lapse video, no significant difference in general motility is seen in cells expressing mutant versions of Rab8 as compared to the parental AX2 strain; however, when under-agarose chemotaxis experiments were performed, cells expressing GFP-Rab8CA chemotaxed towards a cAMP source at a significantly higher rate than cells expressing GFP-Rab8DN or the parental AX2 cells. Interestingly, cells expressing GFP-Rab8DN did not differ significantly from the parental AX2 cells in chemotactic rate. Therefore, while it is possible that cells expressing GFP-Rab8CA are more sensitive to cAMP, perhaps due to increased trafficking of cAMP receptors to the leading edge, it is also likely that the ability of the GFP-Rab8CA expressing cells to polarize actin may give them an advantage in directed movement.

We have shown previously that cells expressing GFP-Rab8DN do not display polarized, actin-rich protrusions as those expressing GFP-Rab8CA, but instead, demonstrate cortical actin staining as seen in parental AX2 cells (Powell and Temesvari, 2004). Future chemotaxis studies using the SCAR null cells expressing GFP-Rab8CA could help elucidate whether the ability to polarize actin gives the GFP-Rab8CA expressing cells an advantage in directed movement. In addition, it would be interesting to measure the kinetics of actin polarization in GFP-Rab8CA expressing cells during

chemotaxis using an RFP-actin expression vector. Based on this information, we concluded that the cells expressing GFP-Rab8CA did not have delayed aggregation due to a chemotactic or general motility defect.

In conclusion, we have established a functional and interactive link between Rab8 and RacF2, which likely mediates early cell-cell adhesion through the regulation of the adhesion molecule, gp24. Additionally, we have established the first functional interaction between Rab8 and a WASp family protein, SCAR, in any cell system. These studies greatly advance our understanding of the trafficking role of Rab8, as well as its "moonlighting" role as a regulator of actin remodeling.

References

Bear, J.E., Rawls, J.F., and Saxe, C.L.,3rd. (1998). SCAR, a WASP-related protein, isolated as a suppressor of receptor defects in late *Dictyostelium* development. *J. Cell Biol. 142,* 1325-1335.

Blagg, S.L., and Insall, R.H. (2004). Control of SCAR activity in *Dictyostelium discoideum.* Biochem. *Soc. Trans. 32,* 1113-1114.

Blagg, S.L., Stewart, M., Sambles, C., and Insall, R.H. (2003). PIR121 regulates pseudopod dynamics and SCAR activity in *Dictyostelium*. *Curr. Biol. 13,* 1480-1487.

Burns, C.G., Reedy, M., Heuser, J., and De Lozanne, A. (1995). Expression of light meromyosin in *Dictyostelium* blocks normal myosin II function. *J. Cell Biol. 130,* 605-612.

Caracino, D., Jones, C., Compton, M., and Saxe, C.L.,3rd. (2007). The N-terminus of *Dictyostelium* Scar interacts with Abi and HSPC300 and is essential for proper regulation and function. *Mol. Biol. Cell 18,* 1609-1620.

Chan, A.Y., Bailly, M., Zebda, N., Segall, J.E., and Condeelis, J.S. (2000). Role of cofilin in epidermal growth factor-stimulated actin polymerization and lamellipod protrusion. *J. Cell Biol. 148,* 531-542.

Chen, Y.T., Holcomb, C., and Moore, H.P. (1993). Expression and localization of two low molecular weight GTP-binding proteins, Rab8 and Rab10, by epitope tag. *Proc. Natl. Acad. Sci. U. S. A. 90,* 6508-6512.

Coates, J.C., and Harwood, A.J. (2001). Cell-cell adhesion and signal transduction during *Dictyostelium* development. *J. Cell. Sci. 114,* 4349-4358.

Eden, S., Rohatgi, R., Podtelejnikov, A.V., Mann, M., and Kirschner, M.W. (2002). Mechanism of regulation of WAVE1-induced actin nucleation by Rac1 and Nck. *Nature 418,* 790-793.

Eichinger, L., and Rivero, F. (2006). *Dictyostelium discoideum Protocols* (Totowa, Humana Press).

Gilbert, S.F. (2003). *Developmental Biology* (Sunderland, Massachusetts: Sinauer Associates, Inc.).

Hall, A. (2000). *GTPases* (Oxford: Oxford University Press).

Ichetovkin, I., Grant, W., and Condeelis, J. (2002). Cofilin produces newly polymerized actin filaments that are preferred for dendritic nucleation by the Arp2/3 complex. *Curr. Biol. 12,* 79-84.

Izumi, G., Sakisaka, T., Baba, T., Tanaka, S., Morimoto, K., and Takai, Y. (2004). Endocytosis of E-cadherin regulated by Rac and Cdc42 small G proteins through IQGAP1 and actin filaments. *J. Cell Biol. 166,* 237-248.

Jordens, I., Marsman, M., Kuijl, C., and Neefjes, J. (2005). Rab proteins, connecting transport and vesicle fusion. *Traffic 6,* 1070-1077.

Kuspa, A., and Loomis, W.F. (1992). Tagging developmental genes in *Dictyostelium* by restriction enzyme-mediated integration of plasmid DNA. *Proc. Natl. Acad. Sci. U. S. A. 89,* 8803-8807.

Legg, J.A., Bompard, G., Dawson, J., Morris, H.L., Andrew, N., Cooper, L., Johnston, S.A., Tramountanis, G., and Machesky, L.M. (2007). N-WASP involvement in dorsal ruffle formation in mouse embryonic fibroblasts. *Mol. Biol. Cell 18,* 678-687.

Loomis, W.F. (1975). *Dictyostelium discoideum: a Developmental System* (New York: Academic Press).

Millard, T.H., Sharp, S.J., and Machesky, L.M. (2004). Signalling to actin assembly via the WASP (Wiskott-Aldrich syndrome protein)-family proteins and the Arp2/3 complex. *Biochem. J. 380,* 1-17.

Muramoto, T., Takeda, S., Furuya, Y., and Urushihara, H. (2005). Reverse genetic analyses of gamete-enriched genes revealed a novel regulator of the cAMP signaling pathway in *Dictyostelium discoideum*. *Mechanisms of Development 122,* 733-743.

Muramoto, T., and Urushihara, H. (2006). Small GTPase RacF2 affects sexual cell fusion and asexual development in *Dictyostelium discoideum* through the regulation of cell adhesion. *Dev. Growth Differ. 48,* 199-208.

Oikawa, T., Yamaguchi, H., Itoh, T., Kato, M., Ijuin, T., Yamazaki, D., Suetsugu, S., and Takenawa, T. (2004). PtdIns(3,4,5)P3 binding is necessary for WAVE2-induced formation of lamellipodia. *Nat. Cell Biol. 6,* 420-426.

Pang, K.M., Lynes, M.A., and Knecht, D.A. (1999). Variables controlling the expression level of exogenous genes in *Dictyostelium*. *Plasmid 41,* 187-197.

Peranen, J., Auvinen, P., Virta, H., Wepf, R., and Simons, K. (1996). Rab8 promotes polarized membrane transport through reorganization of actin and microtubules in fibroblasts. *J. Cell Biol. 135,* 153-167.

Pinyol, R., Haeckel, A., Ritter, A., Qualmann, B., and Kessels, M.M. (2007). Regulation of N-WASP and the Arp2/3 complex by Abp1 controls neuronal morphology. *PLoS ONE 2,* e400.

Pollitt, A.Y., Blagg, S.L., Ibarra, N., and Insall, R.H. (2006). Cell motility and SCAR localisation in axenically growing *Dictyostelium* cells. *Eur. J. Cell Biol. 85,* 1091-1098.

Powell, R.R., and Temesvari, L.A. (2004). Involvement of a Rab8-like protein of *Dictyostelium discoideum*, Sas1, in the formation of membrane extensions, secretion and adhesion during development. *Microbiology 150,* 2513-2525.

Powell, R.R., Welter, B.H., Hwu, R., Bowersox, B., Attaway, C., and Temesvari, L.A. (2006). *Entamoeba histolytica:* FYVE-finger domains, phosphatidylinositol 3-phosphate biosensors, associate with phagosomes but not fluid filled endosomes. *Exp. Parasitol. 112,* 221-231.

Saxe, S.A., and Kimmel, A.R. (1990). SAS1 and SAS2, GTP-binding protein genes in *Dictyostelium discoideum* with sequence similarities to essential genes in *Saccharomyces cerevisiae*. *Mol. Cell. Biol. 10,* 2367-2378.

Stenmark, H., and Olkkonen, V.M. (2001). The Rab GTPase family. *Genome Biol. Reviews 3* 2007.

Suetsugu, S., Miki, H., and Takenawa, T. (1999). Identification of two human WAVE/SCAR homologues as general actin regulatory molecules which associate with the Arp2/3 complex. *Biochem. Biophys. Res. Commun. 260,* 296-302.

Takenawa, T., and Suetsugu, S. (2007). The WASP-WAVE protein network: connecting the membrane to the cytoskeleton. *Nat. Rev. Mol. Cell Biol. 8,* 37-48.

Ward, M.E., Wu, J.Y., and Rao, Y. (2004). Visualization of spatially and temporally regulated N-WASP activity during cytoskeletal reorganization in living cells. *Proc. Natl. Acad. Sci. U. S. A. 101,* 970-974.

Welter, B.H., Laughlin, R.C., and Temesvari, L.A. (2002). Characterization of a Rab7-like GTPase, EhRab7; a marker for the early stages of endocytosis in *E. histolytica*. *Molecular Biochemical Parasitology 121,* 254.

Yamamura, R., Nishimura, N., Nakatsuji, H., Arase, S., and Sasaki, T. (2008). The interaction of JRAB/MICAL-L2 with Rab8 and Rab13 coordinates the assembly of tight junctions and adherens junctions. *Mol. Biol. Cell 19,* 971-983.

CHAPTER THREE

DEVELOPMENT OF A RAB8 ACTIVATION ASSAY AND THE INTERACTION OF RAB8 WITH THE GERMINAL CENTER KINASE, GCK

Abstract

Metastasis, or the spread of cancer cells from a primary tumor to a distant organ, contributes to more than 90% of cancer patient deaths. However, the molecular and genetic mechanisms responsible for metastasis remain largely elusive. One key process involved in metastasis is epithelial to mesenchymal transition (EMT), whereby primary tumor cells gain the ability to migrate. This gain of motility involves the formation of cell extensions in the direction of movement, which requires vesicle trafficking and actin cytoskeletal rearrangement. Interestingly, the small GTPase, Rab8, is involved in vesicle trafficking, but also unexpectedly "moonlights" as an actin cytoskeleton regulator, suggesting its possible role in EMT. Rab8 was first identified in melanoma cells and is homologous to the *mel* transforming oncogene, further suggesting its role in malignant tumor formation. However, no specific link between melanoma and Rab8 has been found.

The germinal center kinase, GCK, has been shown to interact directly with the active, GTP-bound form of Rab8. GCK also plays a role in sensitivity of early stage melanoma cells to UV-induced apoptosis. We have designed a Rab8 activation assay based on its interaction with GCK, and have investigated the effect of expression of mutant versions of Rab8 on GCK cellular levels.

Introduction

Epithelial to mesenchymal transition (EMT) is a normal process that occurs during embryogenesis. The existence of the two distinct cell types, epithelial and mesenchymal, were first noted by developmental biologists as early as 1908. In the late 1960s, Elisabeth Hay provided details of the primitive streak in chick embryos, the formation of which requires epithelial cells to be converted to mesenchymal cells. Later, in 1982, Elisabeth Hay and Gary Greenburg demonstrated that the conversion of epithelial cells to mesenchymal cells was a definable cellular process. As such, EMT has been extensively studied by developmental biologists since the early 1980s (Thiery, 2002). Epithelial mesenchymal transition is vital during developmental processes including gastrulation (Xue, Plieth, *et al.*, 2003). According to Lewis Wolpert's famous statement that "it is not birth, marriage, or death, but gastrulation, that is the most important event in the lifespan of an individual," EMT is a crucial developmental process (Nieto, 2002). Mesenchymal cells are able to migrate to different locations, which in development, allows for the formation of the various tissue and organ systems of the embryo (Grunert, Jechlinger, and Beug, 2003; Kang and Massague, 2004). Pathological EMT is also observed at the onset of cancerous tumor metastasis.

EMT is the transformation of polarized epithelial cells to non-polarized mesenchymal cells through loss of cell-cell contacts accompanied by restructuring of the cytoskeleton (Kang and Massague, 2004; Thiery, 2002). During EMT, epithelial cells downregulate epithelial marker proteins associated with tight junctions and desmosomes, including E-cadherin, α-catenin, and γ-catenin, and upregulate mesenchymal marker

proteins, such as vimentin, fibronectin and N-cadherin (Grunert, Jechlinger, and Beug, 2003; Kang and Massague, 2004).

In 1985, Michael Stocker and Michael Perryman were able to demonstrate EMT of MDCK (Madin Darby Canine Kidney) cells by exposing the cells to a fibroblast culture supernatant. They referred to the EMT inducer as scatter factor. In 1990, the factor was identified as hepatocyte growth factor, which is a ligand of the tyrosine kinase surface receptor, c-met. Since that discovery, other growth factor/tyrosine kinase receptor combinations have been shown to cause EMT (Thiery, 2002).

Researchers began to consider the possibility of a role for EMT in cancer. While this proposal sparked debate within the cancer research community (Kang and Massague, 2004), it soon became clear that there was indeed reason to suspect EMT as a major component of cancer metastasis. According to Yang, *et al.* (Yang, Mani, *et al.*, 2004), "Genes implicated in EMT during embryogenesis are turning up, one after the other, in tumorigenesis."

The most common cause of death in cancer patients is tumor metastasis (Yang, Mani, *et al.*, 2004). Metastasis is a multi-step process that involves the escape of cells from a primary malignant tumor and the establishment of a new tumor at another site in the body. Disease prognosis is heavily dependent upon whether or not a tumor is able to metastasize. The first step in the metastatic process is invasion. This step requires primary tumor cells to lose cell-cell adhesion and to gain the ability to move. This step has been the primary focus of the involvement of EMT in the metastatic process. The second step is intravasation, where invasive cells are able to enter the circulatory system

through capillaries or lymphatic vessels. The third step is extravasation during which metastatic cells exit the circulatory system through the vessel endothelium to enter a tissue sight removed from the primary tumor. These metastatic cells may establish micrometastases. The final step is the proliferation of the micrometastases into secondary tumors (Grille, Bellacosa, *et al.*, 2003; Yang, Mani, *et al.*, 2004).

One of the most dramatic changes observed during EMT is the gain of cellular mobility. Cell migration involves extension of filopodia and/or lamellipodia in the direction of movement. It has been suggested that formation of these structures requires rearrangement of the actin cytoskeleton, as well as recruitment of membrane constituents, via vesicle trafficking, from other parts of the cell for insertion into the cell leading edge (Grunert, Jechlinger, and Beug, 2003; Olson and Sahai, 2009; Ridley, Schwartz, *et al.*, 2003). Cytoskeletal changes during EMT are likely mediated by the Ras-related Rho family of GTPases, including Rac and Cdc42, and vesicle trafficking events are likely mediated by the Ras-related Rab GTPases (Eger and Mikulits, 2005; Sahai, 2005). Rac, Cdc42, and Rabs cycle between active, GTP-bound forms and inactive GDP-bound forms. GTP/GDP exchange factors (GEFs) catalyze the exchange of GDP for GTP on the GTPase. Hydrolysis of GTP is aided by GTPase-activating proteins (GAPs) (Alberts, Johnson, *et al.*, 2008; Lodish, Berk, *et al.*, 2000).

Upon induction of EMT-associated migration, there is a repolarization of the Golgi complex, positioning it between the leading edge of the cell and the nucleus. This allows directed vesicle secretion along the axis of migration. Interestingly, Rab8 has been shown to participate in the regulation of polarized secretion from the trans-Golgi

network to the basolateral surface. It has also been shown to play a role in cell-cell adhesion and restructuring of the actin cytoskeleton, suggesting that it may play an important role in EMT (Peranen, Auvinen, *et al.*, 1996; Powell and Temesvari, 2004). Although the contribution of Rab8 to the maintenance of cell polarity has been investigated, its contribution to EMT has not.

Powell and Temesvari have studied the role of Rab8 (Sas1) in the lower eukaryote, *Dictyostelium discoideum*. *D. discoideum* Rab8 shares 75% homology with human Rab8. The first step in *D. discoideum* development is aggregation of cells. In a *D. discoideum* cell line expressing constitutively active Rab8 as a green fluorescent protein chimera (GFP-Rab8CA), aggregation was inhibited and actin-rich membrane protrusions appeared. Further, cell-cell adhesions and levels of gp24, a cadherin-like cell adhesion molecule, were reduced. The Rab8CA mutants also displayed increased secretion. In contrast, cells expressing an inactive (dominant negative) version of Rab8 (GFP-Rab8DN) exhibited increased aggregation, cell-cell adhesion, and gp24 levels (Powell and Temesvari, 2004). Like mammalian Rab8, *D. discoideum* Rab8 may be a key regulator of actin rearrangement and secretion, suggesting that the dual function of Rab8 is evolutionarily conserved. The phenotypic changes displayed in the Rab8CA expressing mutant were reminiscent of changes observed in EMT, further supporting a role for Rab8 in this process (Powell and Temesvari, 2004).

The purpose of this research was to develop a multi-pronged assay for determining the level of Rab8 activation, and to utilize the assay to investigate the role of Rab8 in differentiation/dedifferentiation as well as its role in signaling pathways leading

to actin restructuring. The activation assay is based on the results of a study by Ren, *et al.*, to identify Rab8 interacting proteins. In a yeast two-hybrid screening of a mouse myeloma expression library, a protein designated as Rab8ip, was shown to bind to Rab8. The Rab8ip was identified as a homologue of human germinal center kinase (GCK). The two proteins share 93% homology. Only the GTP-bound, active form of Rab8 was shown to interact with the GCK-like, Rab8ip protein (Ren, Zeng, *et al.*, 1996). As such, we have developed a GST-GCK Rab8 interacting domain (GST-GCK Rab8id) fusion protein. This fusion protein is the basis for a Rab8 activation assay. The protein has been used as a bait protein for a GST-pulldown assay as well as a bioprobe for immunofluorescence microscopy.

Additionally, we have conducted initial investigations to identify the significance of the Rab8-GTP interaction with Rab8ip. Germinal center kinase, GCK, has been linked to the activation of the JNK/p38 pathway and implicated in the regulation of UV-mediated apoptosis in melanoma cells (Ichijo, 1999; Ivanov, Kehrl, and Ronai, 2000). Our preliminary results indicate a role for Rab8 in the control of cytoplasmic GCK levels. This is intriguing, as Rab8 was first identified as the *mel* oncogene from a melanoma cell expression library (Nimmo, Sanders, *et al.*, 1991), but no link between Rab8 and melanoma has ever been identified.

Because actin cytoskeletal restructuring is so vital to cell-cell adhesion, cell polarity and motility, Rab8 is suspected of playing a role in how epithelial cells undergo epithelial to mesenchymal transition in development and cancer metastasis. The development of our Rab8 activation assay will be a valuable tool in studying the role of

Rab8 in EMT. In addition, the investigation of the interaction between Rab8 and GCK may clarify how Rab8 may be involved in the disease process of melanoma.

Materials and Methods

Cell and culture conditions

MDCK (Madine Darby Canine Kidney) cells were purchased from ATTC. Cells were cultured in DMEM (Lonza, Invitrogen, Carlsbad, CA) supplemented with 10% FBS (fetal bovine serum; Atlas Biologicals, Fort Collins, CO) and 100 μg/ml pen/strep (Gibco, Invitrogen, Carlsbad, CA). HEK 293 (Human Embryonic Kidney) cells were a kind gift from Dr. Karl Franek (Greenwood Genetics Center, Greenwood, South Carolina). Cells were cultured in DMEM supplemented with 10% FBS and 100 μg/ml pen/strep. Cells were maintained at 37^{o}C and 5% CO_2.

Constructs

Human Rab8WT (wildtype), Rab8CA (constitutively active) and Rab8DN (dominant negative) were isolated from constructs provided by Dr. Karl Franek (Greenwood Genetic Center, Greenwood, SC). Rab8 was rendered constitutively active by a point mutation, which converts a glutamine residue at position 67 to a leucine residue (Rab8Q67L). Rab8 was rendered dominant negative by a point mutation, which converts a threonine residue at position 22 to an asparagine residue (Rab8T22N).

We used the EGFP-C1 plasmid (Clontech, gift of Dr. James Cardelli, LSU Health Sciences Center, Shreveport, LA, USA) to construct EGFP-Rab8 fusion proteins. There

was a point deletion in the multicloning site of the EGFP-C1 parent vector. This deletion resulted in a frame shift which added a stop codon between the EGFP and Rab8 coding regions. We corrected for this by designing a forward primer, which added two additional bases in order to place the EGFP and Rab8 coding regions within the same reading frame. We also added a 5-alanine linker between the coding regions for EGFP and Rab8 to ensure that there was adequate flexibility in the fusion protein for proper folding. To accomplish this, two sets of forward primers were used. The first forward primer set added two additional adenosine bases to correct the reading frame and 3 alanines to the 5' end of Rab8, while the reverse primer added a stop codon and BamHI cutsite to the 3' end. The first set of primers used was:

Forward: 5'- GGA AGC TTG CAG CAG CAG CAG CAG CG -3'

Reverse: 5'- GGA TCC TCA CAG AAG AAC ACA TCG G – 3'

The resulting ~ 700 bp PCR product was then used as the template for the second PCR reaction, which added 2 alanines and a HindIII cutsite to the 5' end of the Rab8 coding region. The second set of primers used was:

Forward: 5'- AAG CTT TAG CAG CAG CAG CAG CAG CG – 3'

Reverse: 5'- GGA TCC TCA CAG AAG AAC ACA TCG G – 3'

The resulting ~700 bp PCR product was subcloned into the TOPO-TA vector, pCR2.1 (Invitrogen, Carlsbad, CA).

The pCR2.1 – 5 ala-Rab8 plasmids and the EGFP-C1 plasmid (Clontech, gift of Dr. James Cardelli, LSU Health Sciences Center, Shreveport, LA, USA) were digested with HindIII and BamHI. The 5 ala-Rab8 sequences were ligated into EGFP-C1 according to the manufacturer's instructions using the Epicentre Biotechnologies Fast-Link^{TM} DNA Ligation Kit (Epicentre Biotechnologies, Madison, WI), resulting in the EGFP-5 ala-Rab8WT (EGFP-Rab8WT), EGFP-5 ala- Rab8CA (EGFP-Rab8CA), and EGFP-5ala-Rab8DN (EGFP-5 ala-Rab8CA) constructs.

XL-2 Blue Ultracompetent cells (Stratagene, Agilent Technologies, Santa Clara, CA) were transformed with EGFP-C1, EGFP-Rab8WT, EGFP-Rab8DN, and EGFP-Rab8CA according to the manufacturer's protocol. Cells were grown in 1 ml of Luria Broth for 1 hour at 37^{o}C and 200 rpm shaking. Cells were plated onto agarose plates with kanamycin selection and incubated overnight at 37^{o}C. The resulting clones were screened by restriction enzyme analysis and PCR colony screening. Positive clones were sequenced to verify that the EGFP and Rab8 coding sequences were in frame, and that the correct cut sites, 5-alanine linker and Rab8 point mutations had been maintained throughout the cloning process. Sequences were verified using NCBI BLAST.

Transfection

MDCK and HEK 293 cells were transfected with EGFP-C1, EGFP-Rab8WT, EGFP-Rab8DN, or EGFP-Rab8CA using Lipofectamine 2000 (Invitrogen, Carlsbad,

CA), according to the manufacturer's protocol. Briefly, cells were plated in 6-well plates and incubated overnight at 37^{o}C. Cells were washed twice with 1X PBS and 2 ml Optimem (Gibco, Invitrogen, Carlsbad, CA) was added to each well. DNA (3.2 μg) was diluted in 46.8 μl Optimem. Lipofectamine 2000 (1.5 μl) (Invitrogen, Carlsbad, CA) was diluted in 47.5 μl Optimem and incubated for 5 minutes at room temperature. The diluted DNA and diluted Lipofectamine 2000 were combined and incubated for 20 minutes at room temperature. The DNA-Lipofectamine 2000 mixture (100 μl) was added to each well of cells. The cells were incubated at 37^{o}C for 6 hours. The media was removed and replaced with 3 ml of DMEM supplemented with 10% FBS and 100 μg/ml pen/strep. Cells were examined for fluorescence 24 hours after transfection. For stable clones, 600 μg/ml neomycin (G418) (Mediatech, Inc., Manassas, VA) was added 72 hours after transfection. Media was exchanged every 48 hours until the appearance of clonal colonies. Cloning rings were used to isolate clones. Isolated clones were transferred sequentially to 6-well plates, 12.5 ml culture flasks and 25 ml culture flasks.

Immunofluorescence Microscopy

Cells were washed twice in 1X PBS and trypsinized. Cells were counted, and 1 x 10^{6} cells were plated onto coverslips or Lab-Tek coverglass chamber wells (Nalge Nunc International, Rochester, NY) and allowed to adhere overnight. For HEK 293 cells, coverslips or chamber wells were pretreated with 0.01% Poly-L-lysine (Sigma-Aldrich St. Louis, MO) at 37^{o}C for 1 hour, washed twice with 1X PBS and dried prior to cell plating.

Cells were washed twice with 1X PBS and fixed in 4% paraformaldehyde for 15 minutes at room temperature, and then, incubated in 1X PBS with 20 mM glycine for 20 minutes to quench aldehyde groups from fixation. Cells were permeabilized with 0.2 % Triton-X-100 for 20 minutes at room temperature. Nonspecific binding sites were blocked by incubating with 3%BSA (bovine serum albumin)/10% goat serum in PBS for 20 minutes at room temperature. The cells were then incubated for 2 hours at room temperature with the primary antibody (1:1000 rabbit anti-GCK (Cell Signaling, Santa Cruz Biotechnology, Santa, Cruz, CA); 100 μg/ml GST-GCK Rab8id bioprobe) in PBS with 1% BSA. Cells were washed and incubated for 1 hour at room temperature with a secondary antibody (1:1000 AlexaFluor 647 goat anti-rabbit IgG (Molecular Probes, Eugene, OR); 1:2000 Texas Red conjugated goat anti-GST antibody (Rockland, Gilbertsville, PA) in 1X PBS with 1% BSA. During the last 20 minutes of incubation, 10 μl of propidium iodide was added (Molecular Probes, Eugene, OR). The stained cells were washed with 1X PBS, mounted in 50% PBS/glycerol and observed using a Zeiss LSM 510 confocal microscope (Carl Zeiss, Thornwood, NY)(Powell, Welter, et al, 2006).

GST plasmid construction

Human GCK was cloned from the GCK ImageClone pCMV-SPORT6 (Open Biosystems, Huntsville, AL). Sequence alignment of the ImageClone and the human GCK cDNA showed that 18 bp were missing from the ImageClone sequence. These bases were located at the 5' end of the Rab8 binding domain, which is located at the C-

terminus of the GCK sequence. Therefore, the missing nucleotides were replaced using primers to complete the Rab8-interacting domain and to add EcoRI and SalI cutsites to the sequence. The primers used were:

Forward: 5'- GAA TTC CCT CCT TCA GGC CCC – 3'

Reverse: 5' – GTC GAC TTA GTA GGT GCT CTG – 3'

The resulting ~1200 bp PCR product was subcloned into the TOPO-TA vector, pCR2.1 (Invitrogen, Carlsbad, CA).

The pCR2.1 – GCK Rab8id plasmid and the pGEX-5X-1 plasmid (Amersham Biosciences, Piscataway, NY) were digested with EcoRI and SalI. The GCK Rab8id sequence was ligated downstream of the GST coding region of pGEX-5X-1 plasmid according to the manufacturer's instructions using the Epicentre Biotechnologies Fast-Link™ DNA Ligation Kit (Epicentre Biotechnologies, Madison, WI) resulting in the GST-GCK Rab8id construct.

Competent BL21 *E. coli* cells (Invitrogen, Carlsbad, CA) were transformed with pGEX-5X-1-GCK Rab8id and pGEX-5X-1 alone. A single colony was grown in 2 ml of Luria Broth overnight at 37°C with shaking at 250 rpm. 100 ml of Luria Broth were inoculated with 50 μl of the overnight culture, and incubated at 37°C with shaking at 250 rpm for approximately 3 hours until the OD600 was approximately 0.5. The cells were centrifuged for 15 minutes at 4°C and resuspended in 10 ml of ice cold TSS buffer (TSS Buffer: 100 mL; 10 g Tryptone, 0.5 g Yeast Extract, 0.5 g NaCl, 0.8 g PEG, 5 ml DMSO,

5 ml 1 M $MgCl_2$). Cells (1 ml) were transferred to a prechilled 50 ml conical and placed on ice. DNA (1 ng) was added to the cells, swirled and incubated on ice for 45 minutes. The cells (100 μl) were added to 900 μl of prewarmed LB-glucose (LB + 20 mM glucose) and incubated for 1 hour at 37°C with shaking at 250 rpm. Cells were plated onto LB-glucose-agar plates and incubated overnight at 37°C. The resulting clones were screened by restriction enzyme analysis and PCR colony screening. Positive clones were sequenced to verify that the GST and GCK Rab8id coding sequences were in frame and that the correct cut sites had been maintained throughout the cloning process. Sequences were verified using NCBI BLAST.

Expression and purification of recombinant GST and GST-GCK Rab8id proteins for Silver Stain verification

To verify the expression of GST and GST-GCK Rab8id in the transformed BL21 *E. coli*, a single colony of each was grown in 2 ml of Luria Broth overnight at 37°C with shaking at 250 rpm. Luria Broth (3 ml) was inoculated with 50 μl of the overnight culture and incubated at 37°C with shaking at 250 rpm for approximately 3 hours until the OD600 was 0.5 – 1.0. Then, 1 ml of this culture was removed, placed in a new tube and induced with 2 μl of 0.5 M IPTG (1-thio-β-D-galactopyranoside) for 2 hours at 37°C with shaking at 250 rpm. A 50 μl aliquot of the induced cells was centrifuged. The resulting pellet was resuspended in 100 μl LDS sample buffer buffer (50% LDS (Invitrogen, Carlsbad, CA), 40% water, 10% 2-mercaptoethanol (Bio-Rad Laboratories, Hercules, CA) and heated at 70°C for 10 minutes. Each sample (15 μl) was loaded onto a NuPage

Gel (10% Bis-Tris) (Invitrogen, Carlsbad, CA). The gel was washed twice in ultrapure water and fixed in 30% Ethanol/10% Acetic Acid. Following fixation, it was washed twice with 10% Ethanol and twice with ultrapure water. The SilverSNAP Stain Kit II (Pierce, Rockford, IL) was used to visualize the protein bands according to the manufacturer's protocol. The staining reaction was halted by replacing the developing solution with 5% acetic acid and incubating for 10 minutes. The gel was washed in ultrapure water, placed between two sheets of cellophane and dried in a Tut's Tomb gel drying device (Idea Scientific Company, Minneapolis, MN) in the fume hood.

Expression and batch purification of recombinant GST and GST-GCK Rab8id proteins

To obtain large amounts of protein for use as a bioprobe and for GST pulldown assays, 2 ml of Luria Broth were inoculated with a single colony and grown for 8 hours at 37^{o}C with shaking at 250 rpm. The inoculum was added to 500 ml of Overnight Express Instant TB Medium supplemented with the Overnight Express Autoinduction Components (Novagen, EMD Biosciences, Darmstadt, Germany) according to the manufacturer's protocol and incubated for 16 hours at room temperature with shaking at 250 rpm. The cells were harvested by centrifugation at 6500g for 15 min. The supernatant was discarded, and the pellet was frozen overnight. The following day, the cells were lysed with B-PER Bacterial Protein Extraction Reagent (Pierce, Rockford, IL). Cell lysates were centrifuged at 27000g for 15 min to separate the soluble (GST-fusion protein containing) proteins from the insoluble proteins. The soluble proteins supernatant was supplemented with 20% Triton for a final concentration of 1% Triton and rocked for 30

minutes at room temperature to further aide protein solubilization. The lysate was then centrifuged at 12000g for 10 minutes.

The GST protein and the GST-GCK Rab8id fusion protein were batch purified by adding 20 μl of 50% glutathione sepharose slurry (Amersham Pharmaceia, GE Healthcare, Waukesha, WI) to each ml of lysate. After 30 minutes of rocking at room temperature, the lysate was centrifuged for 5 minutes at 500g in order to sediment the gel. The gel pellet was washed with PBS. The GST and GST-GCK Rab8id proteins were eluted from the gel with glutathione elution buffer (10 mM glutathione in 50 mM Tris-HCl, pH 8.0). The GST and GST-GCK Rab8id proteins were analyzed for purity by SDS-PAGE and silver staining as described above. Western blot analysis was performed as described below (Welter, Laughlin, and Temesvari, 2002) in order to verify the GST tag using a primary antibody to GST (1:10,000). HALT protease inhibitor (Pierce, Rockland, IL) was added to the purified protein and the protein was stored at -80^{o}C.

SDS-PAGE and Western Blot Analysis

SDS-PAGE and Western blot analyses were carried out as previously described by Welter, *et al.* (Welter, Laughlin, and Temesvari, 2002). Cells were washed twice with 1X PBS, trypsinized and resuspended in 1X PBS. Cells were counted, and 1 x 10^6 cells were pelleted by centrifugation. The pellet was resuspended in 60 μl LDS sample buffer with 2-mercaptoethanol (2% v/v) and heated at 70^{o}C for 10 minutes. Cells were centrifuged at 4^{o}C for 90 minutes, and 15 μl of each sample were loaded onto a NuPage Gel (10% Bis-Tris) (Invitrogen, Carlsbad, CA). Samples were electrophoresed at 200 V

for 1 hour and transferred to a PVDF (polyvinylidene difluoride) membrane (Invitrogen, Carlsbad, CA) in Towbin buffer at 100 V for 90 minutes. Blotted membranes were blocked in 5% powdered milk / 0.5% Tween 20/TBS (Tris Buffered Saline) for 2 hours at room temperature. After rinsing with 0.5%Tween 20/TBS, the membrane was incubated overnight at 4^{o}C with primary antibody (1:500 mouse anti-GFP (Zymed, San Francisco, CA), 1:1000 mouse anti-Rab8 (BD Biosciences, San Jose, CA)). The following morning, the membrane was washed and incubated with a secondary horseradish peroxidase-conjugated goat anti-rabbit (1:5000) or goat anti-mouse (1:2000) IgG antibody (Cappel, ICN Pharmaceuticals, Costa Mesa, CA) for 1 hour at room temperature. After washing, proteins were detected with the Enhanced Chemi Luminescence (ECL) Western blotting detection system (Pierce, Rockland, IL), according to the manufacturer's instructions.

GST Pulldown Assays

HEK 293 cells expressing EGFP, EGFP-Rab8WT, EGFP-Rab8DN, and EGFP-Rab8CA were lysed, and protein amounts were determined using an Eppendorf BioPhotometer (Eppendorf, Hamburg, Germany). The cell lysates were diluted to 80 μg/ml (low concentration) or 5.6 mg/ml (high concentration) in interacting buffer (50 mM Tris pH 8.0, 5 mM $MgCl_2$, 100 mM NaCl).

GST-GCK Rab8id or GST was diluted in coupling buffer (for 1 liter: 29 g NaCl, 8.4 g $NaHCO_3$, pH 8.3) and coupled to glutathione sepharose beads (Amersham, GE Healthcare, Waukesha, WI) with rotation at 4^{o}C for 2 hours. The beads were centrifuged and washed with coupling buffer to remove uncoupled proteins.

The HEK cell lysates were added to the GST- and GST-GCK Rab8id- coupled beads, and incubated at 4^{o}C overnight with rotation. The samples were centrifuged and the beads were washed with interacting buffer to remove unbound protein. Bound proteins were eluted from the beads with elution buffer (10 mM glutathione in 50 mM Tris-HCL, pH 8.0). A 25 μl sample of the eluted protein was mixed with 25 μl LDS buffer for analysis by silver staining (Powell and Temesvari, 2004) and Western blot(Welter, Laughlin, and Temesvari, 2002) as described previously.

FACS sorting

MDCK cells were trypsinized and resuspended in 1 X PBS at a concentration of 1x 10^{6} cells/ml. 5 mls of cells were filtered through a 40 micron sterile filter (Millipore, Danvers, MA). FACS sorting was done using a Cytopeia Influx FACS sorter (BD Biosciences, San Jose, CA) capable of high-speed analysis and cell-sorting. The gating was set to capture the highest 1% of EGFP expressing cells. Cells were sorted into a media tube containing DMEM media supplemented with 10% FBS, 100 μg/ml pen/strep and 600 μg/ml G418. Single cells were dispensed into each well of a sterile 96-well plate to obtain single clones.

Results

Establishment of stable Rab8 mutant cell lines

MDCK (Madin Darby Canine Kidney) cells were transfected with N-terminal enhanced green fluorescent protein (EGFP), or EGFP fusions of constitutively active

Rab8 (EGFP-Rab8CA), dominant negative Rab8 (EGFP-Rab8DN), or wildtype Rab8 (EGFP-Rab8WT). In all of the constructs, a 5 alanine linker was added between the EGFP and Rab8 coding regions. This was done to ensure enough flexibility for the correct folding of the protein (Peranen and Furuhjelm, 2001). Stable clones were selected with 600 μg/ml of G418, isolated with cloning rings and transferred to flasks. Each clone was examined using fluorescence microscopy for expression of EGFP or one of the EGFP-Rab8 chimeric proteins. In positive clones, fluorescence microscopy (Figure 3.1 A-D) showed EGFP protein in the cytoplasm and in the nucleus in cells expressing EGFP alone. Cells expressing EGFP-Rab8 fusion proteins showed that the chimeric proteins were expressed in the perinuclear region, and in the case of EGFP-Rab8CA, in membrane extensions. Furthermore, cells expressing EGFP-Rab8CA, displayed long membrane projections. These localization patterns were consistent with a previous report (Peranen and Furuhjelm, 2001). Clones with the highest percentage of cells expressing the EGFP or EGFP-Rab8 proteins were selected for Western blot analysis. Western blot analysis (Figure 3.1 E) was performed in order to verify expression of the EGFP-Rab8 chimeric proteins. The expression of EGFP-Rab8WT was too low to be detected by Western blot.

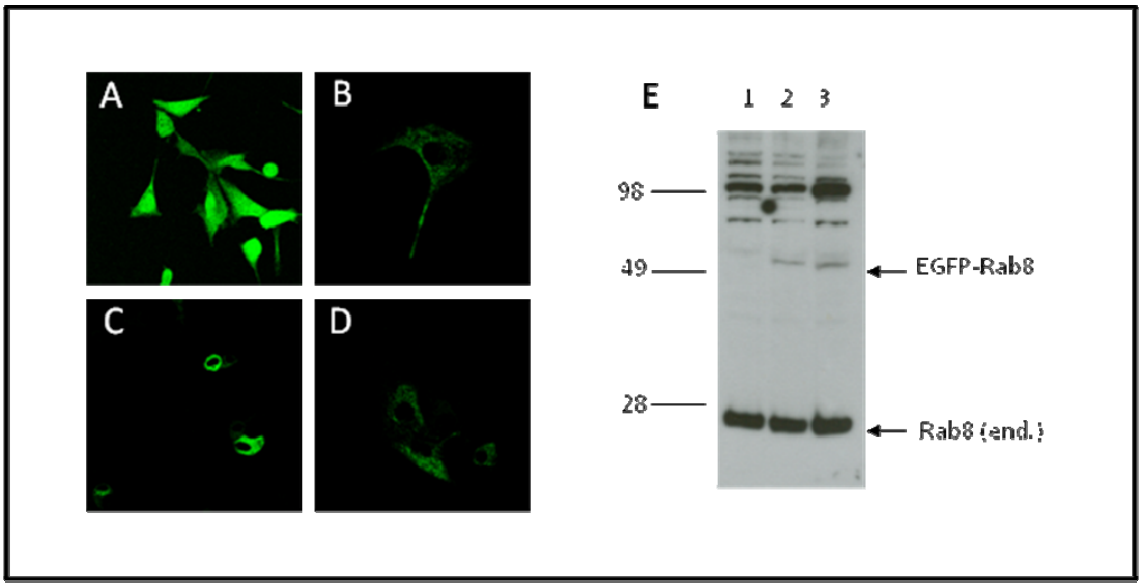

Figure 3.1. Stable Expression of EGFP-Rab8 Constructs in MDCK Cells. Fluorescence microscopy was used to detect expression of (A) EGFP, (B) EGFP-Rab8CA, (C) EGFP-Rab8DN, and (D) EGFP-Rab8WT. Western blot analysis was used to confirm expression of EGFP-Rab8 constructs (E) Lane 1: Untransfected MDCK cells, Lane 2: EGFP-Rab8CA, Lane 3: EGFP-Rab8DN.

The clonal populations did not have 100% of the cells expressing the experimental proteins. Generally, 25-30% of the cells in a field of view were positive for EGFP or EGFP-Rab8 expression. In addition, as the number of transfers increased, the expression levels of the desired proteins decreased. In order to obtain a population with higher percentages of cells positive for expression, FACS sorting was performed to isolate the highest expressing cells from each clonal population. However, this did not improve the overall percent of expressing cells within all of the clonal populations. Western blot analysis (Figure 3.2) was performed to compare the expression levels of EGFP-Rab8 chimeras before and after sorting. In the EGFP-Rab8CA expressing cells,

there was no improvement in the percentage of expressing cells following sorting. While in the EGFP-Rab8DN expressing cells, there was some improvement.

MDCK cells are very difficult to transfect and it is also difficult to obtain highly expressing, stable MDCK clones. More than 16 stable clones of each EGFP-Rab8 chimera were screened. Unfortunately, only one highly expressing EGFP-RAB8DN clone was obtained. As a result of the low expression levels of the EGFP-Rab8 chimeric proteins in the stable MDCK clones, it was decided that transient transfections in a cell line that more readily expresses non-endogenous proteins should be attempted in order to verify the validity of the Rab8 activation assay.

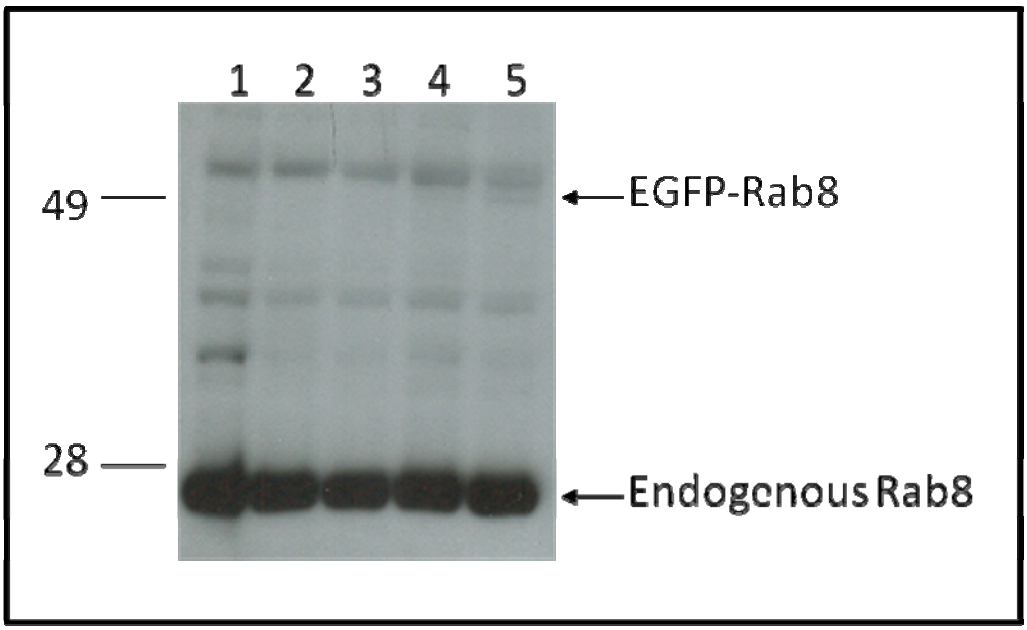

Figure 3.2. Expression of EGFP-Rab8 Constructs in Sorted and Unsorted Cell Populations. Cells were sorted by FACS, and Western blot analysis was used to confirm expression of EGFP-Rab8 constructs in sorted and unsorted populations. Lane 1: Untransfected MDCK cells; Lane 2: Unsorted EGFP-Rab8CA; Lane 3: Sorted EGFP-Rab8CA; Lane 4: Unsorted EGFP-Rab8DN; Lane 5: Sorted EGFP-Rab8DN.

HEK 293 cells, which are often used for the expression of recombinant proteins (Thomas, and Smart, 2005), were transiently transfected with N-terminal enhanced green fluorescent protein (EGFP), or EGFP fusions of constitutively active Rab8, dominant negative Rab8, or wildtype Rab8. Approximately 24 hours following transfection, the expression levels of the EGFP and EGFP- Rab8 proteins were assessed using fluorescence microscopy (Figure 3.3 A-H). Overall population expression was substantially higher in the transiently transfected HEK 293 cells (> 50%) than that seen in the stable MDCK cell lines (approximately 25-30%). Localization of EGFP in the cytoplasm and nucleus and localization of the EGFP-Rab8 chimeras in the perinuclear region was consistent with the localization seen in the stable MDCK cell lines. Western blot analysis (Figure 3.3 I) was performed to verify the expression of EGFP- Rab8CA, EGFP-Rab8WT and EGFP-Rab8DN. All of the chimeric proteins were expressed at high levels in the transiently transfected HEK 293 cells. Therefore, it was decided to verify the efficacy of the Rab8 activation assay utilizing transiently transfected HEK 293 cells.

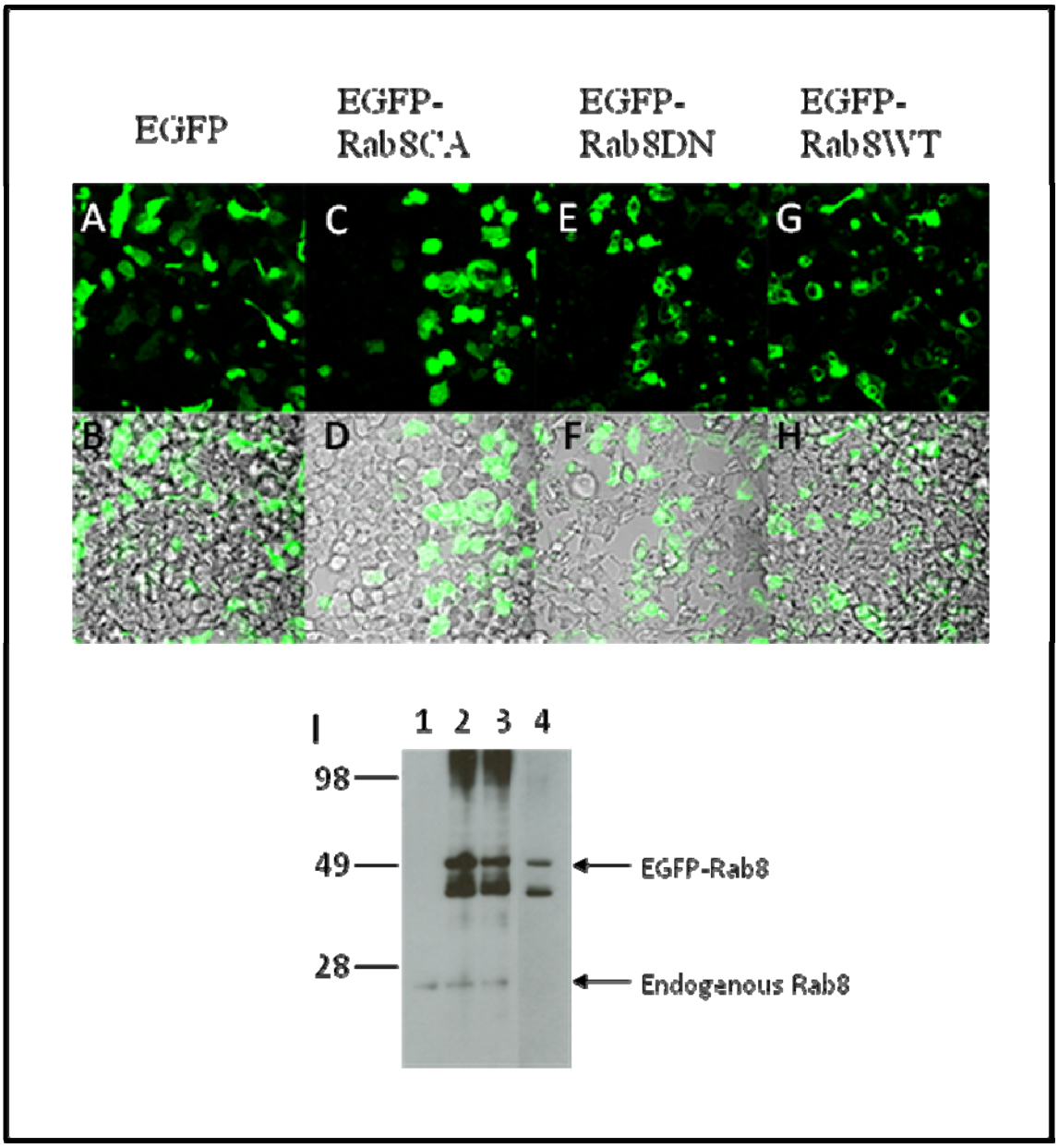

Figure 3.3. Expression of EGFP-Rab8 Constructs in HEK 293 Cells. Fluorescence microscopy was used to detect expression of (A,B) EGFP, (C,D) EGFP-Rab8CA, (E,F) EGFP-Rab8DN, and (G,H) EGFP-Rab8WT. Western blot analysis was used to confirm expression of EGFP-Rab8 constructs (I) Lane 1: Untransfected MDCK cells, Lane 2: EGFP-Rab8CA, Lane 3: EGFP-Rab8WT; Lane 4: EGFP-Rab8DN.

GST-GCK Rab8id Rab8 Activation Pulldown Assay

Ren *et al.* demonstrated that the GCK-like protein, Rab8ip, interacts directly with the constitutively active form of Rab8. It does not interact with the dominant negative form of Rab8 (Ren, Zeng, *et al.*, 1996). Based on this, we designed an assay for the level of Rab8 activation within a cell. We created a glutathione-S-transferase (GST) fusion protein with amino acids 430-819 of human GCK(Figure 3.4). These amino acids contain the Rab8-GTP interacting domain of GCK.

BL21 *E. coli* cells were transformed with plasmids encoding GST and GST-GCK Rab8id. The bacteria were induced with IPTG to produce the GST and GST-GCK Rab8id proteins. The proteins were examined by silver stain (Figure 3.5 A) and Western blot analysis (Figure 3.5 B) using an antibody specific for GST. A protein band was seen at ~72 kD on the silver stain. This corresponded to a ~72 kD band on the Western blot, demonstrating that the protein is recognized by antibodies specific for GST.

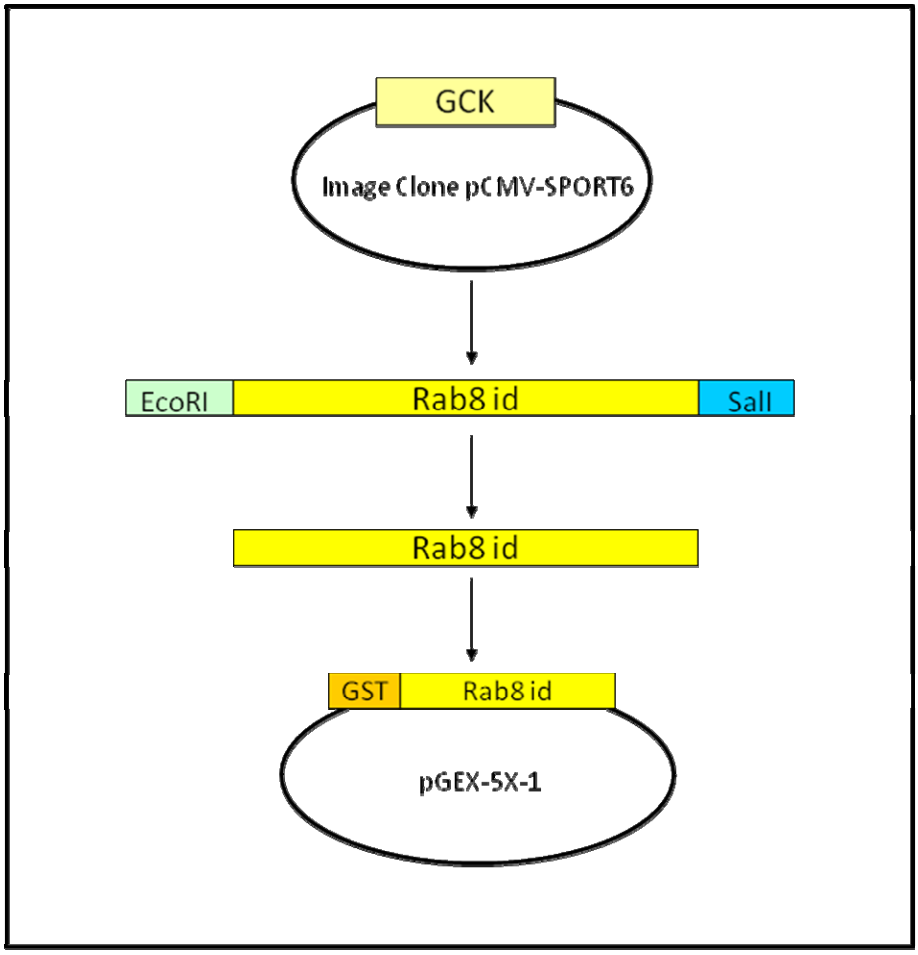

Figure 3.4. GCK-GST Construct. The Rab8-GTP interacting domain of human germinal center kinase (GCK) was cloned from the ImageClone pMV-SPORT6. The resulting PCR product was ligated in pGEX-5X-1 to form the GST-GCK Rab8id fusion construct.

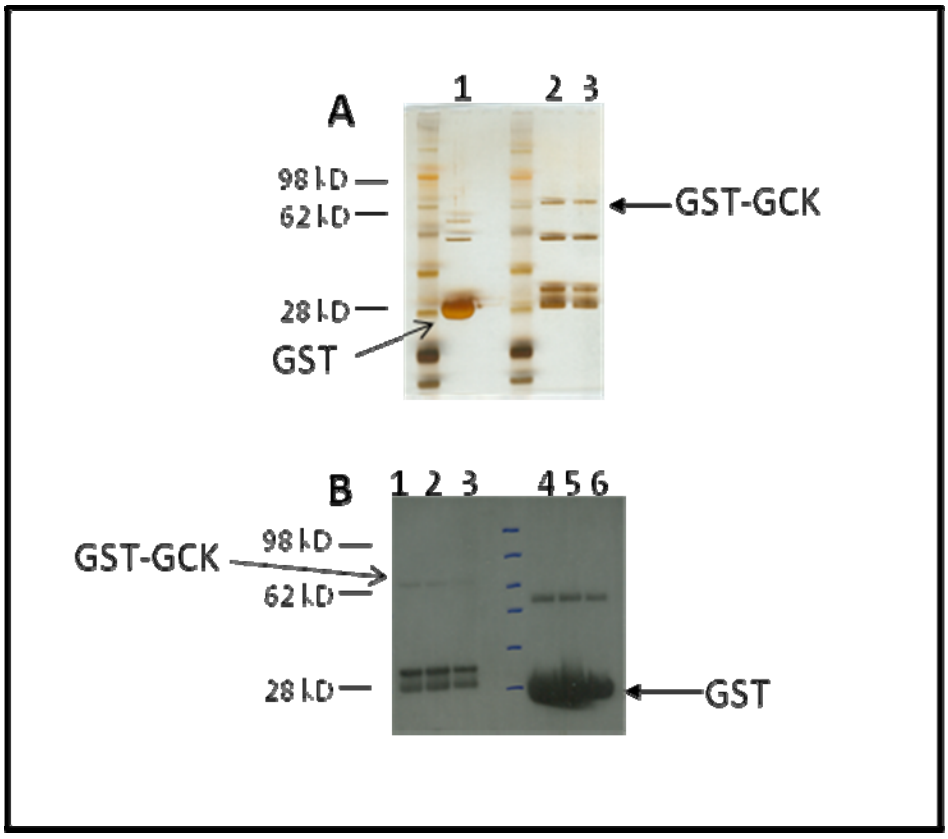

Figure 3.5. Verification of GST-GCK Protein Expression and Isolation. (A) Silver stain was used to verify the expression and purification of the GST-GCK fusion protein. Lane 1: GST; Lane 2, 3: GST-GCK. (B) Western blot analysis was used to verify the expression of the GST-GCK fusion protein. Lane 1,2,3: GST-GCK; Lane 3,4,5: GST.

Next, we incubated recombinant GST or GST-GCK Rab8id with cell lysates of wildtype HEK 293 cells or HEK 293 cells tranfected with EGFP-Rab8CA, or EGFP-Rab8DN (Figure 3.6) . Bands at ~72 kD and ~25 kD can be seen in Lanes 5, 7, and 9. These lanes correspond to cell lysates of wildtype HEK 293 cells (Lane 5), HEK 293 cells transfected with EGFP-Rab8CA (Lane 7) or EGFP-Rab8DN (Lane 8), and incubated with GST-GCK Rab8id- coupled glutathione beads. It appears that the GST-GCK Rab8id bait protein (~72 kD) and endogenous Rab8 (~25 kD), presumably the

GTP-bound form, are present in the precipitated samples. However, there is no evidence of the ~50 kD EGFP-Rab8 chimeric proteins in any of the lanes where the GST-GCK Rab8id bait protein was utilized.

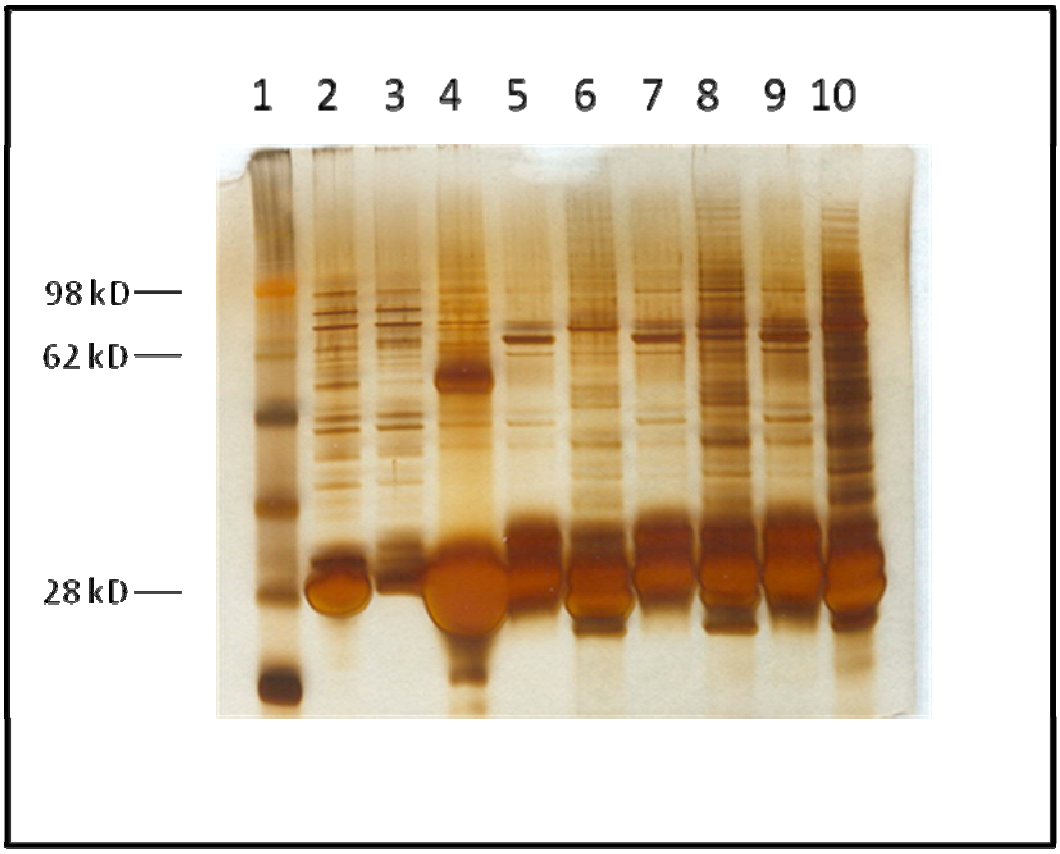

Figure 3.6. GST-GCK Rab8-GTP Pulldown Assay. GST protein or GST-GCK Rab8id protein coupled to glutathione beads were incubated with lysates from wildtype HEK cells or HEK cells expressing EGFP-Rab8CA or EGFP-Rab8DN. Proteins were eluted from the glutathione beads and 20 μl samples were separated using SDS-PAGE and visualized by silver staining. Lane 1: Ladder; Lane 2: GST protein; Lane 3: GST-GCK Rab8id bait protein; Lane 4: GST-bait with wildtype HEK lysate; Lane 5: GST-GCK Rab8id bait protein + 80 μg/ml wildtype HEK lysate; Lane 6: GST-GCK Rab8id bait protein + 5.6 mg/ml wildtype HEK lysate; Lane 7: GST-GCK Rab8id bait protein + 80 μg/ml EGFP-Rab8CA- expressing HEK lysate; Lane 8: GST-GCK Rab8id bait protein + 5.6 mg/ml EGFP-Rab8CA- expressing HEK lysate; Lane 9: GST-GCK Rab8id bait protein + 80 μg/ml EGFP-Rab8DN- expressing HEK lysate; Lane 10: GST-GCK Rab8id bait protein + 5.6 mg/ml EGFP-Rab8DN- expressing HEK lysate.

GST-GCK Rab8id Bioprobe Immunofluorescence Microscopy

HEK 293 cells were plated on poly-L-lysine coated coverslips, and transiently transfected with either EGFP-Rab8CA or EGFP-Rab8DN. Approximately 24 hours later, the cells were fixed with 4% paraformaldehyde and incubated with 100 μg/ml of the GST-GCK Rab8id protein bioprobe for 2 hours at room temperature. The cells were washed, and then, stained with an AlexaFluor-594 conjugated GST-antibody. The cells were washed and mounted in 50% PBS/glycerol. A Zeiss LSM 510 Confocal Microscope (Carl Zeiss, Thornwood, NY) was used to examine the cells for the presence of colocalization of EGFP-Rab8 and the GST-GCK Rab8id bioprobe protein. In the cells expressing EGFP-Rab8CA, colocalization was observed with the GST-GCK Rab8id bioprobe stained with a Alexa-Fluor-594 conjugated GST-antibody (Figure 3.7 A). However, very little colocalization was seen in the cells expressing EGFP-Rab8DN with the AlexaFluor-594 conjugated GST-antibody stained GST-GCK Rab8id bioprobe (Figure 3.7 B).

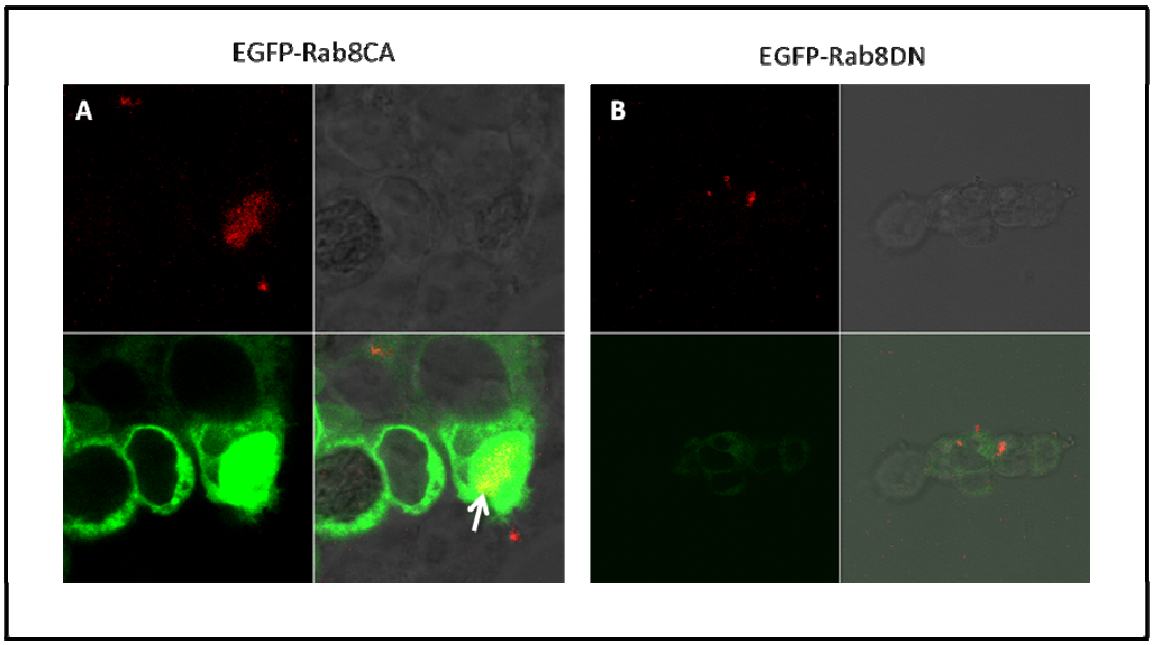

Figure 3.7. GST-GCK Rab8id Bioprobe Staining. HEK 293 cells expressing EGFP-Rab8CA or EGFP-Rab8DN were incubated with the GST-GCK Rab8id protein bioprobe and subsequently stained with an AlexaFluor 594-conjugated anti-GST antibody. Colocalization (yellow, see arrow) of the EGFP-Rab8CA (green) and the GCK-GST Rab8id bioprobe (red) can be seen in (A). However, no colocalization is seen the cells expressing EGFP-Rab8DN (B).

Endogenous GCK Levels in Rab8 Mutant Cell Lines

While it is known that GCK interacts only with activated Rab8, the role of Rab8 in this interaction is unknown. We decided to investigate the endogenous levels and localization of GCK in MDCK cells stably expressing EGFP-Rab8CA and EGFP-Rab8DN. Cells were plated on coverslips and incubated at 37^{o}C overnight. The cells were fixed with 4% paraformaldehyde and then, incubated with a primary antibody to GCK. The cells were washed and then stained with AlexaFluor 647-conjugated goat anti-GST antibody (Rockland, Gilbertsville, PA) . The cell nuclei were stained with propidium iodide (Molecular Probes, Eugene, OR). GCK staining was seen only in the

nucleus in the cells expressing EGFP-Rab8CA (Figure 3.8 A), while GCK staining was seen throughout the cytoplasm of the cell in addition to within the nucleus in cells expressing EGFP-Rab8DN (Figure 3.8 B).

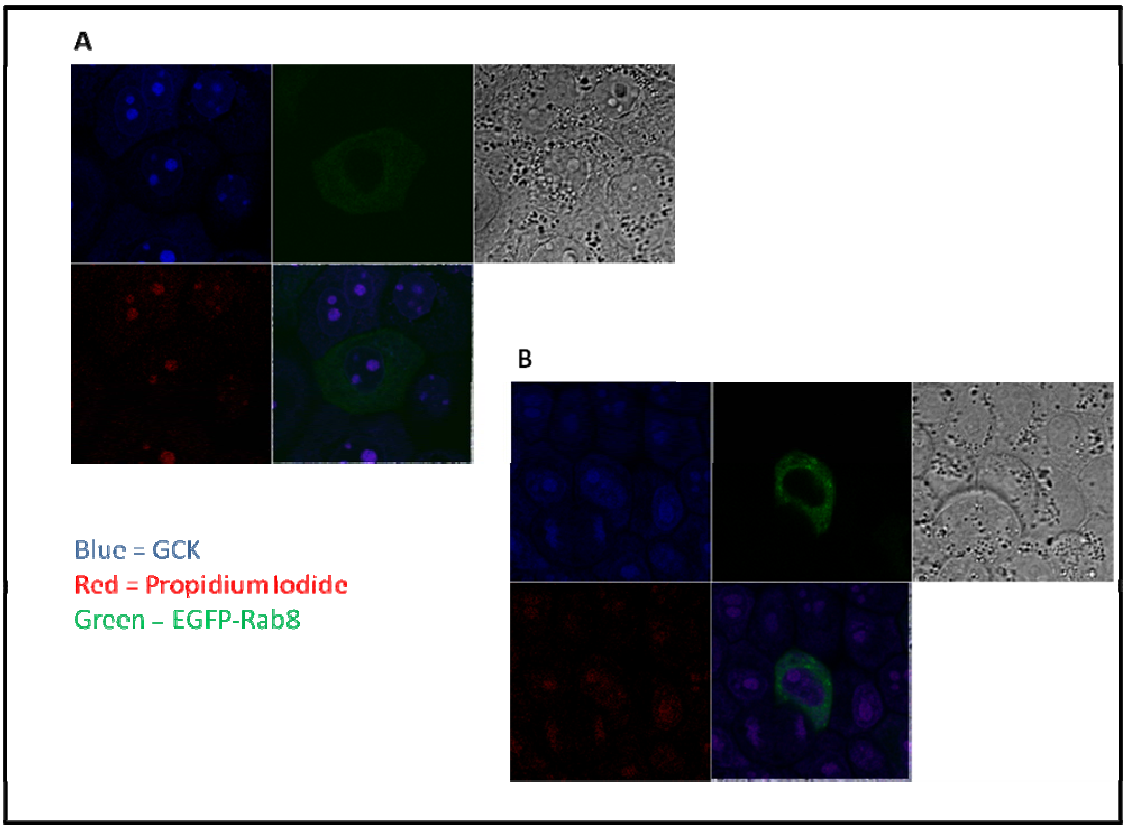

Figure 3.8 Endogenous GCK Levels in Rab8 Mutant Cell Lines. MDCK cells expressing EGFP-Rab8CA showed localization of GCK only within the nucleus (A), while cells expressing EGFP-Rab8DN showed the presence of GCK in the cytoplasm as well as in the nucleus (B).

MDCK cells expressing EGFP-Rab8DN form domes in culture

When MDCK cell lines that were stably expressing EGFP-Rab8DN were examined in culture, a number of dome formations were observed. MDCK cells are

known for their ability to form domes, or hemicysts in monolayer culture; however, dome formation normally occurs following cell confluence (Chang, Lin, *et al.*, 2007; Lever, 1979a). In the case of the MDCK cells expressing EGFP-Rab8DN, domes were seen within single clones immediately following transfection (Figure 3.9 B). Additionally, following normal maintenance transfer, the MDCK cells expressing EGFP-Rab8DN formed multiple domes at subconfluent levels as low as 25%. Untransfected MDCK cells do not display spontaneous dome formation until 1-2 days after reaching 100% confluency (Lever, 1979b). Remarkably, MDCK cells expressing EGFP-Rab8CA were not seen to display domes until 3-4 days after reaching confluency.

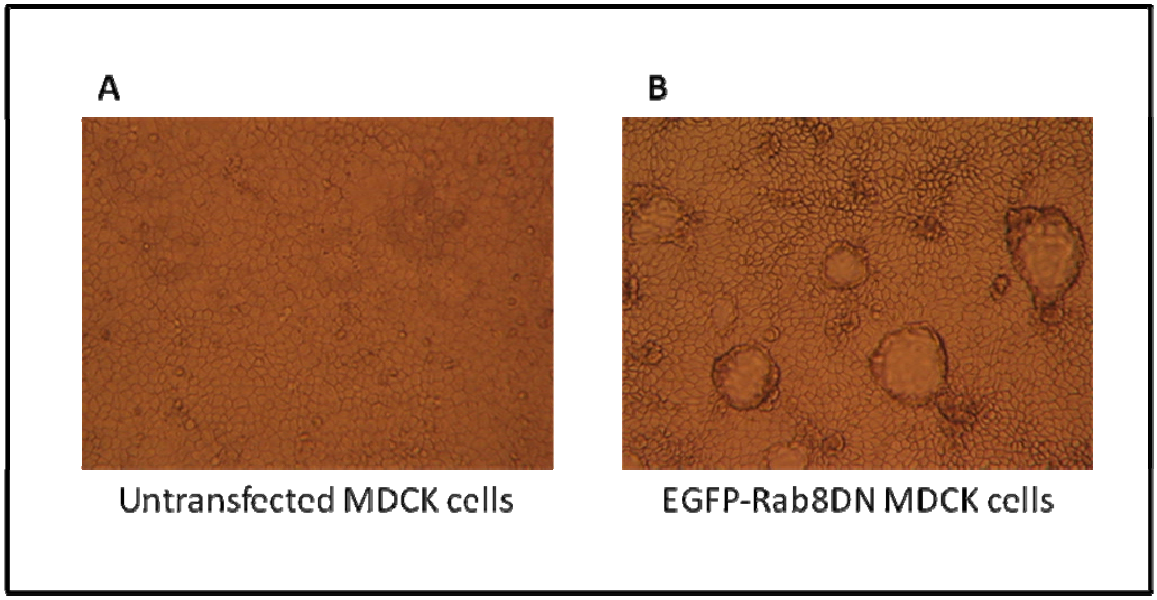

Figure 3.9. Untransfected and EGFP-Rab8DN MDCK Cell Monolayers.
Untransfected MDCK cells (A) and MDCK cells transfected with EGFP-RABDN (B) were photographed in normal culture conditions. The EGFP-Rab8DN-expressing cells show numerous dome structures (B), which are absent in the untransfected cells (A).

Discussion

We have developed a Rab8 activation assay based on the direct binding of only the active, GTP-bound form of Rab8 with the germinal center kinase, GCK (Ren, Zeng, *et al.*, 1996). The Rab8-GTP binding site of GCK was cloned and inserted into the pGEX-5X-1 plasmid in order to add a GST-tag to the GCK Rab8 interacting domain. The glutathione-S-transferase tag allows the GST-GCK Rab8id fusion protein to be selectively "pulled down" from a cell lysate along with any Rab8-GTP that has bound to it. Subsequently, Western blot analysis of the eluted analysis can be utilized to examine relative levels of Rab8-GTP in a population of cells. Additionally, the purified protein may be used as a bioprobe along with a fluorescently tagged GST-antibody in order to visualize active, GTP-bound Rab8 within a cell using immunofluorescence microscopy. This assay will allow us to analyze the possible role of Rab8 activation in the process of epithelial to mesenchymal transition (EMT) and tumor metastasis.

In order to examine the role of Rab8 in EMT, we transfected MDCK (Madin Darby Canine Kidney) cells with constructs to induce expression of EGFP, EGFP-Rab8WT, EGFP-Rab8CA, or EGFP-Rab8DN. MDCK cells were chosen because they are a well studied, epithelial model system (Shaw, Rickwood, and Hames, 1996). Many studies involving induction of EMT and tumor metastasis have utilized MDCK cells (Yang, Mani, *et al.*, 2004).

We attempted to establish stable clones of the EGFP-Rab8 expressing MDCK cells. Stable clones of all of the cell lines were established; however, most of the clonal populations displayed only a low percentage of cells expressing the EGFP-Rab8 chimeric

proteins as evaluated by fluorescence microscopy. FACS sorting of the clonal populations was attempted; however, no increase in expression levels was obtained. Only one stable EGFP-Rab8DN clone with a high percentage of the cell population expressing the EGFP-Rab8DN protein was established. According to personal correspondence with other laboratories that have worked with EGFP expression and the cultivation of stable EGFP-expressing MDCK clones, the establishment of these clones can be particularly difficult. MDCK cells do not generally have high levels of transient transfection, and as a result, the probability of obtaining stably expressing clones is reduced. In addition, stable clonal populations have a tendency to lose expression over time as a result of transcriptional silencing through DNA methylation (Williams, Mustoe, *et al.*, 2005).

Because of the difficulties we encountered in trying to establish stable MDCK clones, we decided to utilize a different cell line and to perform transient transfections in order to test the GST-GCK Rab8id pulldown assay. We transiently transfected HEK 293 cells (human embryonic kidney). This cell line is frequently used for the expression of recombinant mammalian proteins, is easily transfected and shows high levels of transfection efficiency (Thomas and Smart, 2005) When these cells were transfected with EGFP, EGFP-Rab8WT, EGFP-Rab8CA, or EGFP-Rab8CA, high levels of transfection efficiency and expression were seen by fluorescence microscopy and Western blot analysis. Thus, we were able to utilize HEK 293 cells to generate cell lysates upon which to test the validity of the Rab8 activation pulldown assay. At the time of this report, only one pulldown assay has been performed. Silver stain analysis showed that the GST-GCK bait protein was present, although at low levels, in the eluates. Interestingly, a prominent

band corresponding to the same size as endogenous Rab8 was detected in the cell lysates incubated with the GST-GCK Rab8id bait protein. There could be several reasons for these results including too little bait protein or not enough EGFP-Rab8 prey protein in the lysates. In addition, interference by the EGFP-tag to the binding of the active, GTP-bound Rab8 to the GST-GCK Rab8id could be a problem. In a similar experiment with the Rab8-GTP interacting protein, FIP-2, EGFP-Rab8 constructs were utilized for evaluation of colocalization of FIP-2 and Rab8. However, His-Rab8 constructs were built in order to evaluate the *in vitro* binding of Rab8 to a GST-FIP2 fusion protein (Hattula and Peranen, 2000). Several optimization experiments will be required before the pulldown assay can be effectively utilized to determine Rab8 activation levels in cell lysates.

The stable EGFP-Rab8CA and EGFP-Rab8DN expressing MDCK cell lines that were established were utilized in order to evaluate the effectiveness of the GST-GCK Rab8id as a bioprobe for immunofluorescence microscopy. Previous studies in our lab have established a GST-tagged, FYVE-finger domain-based biosensor for PIP_3 (phosphotidylinositol 3-phosphate) (Powell, Welter, *et al.*, 2006). Therefore, initial experiments were conducted according to the biosensor staining protocols established in the previous study. At the time of this report, only one staining procedure has been completed. However, the results from this experiment show promising results. In MDCK cells stably expressing EGFP-Rab8CA, there is considerable colocalization of the EGFP-Rab8CA and the GST-GCK Rab8id bioprobe. However, in MDCK cells stably expressing EGFP-Rab8DN, little to no colocalization of the EGFP-Rab8DN and the

GST-GCK Rab8id is seen. As in the Rab8 activation pulldown assay, optimization of this staining technique is still required.

In addition to the establishment of the Rab8 activation assay, this research has also generated preliminary data that suggests a role for Rab8 in the regulation of GCK localization. In MDCK cells expressing EGFP-Rab8CA, GCK staining is seen primarily in the nucleus. In neighboring cells that are not expressing EGFP-Rab8CA, some GCK staining is visible within the cytoplasm. In MDCK cells expressing EGFP-Rab8DN, GCK staining is equivalent to or greater than MDCK cells not expressing EGFP-Rab8 constructs. The idea that Rab8 may play a regulatory role on the amount of GCK within the cytoplasm is intriguing. GCK is a constitutively active kinase. The kinase activity of the protein is necessary for its ubiquitination and degradation by the proteosome. In resting cells, GCK is turned over rapidly (Zhong and Kyriakis, 2004; Zhong and Kyriakis, 2007). However, GCK levels inside the cell have been shown to increase in response to stimuli, including the binding of PAMPS (pathogen-associated molecular patterns), such as LPS, peptidoglycan, bacterial flagellin, DNA and RNA from microbial and viral pathogens, to TLRs (toll-like receptors), which activate the TNF receptor-associated (TRAF) family members, TRAF2 and TRAF6. These TRAF family members have been implicated in the stabilization of GCK, protecting it from degradation by the proteosome, and allowing it to activate the JNK (Jun N-terminal kinase) pathway (Zhong and Kyriakis, 2004).

The human germinal center kinase, in conjunction with TRAF2, has been shown to interact with and activate the MAP 3-kinase, MEKK1. This member of the MEK

kinase family of MAP 3-kinases has been shown to contribute to the stabilization of the endogenously ubiquitinated GCK protein within the cytoplasm (Chadee, Yuasa, and Kyriakis, 2002). Interestingly, MEKK1 also contains a CRIB domain, which allows it to bind to and be activated by Rac1 and Cdc42 (Ichijo, 1999). Additionally, GCK has been shown to interact with the MAP3Ks of the mixed lineage kinase (MLK) pathway, MLK2 and MLK3. In response to PAMPS, GCK activates the JNK/p38 pathways through MLK2 and MLK3 (Zhong and Kyriakis, 2007).

Our preliminary results demonstrate that the status of Rab8 activation has an effect on the levels of GCK within the cytoplasm. Rab8 was first identified as the *mel* oncogene when murine NIH3T3 cells were transfected with an expression library derived from the human melanoma cell line, NK14 (Nimmo, Sanders, *et al.*, 1991); however, no link to Rab8 has ever been identified in melanoma cells. Interestingly, TRAF2/GCK have been shown to play a role in melanoma sensitivity to UV-induced apoptosis (Ivanov, Kehrl, and Ronai, 2000). Therefore, the possible key to the connection between Rab8 and melanoma may lie in its interaction with GCK.

The association with GCK also indicates a possible role of Rab8 in the activation of the JNK/p38 pathways (Ichijo, 1999). These pathways have been linked to the regulation of cellular apoptosis. In the stable EGFP-Rab8DN expressing MDCK cells, we observed the early appearance of dome formations, or hemicysts. In confluent epithelial monolayers, the appearance of domes is a result of enhanced cellular differentiation (Chang, Lin, *et al.*, 2007). With enhanced cellular differentiation, MDCK cells gain the ability to perform transepithelial transport of liquids. This causes the accumulation of

fluid between the cell monolayer and the culture flask (Chang, Lin, *et al.*, 2007; Lever, 1979a; Lever, 1979b; Su, Yeh, *et al.*, 2007). Apoptosis is also enhanced in confluent cell monolayers which have undergone enhanced cellular differentiation. Chang *et al.* demonstrated that this apoptosis is the result of caspase 8 signaling and the decrease of ERK1/2 signaling (Chang, Lin, *et al.*, 2007; Schlesinger, Bonvin, *et al.*, 2002). Remarkably, caspase 8 has been tied to both MEKK1 and MLK3, which both bind to GCK. Caspase 8 has been shown to be a modifier of MEKK1 (Schlesinger, Bonvin, *et al.*, 2002), and is involved in the TNF pathway, in which MLK3 is involved, which leads to apoptosis (Brancho, Ventura, *et al.*, 2005). The inactive, GDP-bound form of Rab8 has been shown to lead to the death of transgenic *Xenopus* rods (Moritz, Tam, *et al.*, 2001). These results are consistent with our observation of increased frequency of dome formation in MDCK monolayers, further supporting a possible role for Rab8 in apoptosis.

In conclusion, this report outlines the development of a Rab8 activation assay, which should prove useful in the study of the role of Rab8 in EMT and cancer metastasis. Additionally, the preliminary data from this study highlights the fact that the relationship between the germinal center kinase, GCK, and Rab8 should be investigated further. The elucidation of this interaction could lead to new insights into the causes of many of the phenotypic changes observed in Rab8 mutants.

References

Alberts, B., Johnson, A., Lewis, J., Raff, M., Roberts, K., and Walter, P. (2008). *Molecular Biology of the Cell* (New York, Garlan Science, Taylor & Francis Group, LLC).

Brancho, D., Ventura, J.J., Jaeschke, A., Doran, B., Flavell, R.A., and Davis, R.J. (2005). Role of MLK3 in the regulation of mitogen-activated protein kinase signaling cascades. *Mol. Cell. Biol. 25,* 3670-3681.

Chadee, D.N., Yuasa, T., and Kyriakis, J.M. (2002). Direct activation of mitogen-activated protein kinase kinase kinase MEKK1 by the Ste20p homologue GCK and the adapter protein TRAF2. *Mol. Cell. Biol. 22,* 737-749.

Chang, Y.H., Lin, H.H., Wang, Y.K., Chiu, W.T., Su, H.W., and Tang, M.J. (2007). Activation of caspase-8 and Erk-1/2 in domes regulates cell death induced by confluence in MDCK cells. *J. Cell. Physiol. 211,* 174-182.

Eger, A., and Mikulits, W. (2005). Models of epithelial-mesenchymal transition. *Drug Discovery Today: Disease Models 2,* 57-57-63.

Grille, S.J., Bellacosa, A., Upson, J., Klein-Szanto, A.J., van Roy, F., Lee-Kwon, W., Donowitz, M., Tsichlis, P.N., and Larue, L. (2003). The protein kinase Akt induces epithelial mesenchymal transition and promotes enhanced motility and invasiveness of squamous cell carcinoma lines. *Cancer Res. 63,* 2172-2178.

Grunert, S., Jechlinger, M., and Beug, H. (2003). Diverse cellular and molecular mechanisms contribute to epithelial plasticity and metastasis. *Nat. Rev. Mol. Cell Biol. 4,* 657-665.

Hattula, K., and Peranen, J. (2000). FIP-2, a coiled-coil protein, links Huntingtin to Rab8 and modulates cellular morphogenesis. *Curr. Biol. 10,* 1603-1606.

Ichijo, H. (1999). From receptors to stress-activated MAP kinases. *Oncogene 18,* 6087-6093.

Ivanov, V.N., Kehrl, J.H., and Ronai, Z. (2000). Role of TRAF2/GCK in melanoma sensitivity to UV-induced apoptosis. *Oncogene 19,* 933-942.

Kang, Y., and Massague, J. (2004). Epithelial-mesenchymal transitions: twist in development and metastasis. *Cell 118,* 277-279.

Lever, J.E. (1979a). Inducers of mammalian cell differentiation stimulate dome formation in a differentiated kidney epithelial cell line (MDCK). *Proc. Natl. Acad. Sci. U. S. A. 76,* 1323-1327.

Lever, J.E. (1979b). Regulation of dome formation in differentiated epithelial cell cultures. *J. Supramol. Struct. 12,* 259-272.

Lodish, H., Berk, A., Zipursky, S.L., Matsudaira, P., Baltimore, D., and Darnell, J. (2000). *Molecular Cell Biology*. (New York, W.H. Freeman & Company).

Moritz, O.L., Tam, B.M., Hurd, L.L., Peranen, J., Deretic, D., and Papermaster, D.S. (2001). Mutant rab8 Impairs docking and fusion of rhodopsin-bearing post-Golgi membranes and causes cell death of transgenic *Xenopus* rods. *Mol. Biol. Cell 12,* 2341-2351.

Nieto, M.A. (2002). The snail superfamily of zinc-finger transcription factors. *Nat. Rev. Mol. Cell Biol. 3,* 155-166.

Nimmo, E.R., Sanders, P.G., Padua, R.A., Hughes, D., Williamson, R., and Johnson, K.J. (1991). The MEL gene: a new member of the RAB/YPT class of RAS-related genes. *Oncogene 6,* 1347-1351.

Olson, M.F., and Sahai, E. (2009). The actin cytoskeleton in cancer cell motility. *Clin. Exp. Metastasis 26, 273-287.*

Peranen, J., Auvinen, P., Virta, H., Wepf, R., and Simons, K. (1996). Rab8 promotes polarized membrane transport through reorganization of actin and microtubules in fibroblasts. *J. Cell Biol. 135,* 153-167.

Peranen, J., and Furuhjelm, J. (2001). Expression, purification, and properties of Rab8 function in actin cortical skeleton organization and polarized transport. *Methods Enzymol. 329,* 188-196.

Powell, R.R., and Temesvari, L.A. (2004). Involvement of a Rab8-like protein of *Dictyostelium discoideum*, Sas1, in the formation of membrane extensions, secretion and adhesion during development. *Microbiology 150,* 2513-2525.

Powell, R.R., Welter, B.H., Hwu, R., Bowersox, B., Attaway, C., and Temesvari, L.A. (2006). *Entamoeba histolytica*: FYVE-finger domains, phosphatidylinositol 3-phosphate biosensors, associate with phagosomes but not fluid filled endosomes. *Exp. Parasitol. 112,* 221-231.

Ren, M., Zeng, J., De Lemos-Chiarandini, C., Rosenfeld, M., Adesnik, M., and Sabatini, D.D. (1996). In its active form, the GTP-binding protein rab8 interacts with a stress-activated protein kinase. *Proc. Natl. Acad. Sci. U. S. A. 93,* 5151-5155.

Ridley, A.J., Schwartz, M.A., Burridge, K., Firtel, R.A., Ginsberg, M.H., Borisy, G., Parsons, J.T., and Horwitz, A.R. (2003). Cell migration: integrating signals from front to back. *Science 302,* 1704-1709.

Sahai, E. (2005). Mechanisms of cancer cell invasion. *Curr. Opin. Genet. Dev. 15,* 87-96.

Schlesinger, T.K., Bonvin, C., Jarpe, M.B., Fanger, G.R., Cardinaux, J.R., Johnson, G.L., and Widmann, C. (2002). Apoptosis stimulated by the 91-kDa caspase cleavage MEKK1 fragment requires translocation to soluble cellular compartments. *J. Biol. Chem. 277,* 10283-10291.

Shaw, A.J., Rickwood, D., and Hames, B.D. (1996). *Epithelial Cell Culture: A Practical Approach.* (New York, Oxford University Press).

Su, H.W., Yeh, H.H., Wang, S.W., Shen, M.R., Chen, T.L., Kiela, P.R., Ghishan, F.K., and Tang, M.J. (2007). Cell confluence-induced activation of signal transducer and activator of transcription-3 (Stat3) triggers epithelial dome formation via augmentation of sodium hydrogen exchanger-3 (NHE3) expression. *J. Biol. Chem. 282,* 9883-9894.

Thiery, J.P. (2002). Epithelial-mesenchymal transitions in tumour progression. *Nat. Rev. Cancer 2,* 442-454.

Thomas, P., and Smart, T.G. (2005). HEK293 cell line: a vehicle for the expression of recombinant proteins. *J. Pharmacol. Toxicol. Methods 51,* 187-200.

Welter, B.H., Laughlin, R.C., and Temesvari, L.A. (2002). Characterization of a Rab7-like GTPase, EhRab7; a marker for the early stages of endocytosis in *E. histolytica*. *Molecular Biochemical Parasitology 121,* 254.

Williams, S., Mustoe, T., Mulcahy, T., Griffiths, M., Simpson, D., Antoniou, M., Irvine, A., Mountain, A., and Crombie, R. (2005). CpG-island fragments from the HNRPA2B1/CBX3 genomic locus reduce silencing and enhance transgene expression from the hCMV promoter/enhancer in mammalian cells. *BMC Biotechnol. 5,* 17.

Xue, C., Plieth, D., Venkov, C., Xu, C., and Neilson, E.G. (2003). The gatekeeper effect of epithelial-mesenchymal transition regulates the frequency of breast cancer metastasis. *Cancer Res. 63,* 3386-3394.

Yang, J., Mani, S.A., Donaher, J.L., Ramaswamy, S., Itzykson, R.A., Come, C., Savagner, P., Gitelman, I., Richardson, A., and Weinberg, R.A. (2004). Twist, a master regulator of morphogenesis, plays an essential role in tumor metastasis. *Cell 117*, 927-939.

Zhong, J., and Kyriakis, J.M. (2007). Dissection of a signaling pathway by which pathogen-associated molecular patterns recruit the JNK and p38 MAPKs and trigger cytokine release. *J. Biol. Chem. 282*, 24246-24254.

Zhong, J., and Kyriakis, J.M. (2004). Germinal center kinase is required for optimal Jun N-terminal kinase activation by Toll-like receptor agonists and is regulated by the ubiquitin proteasome system and agonist-induced, TRAF6-dependent stabilization. *Mol. Cell. Biol. 24*, 9165-9175.

CHAPTER FOUR

CONCLUSIONS

The small GTPase, Rab8, has been implicated in vesicle trafficking, cell-cell adhesion and the restructuring of the actin cytoskeleton. The unexpected "moonlighting" capability of Rab8 to affect changes in the actin cytoskeleton has been reported by many research groups, but no specific pathway for this action has been identified. This project provides insight into the unique "moonlighting" role of Rab8 as a regulator of actin, as well as its role as a regulator of cell-cell adhesion. In addition, this project provides preliminary data for the investigation of Rab8 in a mammalian cell system.

Clues to the role of Rab8 initially came from our studies of its homolog, Sas1, in *Dictyostelium discoideum*, which undergoes a developmental cycle involving changes in cell motility and cell-cell adhesion. Cells expressing constitutively activated Rab8 (Sas1CA) displayed reduced cell-cell adhesion and increased actin-rich protrusions (Powell and Temesvari, 2004). It was hypothesized that changes in actin, observed as actin-rich protrusions, may contribute to this change. In other systems, actin-rich membrane extension formation is regulated by WASp family proteins including SCAR (Blagg, Stewart, *et al.*, 2003; Blagg and Insall, 2004). To test the hypothesis, we have expressed constitutively active Rab8 in a SCAR-knockout *D. discoideum* cell line. Interestingly, adhesion was normal in this double mutant, suggesting that the adhesion defect was a result of aberrant signaling through SCAR and that Rab8 may be upstream

of SCAR in a signaling cascade. This provides the first genetic evidence in any cell system of a functional interaction between Rab8 and a WASp family protein.

Since SCAR is directly activated by Rac (Caracino, Jones, *et al.*, 2007; Eden, Rohatgi, *et al.*, 2002), we hypothesized that Rab8 may induce changes in actin by acting upstream of Rac to induce aberrant signaling through SCAR. Therefore, we expressed constitutively active Rab8 in conjunction with a dominant negative version of RacF2. We chose RacF2 because of its similar developmental phenotype to our own dominant negative Rab8 expressing cells. Cells expressing dominant negative Rab8 or dominant negative RacF2 demonstrate increased EDTA-sensitive cell-cell adhesion and early, or precocious, aggregation as compared to parental AX2 cells (Muramoto and Urushihara, 2006; Powell and Temesvari, 2004). Our results indicate that the expression of the dominant negative version of RacF2 rescues the aggregation defect of cells expressing constitutively active Rab8. In addition, we have demonstrated that the interaction between Rab8 and RacF2 is direct. Our data suggests that Rab8 and RacF2 likely work together to control cell-cell adhesion during early development. It is likely that this early cell-cell adhesion is controlled through regulation of expression or trafficking of the EDTA-sensitive cell adhesion molecule, gp24 (Muramoto and Urushihara, 2006; Powell and Temesvari, 2004). Tests to establish the role of Rab8 and RacF2 in the regulation of gp24 are currently ongoing. Furthermore, we have also demonstrated that RacF2 does not interact with SCAR. In addition, expression of dominant negative RacF2 does not alter the actin-rich protrusion phenotype of cells expressing constitutively active Rab8.

SCAR-null cells expressing constitutively active Rab8 are able to aggregate, therefore, we decided to investigate the actin distribution in these cells, assuming that alterations in the actin cytoskeleton could affect early development. We demonstrated that SCAR-null cells expressing constitutively active Rab8 still had actin-rich protrusions under nutrient conditions; however, under starvation conditions, these actin-rich protrusions disappeared. We have demonstrated that Rab8 likely interacts functionally with SCAR under starvation conditions, but not necessarily under nutrient conditions. Differences in SCAR activation during starvation and nutrient conditions have been documented previously (Pollitt, Blagg, *et al.*, 2006), so this result is not surprising. It is, however, interesting when we consider the fact that *D. discoideum* cells undergo chemotactic movement during early development.

Additionally, we have demonstrated that the general motility of cells expressing either dominant negative or constitutively active Rab8 does not appear to be adversely affected as compared to parental AX2 cells. However, chemotaxis is significantly enhanced in cells expressing constitutively active Rab8 as compared to cells expressing dominant negative Rab8 or parental AX2 cells. Further studies to determine if the cells expressing constitutively active Rab8 have an advantage in chemotaxis due to the ability to polarize actin quickly could prove interesting.

Epithelial to mesenchymal transition is the transformation of polarized epithelial cells to non-polarized mesenchymal cells through loss of cell-cell contacts and cytoskeletal restructuring (Kang and Massague, 2004; Thiery, 2002). During embryogenesis, mesenchymal cells migrate, allowing formation of tissues and organs

(Grunert, Jechlinger, and Beug, 2003; Kang and Massague, 2004). EMT is also observed at the onset of cancerous tumor metastasis. One dramatic change during EMT is gain of motility, which involves formation of cell extensions in the direction of movement (Grunert, Jechlinger, and Beug, 2003). The reduced cell-cell adhesion and increased actin-rich protrusions seen in *D. discoideum* cells expressing constitutively active Rab8 is reminiscent of changes associated with EMT.

Although the role of Rab8 in cell polarity has been studied, its contribution to EMT has not. Therefore, we have designed a Rab8 expression system for use in mammalian cells for the future study of the role of Rab8 in EMT. To this end, we have designed and developed EGFP (enhanced green fluorescent protein) chimeras of constitutively active, dominant negative and wildtype forms of Rab8. We have stably transfected MDCK (Madin Darby Canine Kidney) and transiently transfected HEK 293 (Human Embryonic Kidney) cells with these constructs and have verified expression of the EGFP-Rab8 chimeric proteins in these cells. In addition, we have designed an activation assay that may be used to determine the activation state of Rab8 within a cell.

The Rab8 activation assay was designed utilizing a Rab8 binding protein, GCK (germinal center kinase). GCK binds only to the active, GTP-bound form of Rab8 (Ren, Zeng, *et al.*, 1996). We designed a GST (glutathione-S-transferase) fusion of the Rab8 binding domain of GCK. We incubated cells expressing EGFP chimeras of constitutively active or dominant negative Rab8 with the GST-GCK purified protein, and subsequently stained with a fluorescent secondary antibody to GST. Immunofluorescence microscopy only showed colocalization of GST-GCK with EGFP-Rab8CA, demonstrating that the

GST-GCK preferentially bound to the EGFP-Rab8CA chimeric protein. While the assay still requires optimization, we have demonstrated proof of principle in this study that the GST-GCK fusion protein can be utilized as a bioprobe to indicate active, GTP-bound Rab8 in cells.

Interestingly, we have also demonstrated an effect of Rab8 activation status on intracellular GCK levels. Our preliminary results show that constitutively active Rab8 expressing cells had lower amounts of intracellular GCK than cells expressing dominant negative Rab8. While GCK has been recognized as a Rab8 binding protein (Ren, Zeng, *et al.*, 1996), the significance of this interaction has never been documented. It is an intriguing connection because while Rab8 was first identified as the *mel* oncogene from the human melanoma cell line, NK14, (Nimmo, Sanders, *et al.*, 1991) its method of involvement in melanoma has never been established. GCK, however, has been shown to play a role in melanoma sensitivity to UV-induced apoptosis (Ivanov, Kehrl, and Ronai, 2000).

Through our study of the role of Rab8 in the lower eukaryote, *Dictyostelium discoideum*, we have provided valuable insight into the evolutionarily conserved role of Rab8 in regulation of actin cytoskeleton restructuring. Because actin cytoskeletal restructuring is so vital to cell-cell adhesion, cell polarity and motility, this study also provides new information which may help us to understand the complex processes of development of multicellularity and how epithelial cells undergo epithelial to mesenchymal transition in development and cancer metastasis.

References

Blagg, S.L., and Insall, R.H. (2004). Control of SCAR activity in *Dictyostelium discoideum*. *Biochem. Soc. Trans. 32,* 1113-1114.

Blagg, S.L., Stewart, M., Sambles, C., and Insall, R.H. (2003). PIR121 regulates pseudopod dynamics and SCAR activity in *Dictyostelium*. *Curr. Biol. 13,* 1480-1487.

Caracino, D., Jones, C., Compton, M., and Saxe, C.L.,3rd. (2007). The N-terminus of *Dictyostelium* Scar interacts with Abi and HSPC300 and is essential for proper regulation and function. *Mol. Biol. Cell 18,* 1609-1620.

Eden, S., Rohatgi, R., Podtelejnikov, A.V., Mann, M., and Kirschner, M.W. (2002). Mechanism of regulation of WAVE1-induced actin nucleation by Rac1 and Nck. *Nature 418,* 790-793.

Grunert, S., Jechlinger, M., and Beug, H. (2003). Diverse cellular and molecular mechanisms contribute to epithelial plasticity and metastasis. *Nat. Rev. Mol. Cell Biol. 4,* 657-665.

Ivanov, V.N., Kehrl, J.H., and Ronai, Z. (2000). Role of TRAF2/GCK in melanoma sensitivity to UV-induced apoptosis. *Oncogene 19,* 933-942.

Kang, Y., and Massague, J. (2004). Epithelial-mesenchymal transitions: twist in development and metastasis. *Cell 118,* 277-279.

Muramoto, T., and Urushihara, H. (2006). Small GTPase RacF2 affects sexual cell fusion and asexual development in *Dictyostelium discoideum* through the regulation of cell adhesion. *Dev. Growth Differ. 48,* 199-208.

Nimmo, E.R., Sanders, P.G., Padua, R.A., Hughes, D., Williamson, R., and Johnson, K.J. (1991). The MEL gene: a new member of the RAB/YPT class of RAS-related genes. *Oncogene 6,* 1347-1351.

Pollitt, A.Y., Blagg, S.L., Ibarra, N., and Insall, R.H. (2006). Cell motility and SCAR localisation in axenically growing *Dictyostelium* cells. *Eur. J. Cell Biol. 85,* 1091-1098.

Powell, R.R., and Temesvari, L.A. (2004). Involvement of a Rab8-like protein of *Dictyostelium discoideum*, Sas1, in the formation of membrane extensions, secretion and adhesion during development. *Microbiology 150,* 2513-2525.

Ren, M., Zeng, J., De Lemos-Chiarandini, C., Rosenfeld, M., Adesnik, M., and Sabatini, D.D. (1996). In its active form, the GTP-binding protein rab8 interacts with a stress-activated protein kinase. *Proc. Natl. Acad. Sci. U. S. A. 93,* 5151-5155.

Thiery, J.P. (2002). Epithelial-mesenchymal transitions in tumour progression. *Nat. Rev. Cancer 2*, 442-454.